CHAPTER

10 Ultrasonography and Nuclear Medicine

Frederic Rahbari-Oskoui • Andrew T. Taylor • William Charles O'Neill

Sonography and nuclear medicine are important tools in the evaluation of the kidneys and urinary tract. Due to its simplicity and ready availability, sonography is usually the initial imaging performed and, in many cases, the only examination required. The low cost and portability of modern equipment enable sonography to be an office-based or bedside procedure performed by the practitioner, adding to its convenience and attractiveness. Nuclear medicine can obtain important functional data and complements other imaging modalities that cannot provide this information. This functional assessment can be critical for clinical decisions and often avoids the necessity of invasive testing. This chapter reviews the advantages, disadvantages, and indications for each modality in the kidneys and urinary tract along with the basics of interpretation and common findings.

ULTRASONOGRAPHY

The introduction and extensive use of ultrasonography over the past four decades has dramatically simplified the diagnostic evaluation of the urinary tract. The acoustic properties, limited spectrum of pathology, and ease of visualization of the kidneys—coupled with the safety, simplicity, lack of radiation, and low cost—of sonography make it the initial modality of choice. The improved portability and affordability of equipment and availability of training provide an opportunity for nephrologists to become skilled at this technique, thereby enhancing the diagnosis and care of their patients.

Sonographic images are acquired by analyzing the amplitude and interval of reflected pulses of high-frequency sound. Time is converted to depth and amplitude is converted to brightness (echogenicity) to yield a pixel-based image. Highly reflective structures such as a stone appear bright and cast a dark, distal shadow. In contrast, fluid collections such as cysts do not reflect sound and appear dark but enhance the echogenicity of distal tissue (distal enhancement or through transmission).[1] Tissues such as renal parenchyma have an intermediate echogenicity related to backscatter of sound from the microscopic architecture. Indications for ultrasound imaging of the kidneys and the bladder are diverse and include evaluation of acute renal failure, chronic kidney disease (CKD), cystic diseases, pain, hematuria, severe hypertension, urinary tract infections, and guidance for kidney biopsies.

Imaging and Normal Appearance of the Kidneys

The adult kidney contains several lobules, each consisting of a rim of cortex surrounding a medullary pyramid that terminates in a papilla protruding into a minor calyx. The lobules fuse in utero or shortly after birth in most individuals. The cortex between two pyramids is called a column of Bertin. Minor calyces converge into major calyces that, in turn, converge to form the renal pelvis. The portion of the kidneys that is not parenchyma or urinary space is the sinus, which, in adults, is filled with adipose tissue (Fig. 10.1). Longitudinal views of the kidney are obtained in the supine position with the probe positioned so that the upper pole appears on the left side of the image. In the longitudinal plane, the normal kidney has a characteristic oval shape with a hypoechoic (dark) rim of cortex and medulla surrounding the echogenic (bright) sinus fat[2–4] that obscures the calyces and blood vessels (Fig. 10.2). The medullary pyramids are slightly less echogenic than the cortex[2] and can often be discerned. They are particularly prominent when cortical echogenicity is increased. Transverse images are obtained perpendicular to the longitudinal axis and the kidney appears circular at each pole and C-shaped through the center due to the break in the parenchyma where the ureter and vessels enter, thereby providing the best views of the renal pelvis and hilum.

The appearance of the kidneys is subject to normal variations related primarily to incomplete fusion of the ranunculi. These include complete duplication of the collecting system, which appears as a band of cortex separating the sinus fat into two compartments (Fig. 10.3) and is present in 5% of kidneys, and hypertrophied columns of Bertin, where the cortex extends into the sinus but does not completely bridge

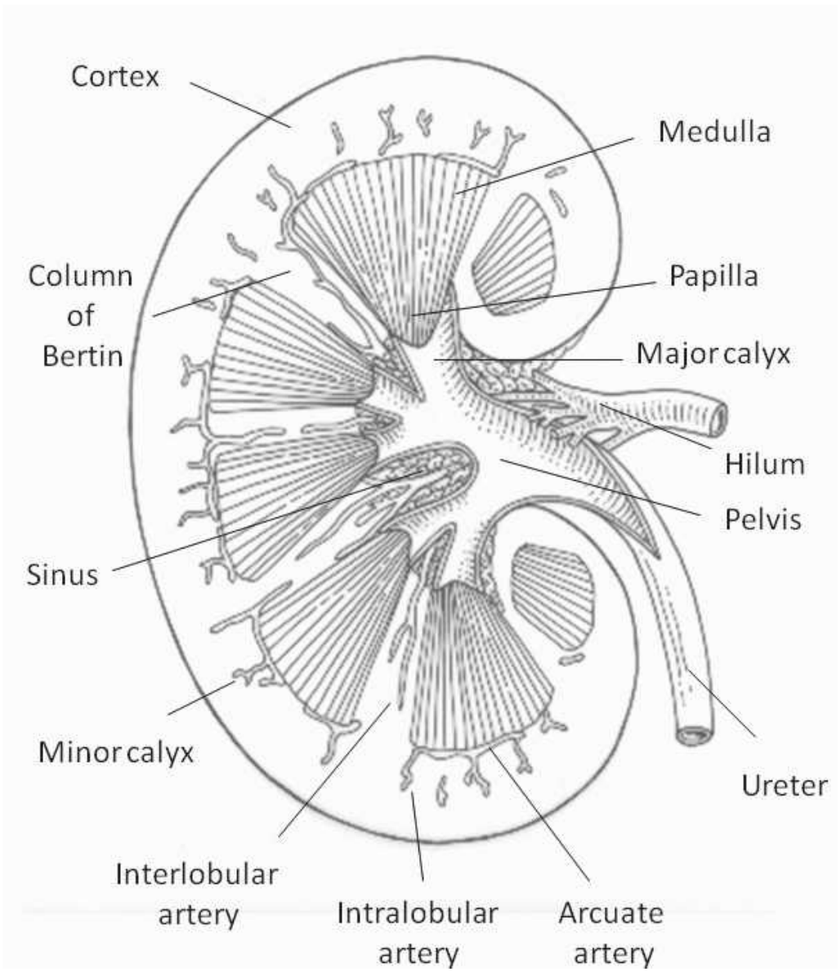

FIGURE 10.1 Intrarenal anatomy, midline coronal section. (Adapted from O'Neill WC. Sonographic evaluation of renal failure. *Am J Kidney Dis*. 2000;35:1021, with permission.)

it (Fig. 10.4) and is present in 15% of kidneys.[5,6] Junctional parenchymal defects are the most subtle manifestation of incomplete fusion, presenting as a wedge-shaped defect in the outer cortex filled with echogenic fat that is continuous with the renal sinus fat by a thin strand.[6] In some individuals, the lobules fail to completely fuse and persist into adulthood. These so-called fetal lobulations appear as regularly spaced convexities, each containing a pyramid.[7] Lobulation may reappear in chronic kidney disease due to atrophy of the columns of Bertin (Fig. 10.5).

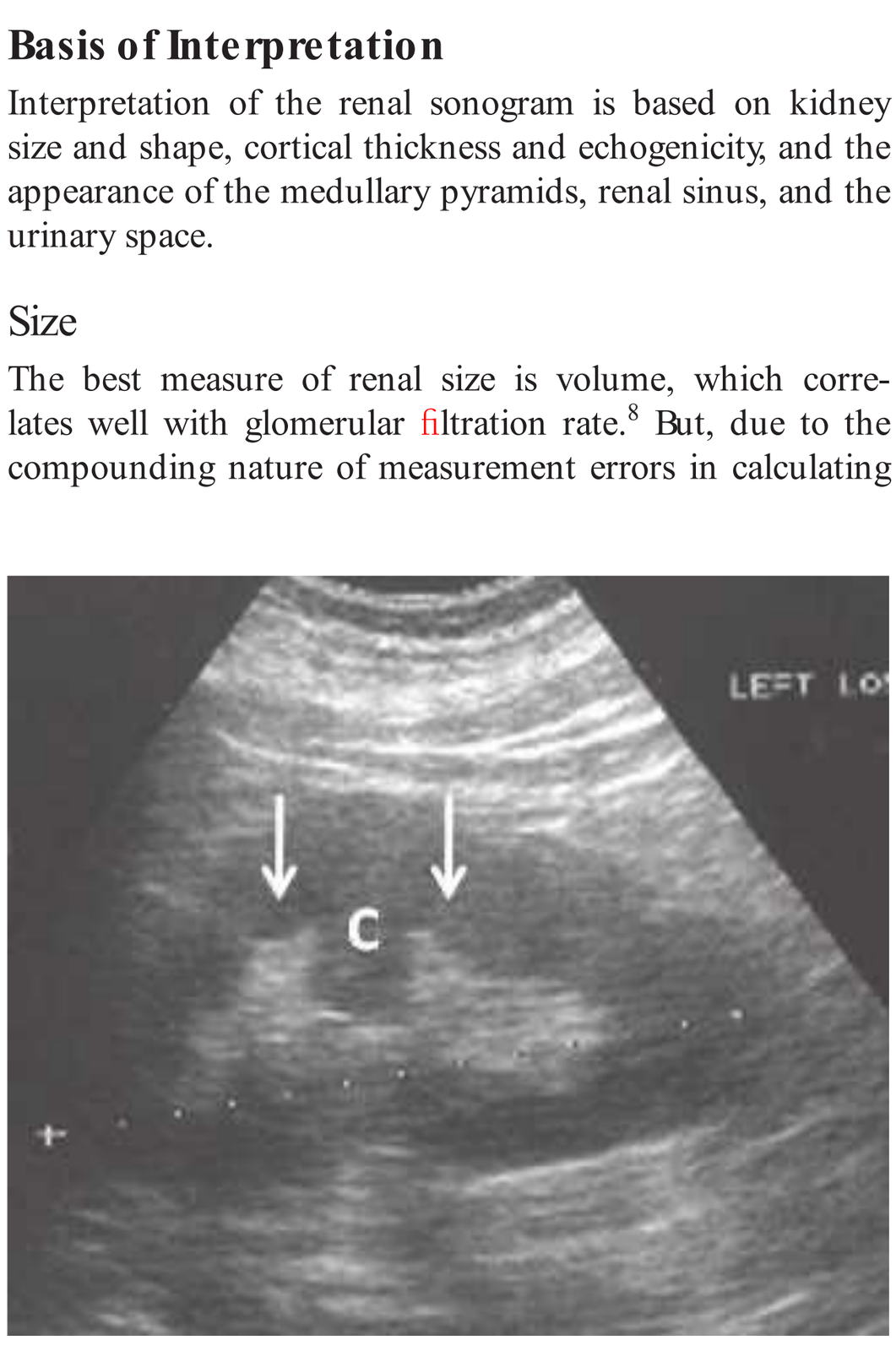

FIGURE 10.3 Duplication of the collecting system. Longitudinal view of the kidney showing a band of tissue (*arrow*) demarcating two separate renal sinuses (*S*).

Basis of Interpretation

Interpretation of the renal sonogram is based on kidney size and shape, cortical thickness and echogenicity, and the appearance of the medullary pyramids, renal sinus, and the urinary space.

Size

The best measure of renal size is volume, which correlates well with glomerular filtration rate.[8] But, due to the compounding nature of measurement errors in calculating

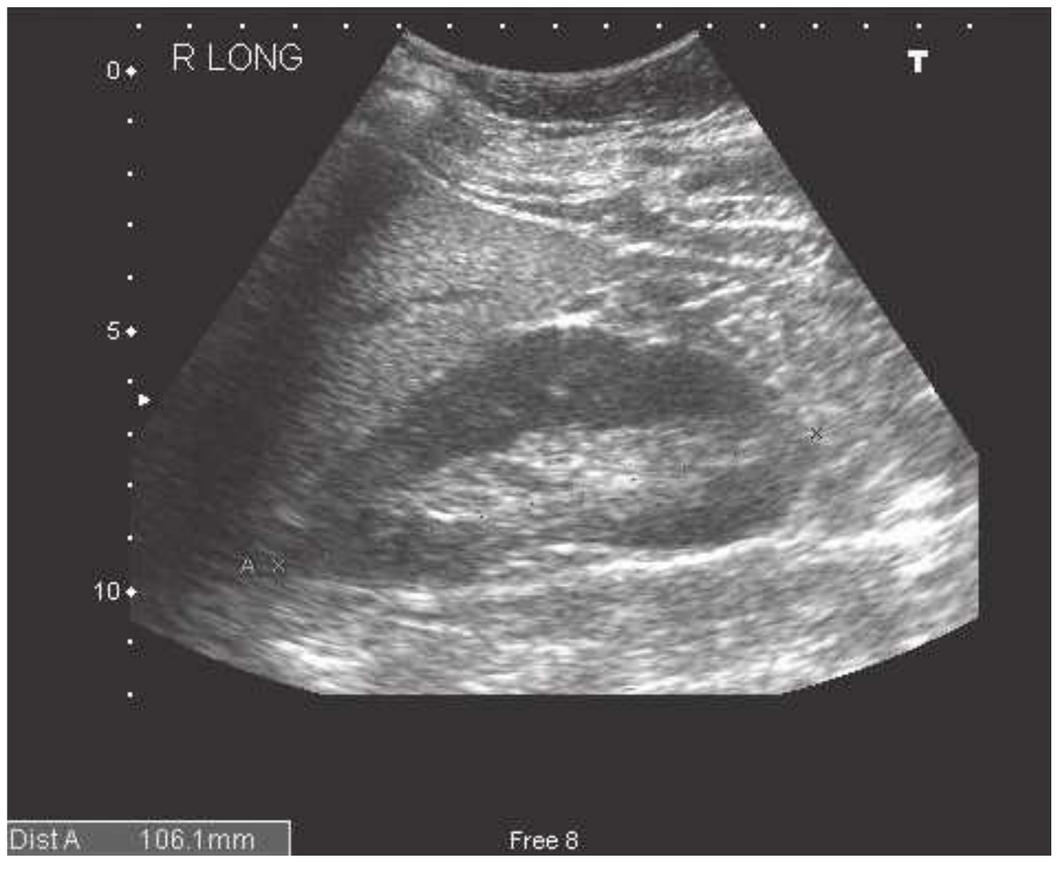

FIGURE 10.2 Longitudinal image of a normal right kidney. Compared to the liver, the renal parenchyma appears as a relatively hypoechoic, oval rim around the echogenic sinus fat.

FIGURE 10.4 Hypertrophied column of Bertin. Longitudinal image of the left kidney showing cortex (*C*) protruding into the renal sinus between two medullary pyramids (*arrows*).

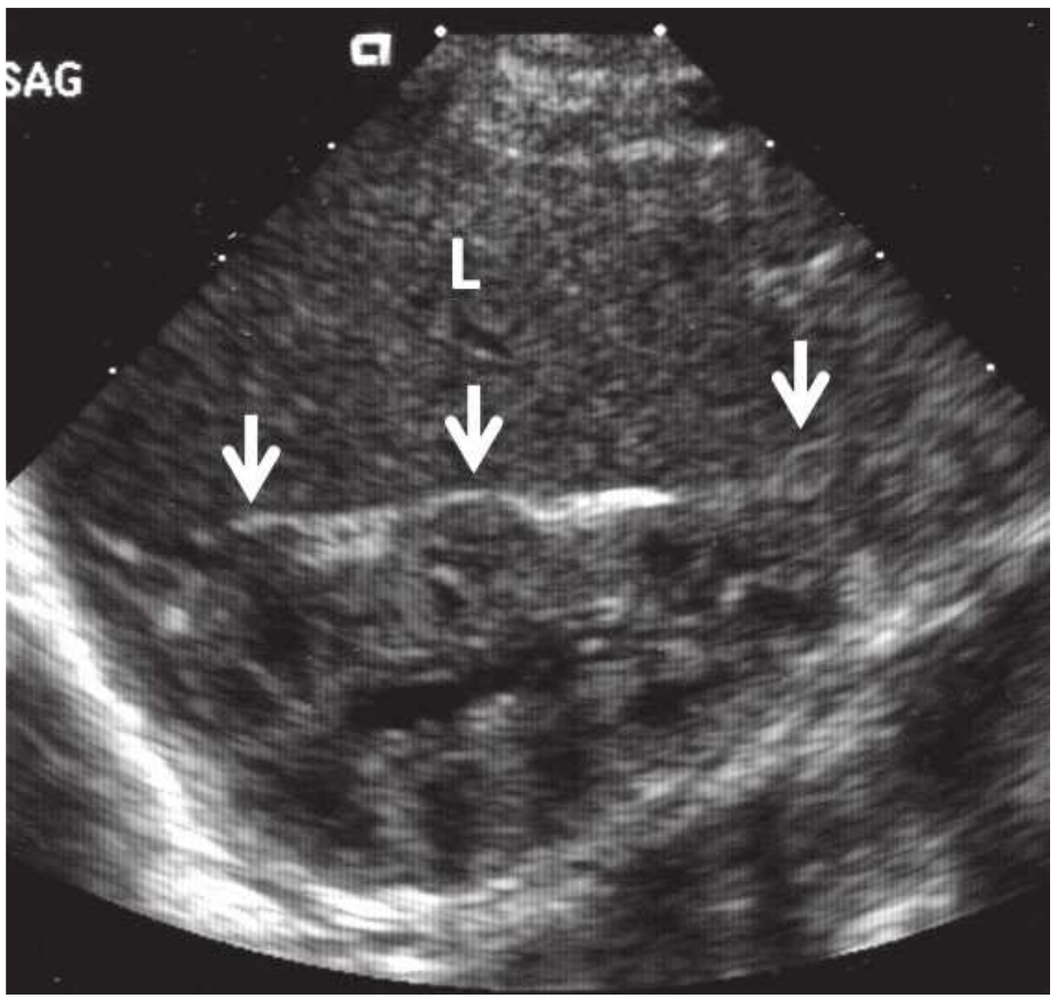

FIGURE 10.5 Normal neonatal kidney. Longitudinal view of the right kidney in a neonate showing accentuated lobules (*arrows*) and the medullary pyramid centered within each lobule. The cortex is more echogenic than the liver and there is no sinus fat.

volume, and the good correlation between maximum kidney length and renal volume,[9,10] maximum renal length is preferred for assessment of renal size on sonograms. Additional measurements in the transverse axes are very inaccurate and of no utility. Renal length averages 11 cm in adults,[10] and 10 cm to 12 cm is a useful range for normal renal length at average body height. Because the variability in measurements is 5%,[9] differences up to 1 cm may not be significant. The variability may be greater in children, comprising as much as 2 to 3 years in the comparison of kidney length to age.[11] Kidney length correlates best with body height in both adults and children (Fig. 10.6A)[10,12–14] and, after correction for body height, does not vary between sexes. Kidney length rapidly increases during the first year of life with a more gradual enlargement up to about 18 years[14,15] (Fig. 10.6B). Progressive enlargement occurs during pregnancy that resolves by 12 weeks postpartum, due primarily to parenchymal enlargement—although some pelvocaliceal enlargement occurs, particularly in the right kidney.[16] Proper interpretation of kidney size must take into account the effect of these nonpathologic factors. Compensatory hypertrophy is common in solitary kidneys in children (up to 80%–90% increase in volume),[17,18] and after nephrectomy in adults (5%–30% increase).[19,20] Enlargement of the kidneys occurs in nephritis and infiltrative diseases, often accompanied by a rounded shape and increased echogenicity.

Cortical Thickness

The thickness of the renal cortex is measured from the renal capsule to either the outer border of the medullary pyramids or to the arcuate arteries. A normal value of 9.3 ± 1.1 mm was obtained in 23 renal transplant donors.[21] If medullary pyramids are not discernible, the parenchymal thickness between the sinus fat and the renal capsule (mean value of 15 to 16 mm) may be used.[10] However, both parameters can vary within a kidney and are difficult to measure precisely. Cortical thinning is a sign of advanced chronic kidney disease. Increased cortical thickness is usually due to edema or

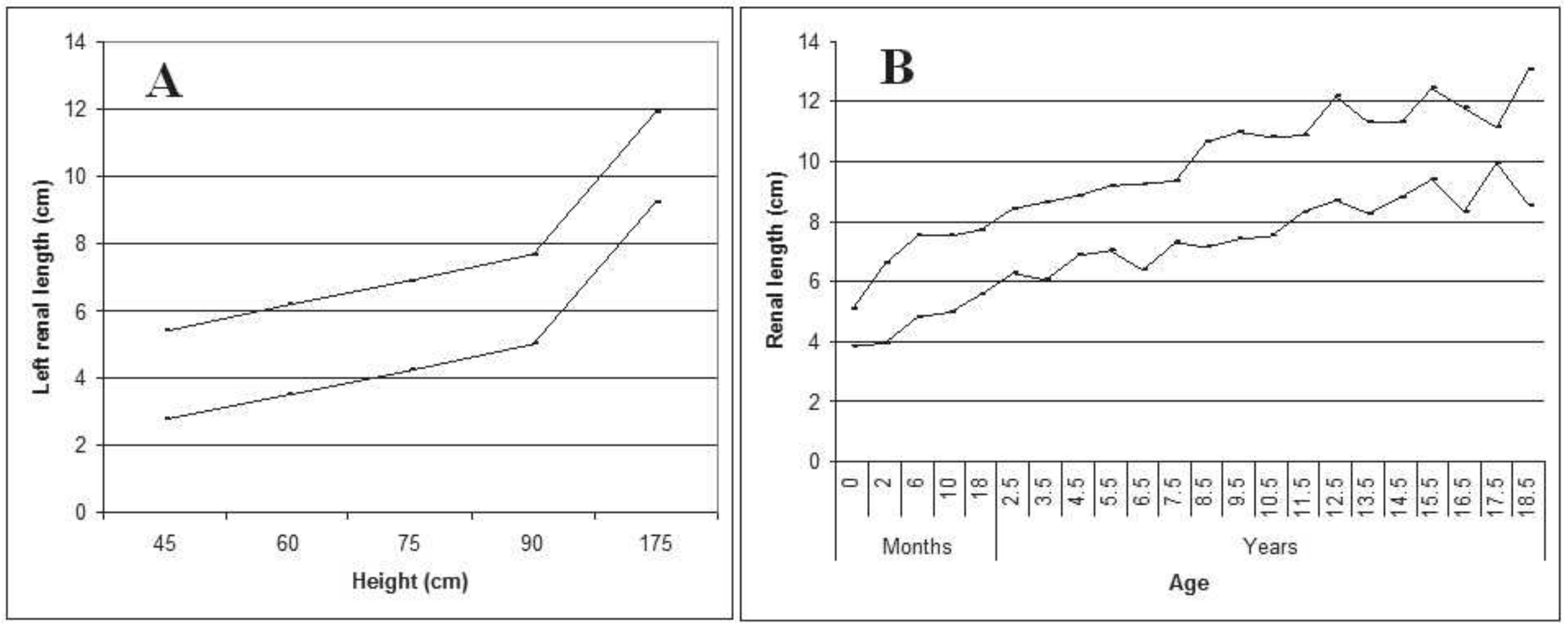

FIGURE 10.6 **A:** Nomogram of renal length based on body height showing 95% confidence limits for maximum length of the left kidney as a function of body height in children. (Adapted from Dinkel E, Ertel M, Dittrich M, et al. Kidney size in childhood: sonographic growth charts for kidney length and volume. *Pediatr Radiol.* 1985;15:38, with permission.) **B:** Nomogram of renal length and age: presenting 95% confidence limits for kidney length versus age in children. (Adapted from O'Neill WC. *Atlas of Renal Ultrasonography*. Philadelphia: WB Saunders; 2011, with permission.)

inflammation and is often accompanied by kidney enlargement, a globular shape, and obliteration of the sinus fat.

Cortical Echogenicity

Comparison of renal cortex to the liver or spleen, at the same depth, is the basis for determination of cortical echogenicity. Renal cortical echogenicity depends on age and is often greater than liver echogenicity in neonates but should be less than or equal to[22,23] that of the liver or spleen by 6 months of age.[24] After several years of age, the renal cortical echogenicity should always be less than the liver. Fibrosis, infiltrating cells, and tubular debris and dilation can increase echogenicity. Transmission artifacts related to overlying fluid and ribs, and increased hepatic echogenicity in steatosis or cirrhosis, can bias the interpretation of cortical echogenicity.

Medullary Pyramids

The medulla should be less echogenic than the cortex but visibility depends on overlying structures and the frequency of sound. Medullary disease usually causes increased echogenicity.

Renal Sinus

The neonatal kidney contains very little fat but the normal renal sinus in adults should exhibit only echogenic fat. Occasionally, the calyces are visible in otherwise normal kidneys, particularly during a brisk diuresis[25,26] or during pregnancy.[27,28] Blood vessels may also be visible, particularly in children and young adults or in states of increased central venous pressure.

Parenchymal Diseases

Glomerular or tubulointerstitial disorders usually present with diffuse changes in the kidneys. However, the changes can be similar in different disorders and the kidneys may appear normal. Thus, interpretation is very dependent on the clinical findings.

The most common parenchymal disorder that causes acute kidney injury is acute tubular necrosis (ATN). The renal sonogram can be normal in ATN[29–31] but increased cortical echogenicity and cortical expansion have been observed in both animal and human studies,[32–35] especially with nephrotoxic ATN,[32,35,36] whereas an enlarged hypoechoic cortex may be more typical of ischemic ATN.[6,32] The cortical enlargement presumably represents edema whereas increases in cortical echogenicity may be due to cellular and proteinaceous casts and debris within the tubules. The degree of renal enlargement has been shown to inversely correlate with recovery time from ATN.[34] In general, sonography is rarely useful in the workup of acute renal failure when the clinical picture suggests ATN and urinary obstruction is unlikely. However, it may be helpful in identifying underlying chronic kidney disease in this setting.

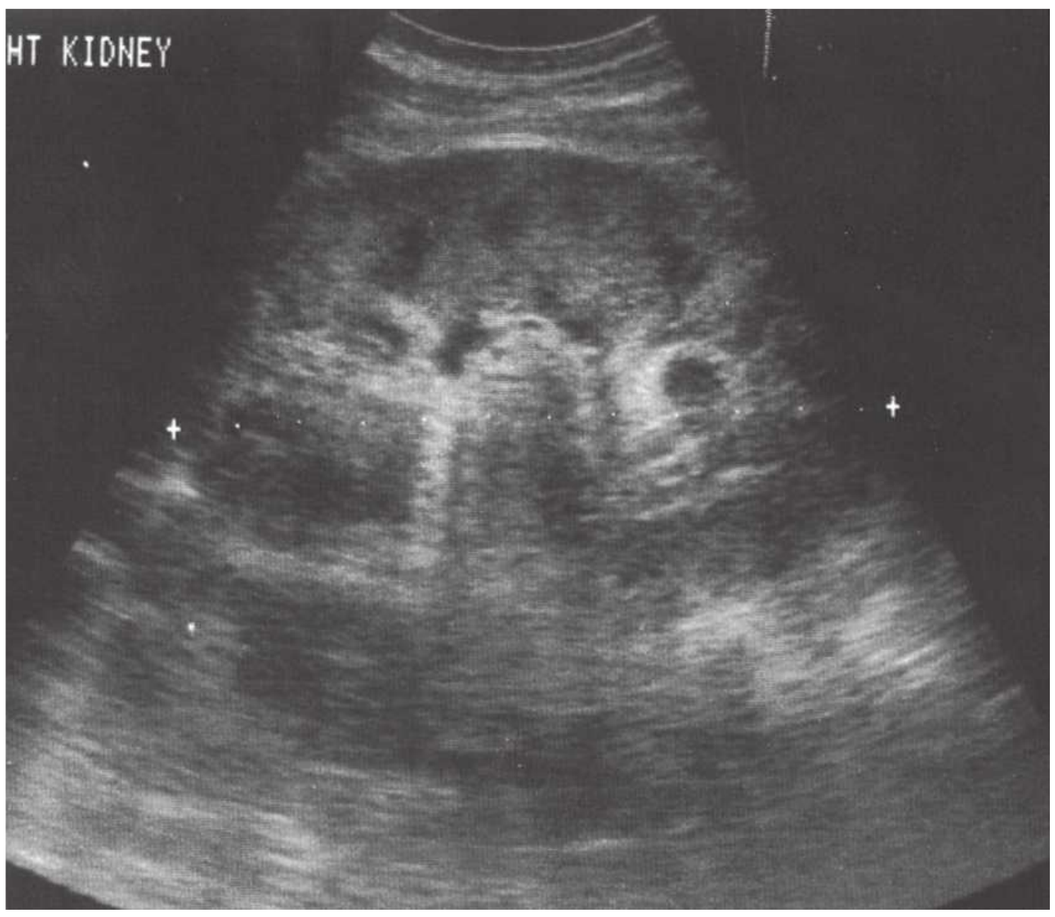

FIGURE 10.7 Acute glomerulonephritis. Longitudinal view of the right kidney showing a globular kidney with diminished sinus fat indicating cortical swelling. Note the prominence of the medullary pyramids due to increased cortical echogenicity.

Glomerulopathies

Although sonography is usually normal in glomerular diseases, acute glomerulonephritis and thrombotic microangiopathies can appear as cortical enlargement and increased cortical echogenicity.[30,31,37,38] When taken in the context of chronic renal failure, even a normal cortical thickness is suggestive of glomerular disease (diabetic nephropathy) because other disorders usually lead to cortical thinning.[39] The cortex is typically normal in membranous nephropathy or immunoglobulin A (IgA) nephropathy.[30,31,40] In severe glomerulonephritis, the kidney may take a rounded shape and echogenic appearance that is barely recognizable as a kidney (Fig. 10.7). Enlarged, echogenic kidneys can also be seen in HIV nephropathy,[41,42] amyloidosis, and preeclampsia.[43]

Tubulointerstitial Disease

Acute interstitial nephritis produces enlarged echogenic kidneys[30,44,45] that have the same appearance as glomerulonephritic kidneys. Chronic interstitial nephritis, particularly analgesic nephropathy (Fig. 10.8), presents with hyperechoic medullary pyramids, often with cortical atrophy.[31,46,47] At a more advanced stage, papillary necrosis and calcifications may be seen.[47–50] Medullary echogenicity can also be increased by uric acid deposition and nephrocalcinosis (Fig. 10.9), sickle hemoglobinopathies, Sjögren syndrome, and chronic hypokalemia.[51] Although acute pyelonephritis rarely produces renal failure, chronic pyelonephritis may cause chronic kidney disease and present with focal cortical scarring and thinning of the cortex often accompanied by caliectasis (Fig. 10.10). Xanthogranulomatous pyelonephritis may lead to enlarged, cystic appearing kidneys.[52,53]

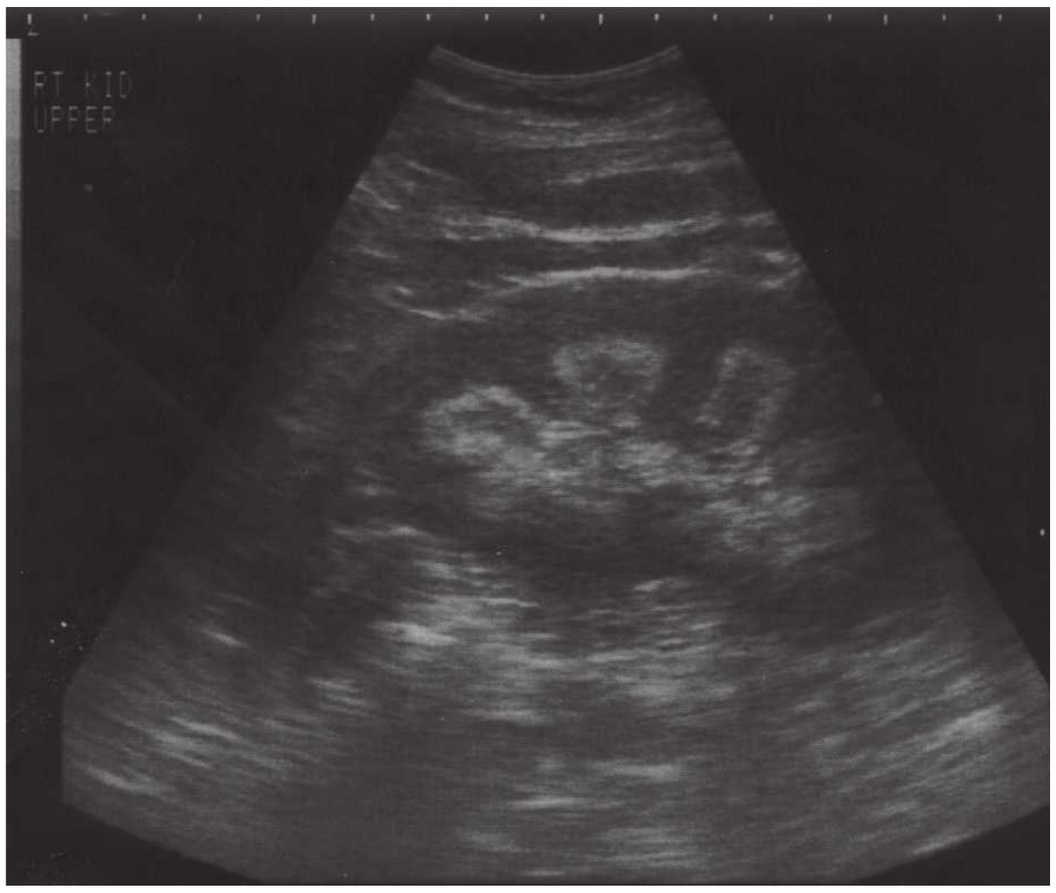

FIGURE 10.8 Analgesic nephropathy. Longitudinal view of the right kidney showing hyperechoic pyramids with relative sparing of the central portions.

Renal atrophy is usually the consequence of long standing renal disease or congenital defects, and presents as small kidneys with a thin cortex and accentuated lobulations (Fig. 10.11). The presence of renal atrophy does not provide any information on the underlying renal pathology but usually indicates that a renal biopsy will be uninformative.

Cysts

Cysts are fluid-filled structures with an epithelial lining usually originating from renal tubules. The typical sonographic features of cysts (anechoic structures with distal enhancement) make them very easily discernible by ultrasonography. The most common type of cyst is a sporadic acquired cyst, which can be present without any kidney disease. Cysts can be simple (Fig. 10.12) or complex (Fig. 10.13), with

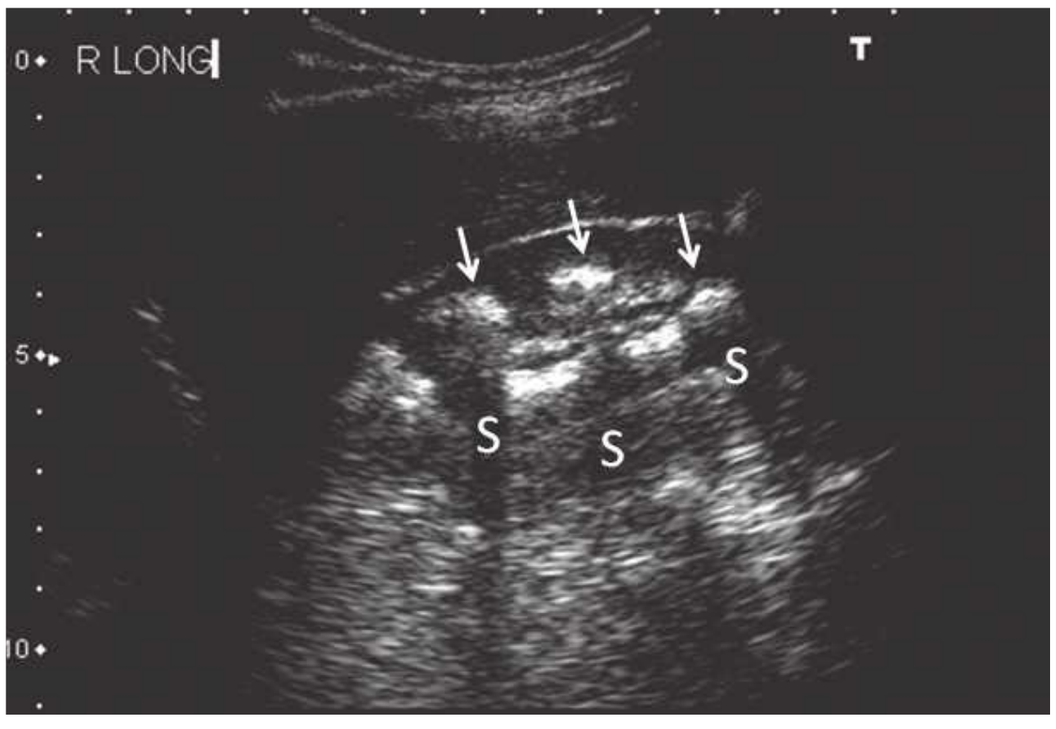

FIGURE 10.9 Nephrocalcinosis. Longitudinal image of the right kidney showing multiple calcifications in the inner medullae (*arrows*) producing acoustic shadows (*S*).

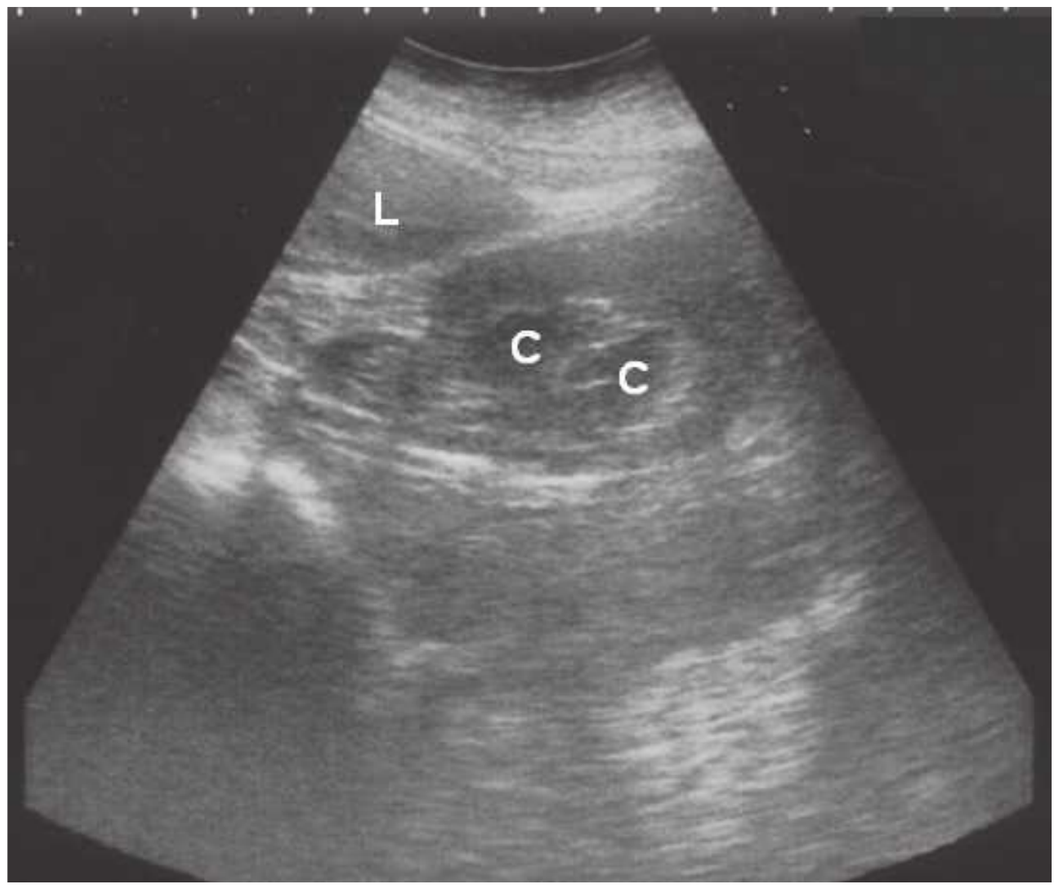

FIGURE 10.10 Chronic pyelonephritis. Longitudinal view of the right kidney shows caliectasis of the lower pole (*C*), and loss of parenchyma with scarring of the upper pole (*arrows*). *L*, liver.

the criteria for complexity including thickening of the wall, calcifications, more than two septations, and luminal echogenicity. Even though the great majority of complex cysts are benign, any complex cyst should be closely followed up with ultrasound or additional imaging studies (computed tomography [CT] and magnetic resonance imaging [MRI]), given the possibility of cystic renal cell carcinomas.[54]

Acquired cystic kidney disease (ACKD) and autosomal dominant polycystic kidney disease (ADPKD) are the most common types of multicystic renal disease. ACKD is often encountered in patients with advanced chronic kidney disease (CKD) or end-stage renal disease (ESRD). Cysts are

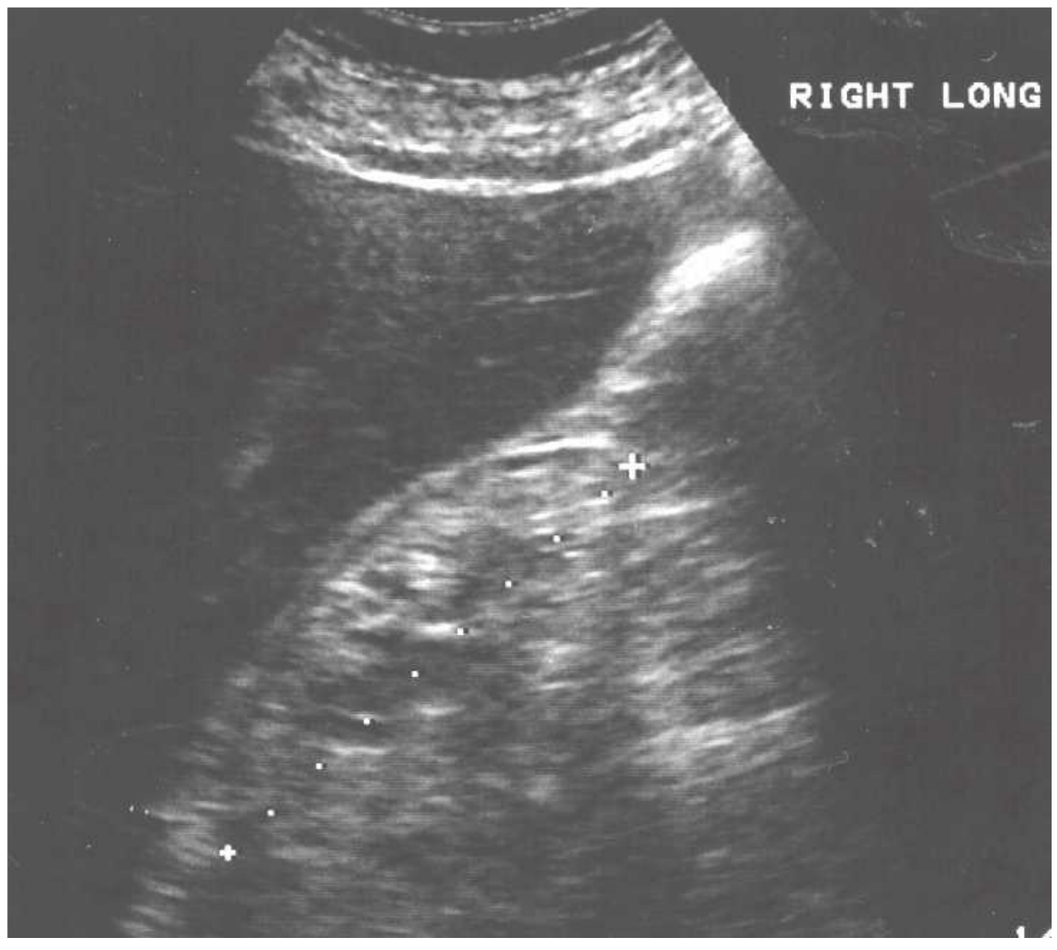

FIGURE 10.11 Renal atrophy. Longitudinal image of the right kidney showing a small kidney with a thin and hyperechoic cortex.

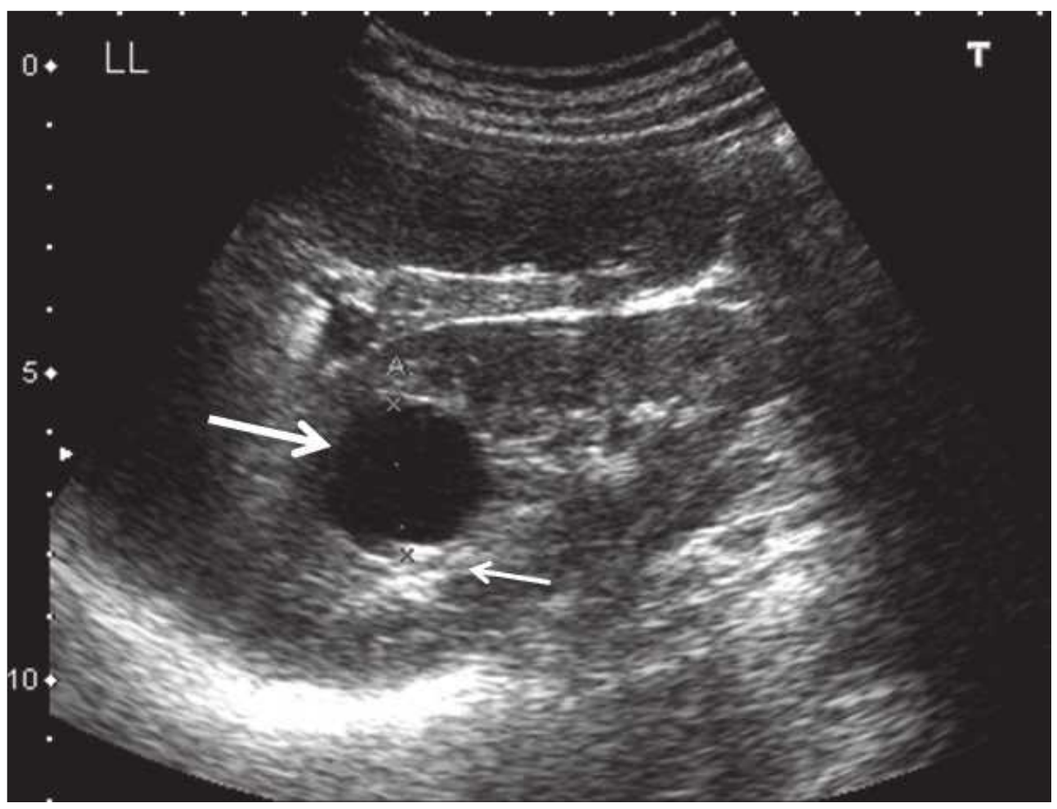

FIGURE 10.12 Simple cyst. Longitudinal image of the left kidney showing a round hypoechoic structure (*large arrow*) in the lower pole, which presents with distal acoustic enhancement (*small arrows*), consistent with a simple cyst.

typically of smaller size and the kidney is usually echogenic and small[55] (Fig. 10.14). ADPKD is the most common inherited cause of renal failure, and sonography is the cornerstone of diagnosis using specific criteria established by Ravine et al.[56] The performance of these criteria was found to be suboptimal in the PKD-2 genotype and revised unified criteria have recently been published by an international group of investigators (Table 10.1).[57]

The pathognomonic sonographic appearance of ADPKD includes presence of multiple bilateral renal cysts (Fig. 10.15) and liver cysts (in 83%–90% of patients)[58] with

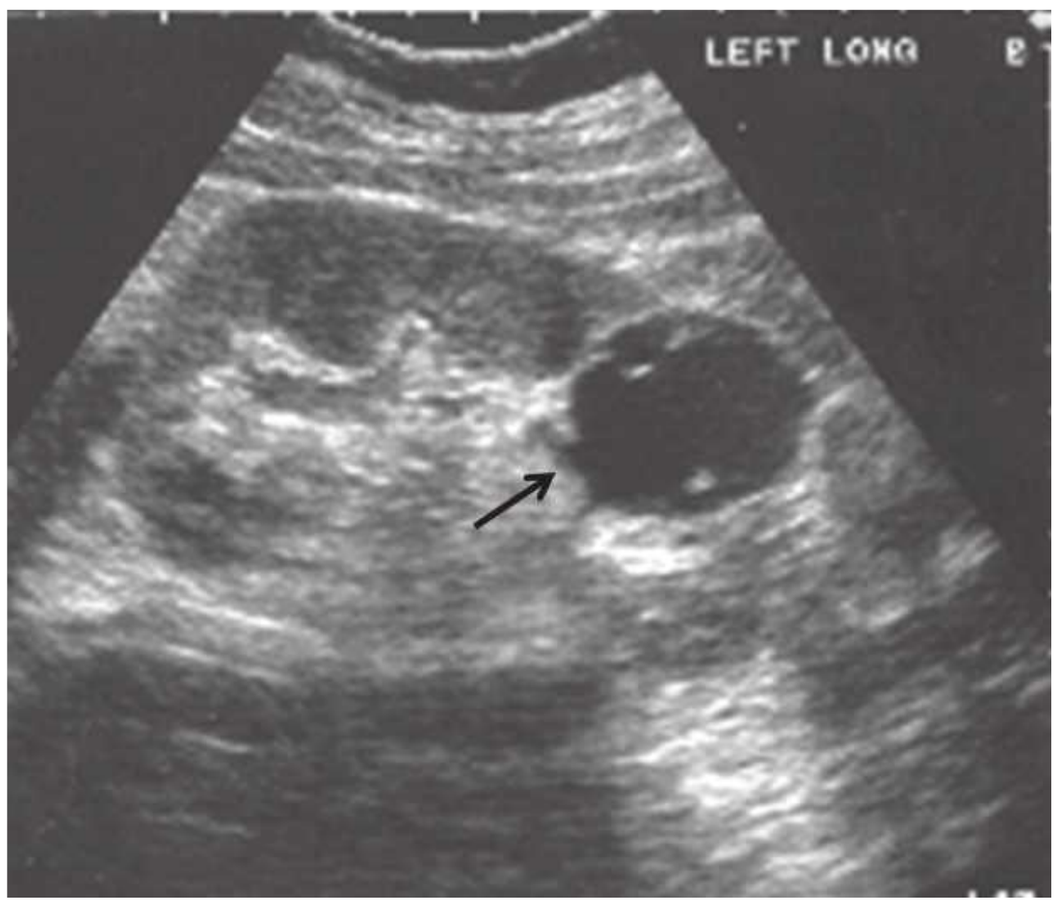

FIGURE 10.13 Complex cyst. Longitudinal view of the left kidney shows a cyst with an irregular wall (*black arrow*) and several internal echoes.

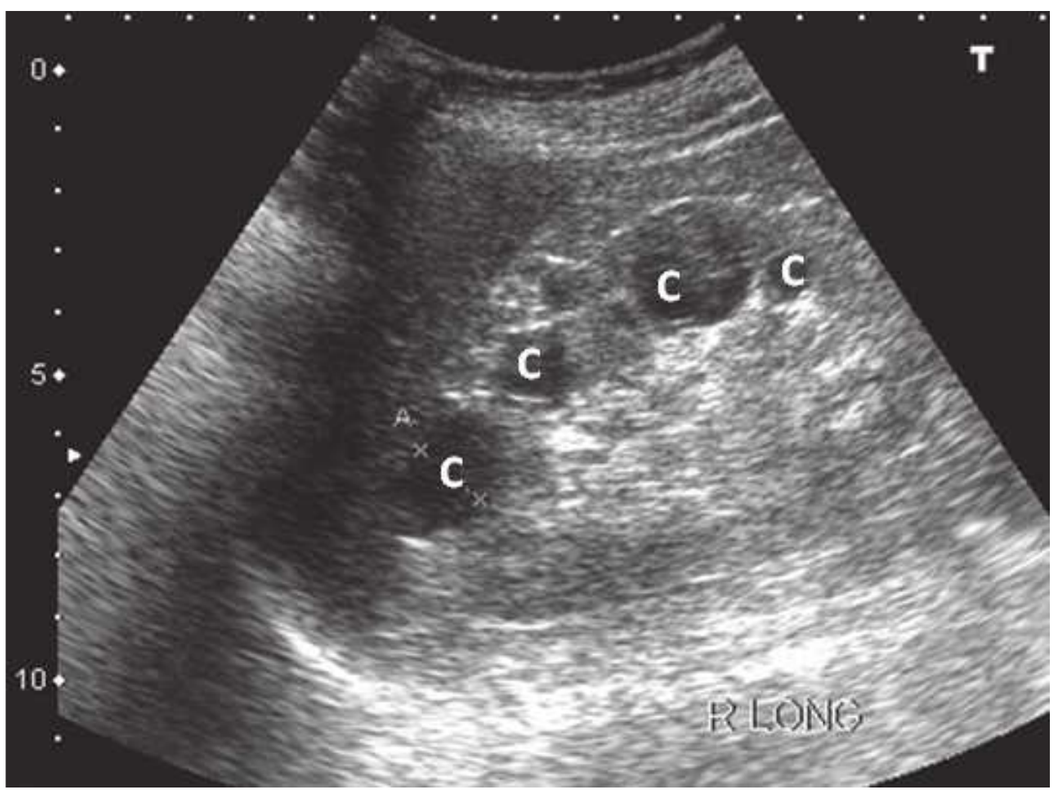

FIGURE 10.14 Acquired cystic kidney disease. Longitudinal view of the right kidney showing multiple cysts (*c*) with an intervening echogenic cortex.

significant renal enlargement. Other multicystic diseases such as medullary cystic kidney disease (MCKD), juvenile nephronophthisis, ACKD, or medullary sponge kidney[59,60] do not present with renomegaly. Multiple cysts with renal enlargement can be seen in von Hippel-Lindau disease, tuberous sclerosis, and multicystic dysplastic disease. Complex cysts are also commonly seen in ADPKD and the main etiologies are intracystic hemorrhage and infection. Even though renal cell carcinoma can be seen in this ADPKD, these patients are not at increased risk.[61]

Urinary Obstruction

Urinary obstruction typically results in hydronephrosis: a dilatation of the collecting system which may be predominantly seen in the minor calyces, the major calyces, or both. More atypical cases may present with minimal dilatation of the collecting system, particularly in the acute setting.[62] Hydronephrosis is only an anatomic diagnosis and may not indicate urinary obstruction. Brisk diuresis (such as in diabetes insipidus), papillary necrosis, and pregnancy can all result in nonobstructive calyceal dilatation.[28,62–64] Grading systems for severity of the hydronephrosis have proven to be of limited clinical utility because the degree of hydronephrosis may correlate poorly with the extent of obstruction. When obstruction is the primary cause of renal failure, it is always associated with hydronephrosis. In acute obstruction, the cortex is intact (Fig. 10.16) whereas chronic obstruction can lead to marked thinning of the cortex (Fig. 10.17). Failure to visualize the proximal ureter suggests obstruction at the ureteropelvic junction, whereas a dilated proximal ureter (hydroureter) (Fig. 10.16) indicates either obstruction at the level of the ureter or bladder. A large postvoid bladder indicates urinary retention, where sometimes the distal ureters can also be visualized (Fig. 10.18), whereas an empty bladder with dilatation of the distal ureters suggests obstruction

10.1 Performance Characteristics of Ultrasonographic Diagnostic Criteria for Autosomal Dominant Polycystic Kidney Disease in At-Risk Individuals Without Information on Genotype

Age Group (years)	Diagnostic Criterion	NPV	PPV	Accuracy
15–29	≥1 renal cyst	0.908	0.966	0.934
	≥2 renal cysts	0.877	0.992	0.924
	≥3 renal cysts	0.855	1.0	0.912
30–39	≥2 renal cysts in each kidney	0.875	1.0	0.922
	≥1 renal cyst	0.983	0.94	0.962
	≥2 renal cysts	0.97	0.979	0.974
	≥3 renal cysts	0.964	1.0	0.984
40–59	≥2 renal cysts in each kidney	0.948	1.0	0.965
	≥1 renal cyst	1.0	0.897	0.960
	≥2 renal cysts	1.0	0.967	0.988
	≥3 renal cysts	0.984	0.965	0.978

NPV, negative predictive value; PPV, positive predictive value.

Adapted from Pei Y, Obaji J, Dupuis A, et al. Unified criteria for the ultrasonographic diagnosis of ADPKD. J Am Soc Nephrol. 2009;19:205–212, with permission.

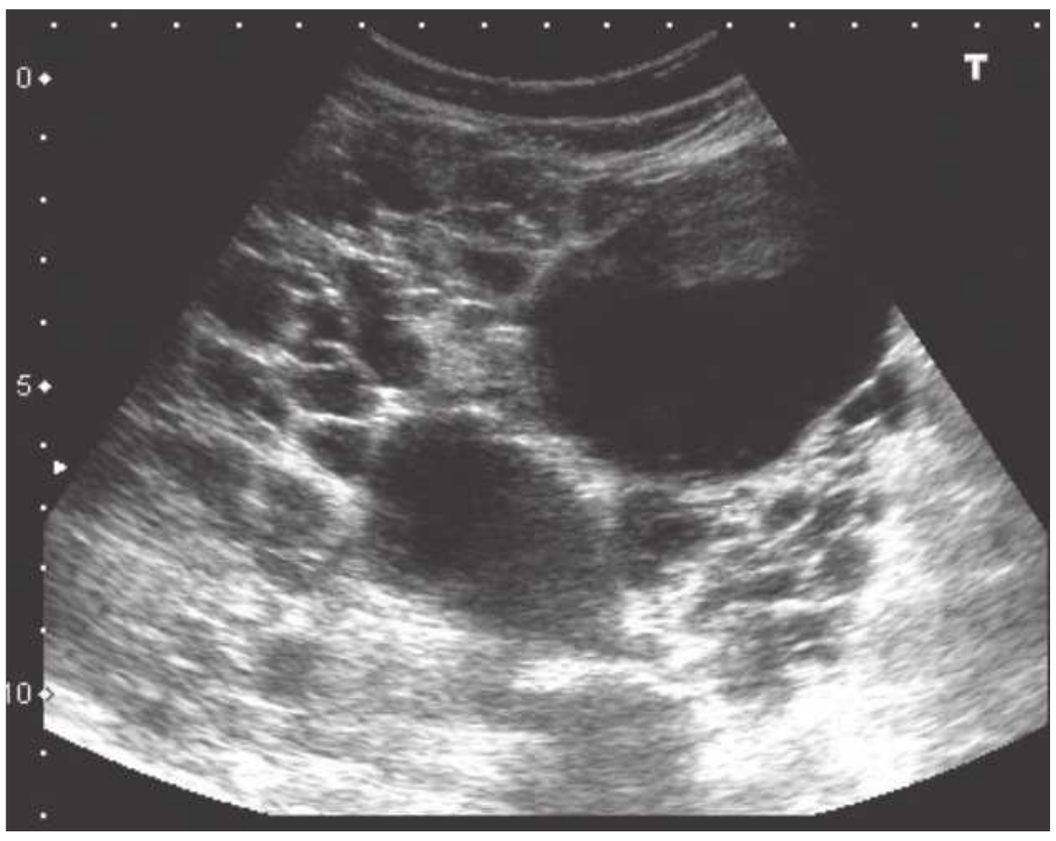

FIGURE 10.15 Autosomal dominant polycystic kidney disease. Longitudinal view of the right kidney showing an enlarged kidney with numerous cysts (hypoechoic structures) of different sizes.

at the bladder inlet. Recognition of hydronephrosis can be difficult in polycystic kidney disease (PKD), where massive cyst formation can prevent or obscure calyceal dilatation and more subtle signs should be sought (Fig. 10.19). This is an important cause of acute renal failure and can be due to stones or blood clots from cyst rupture. Radioisotope scanning may confirm obstruction when sonographic findings are not characteristic.

Occasionally, peripelvic cysts may also mimic hydronephrosis (Fig. 10.20). These are actually dilated lymphatics and, because they track with the blood vessels, can sometimes have a branching pattern. A rim of sinus fat separating the "cysts" from the parenchyma and the absence of a dilated ureter are useful hints toward peripelvic cysts. Another differential diagnosis for hydronephrosis is venous engorgement often seen in cases of volume overload or renal vein thrombosis. In general, the renal vein branches before entering the renal sinus (bush appearance) whereas the collecting system branches in the sinus (pruned tree appearance). The presence of venous pulsations and the tracking of the vein medially to the vena cava, as well as the

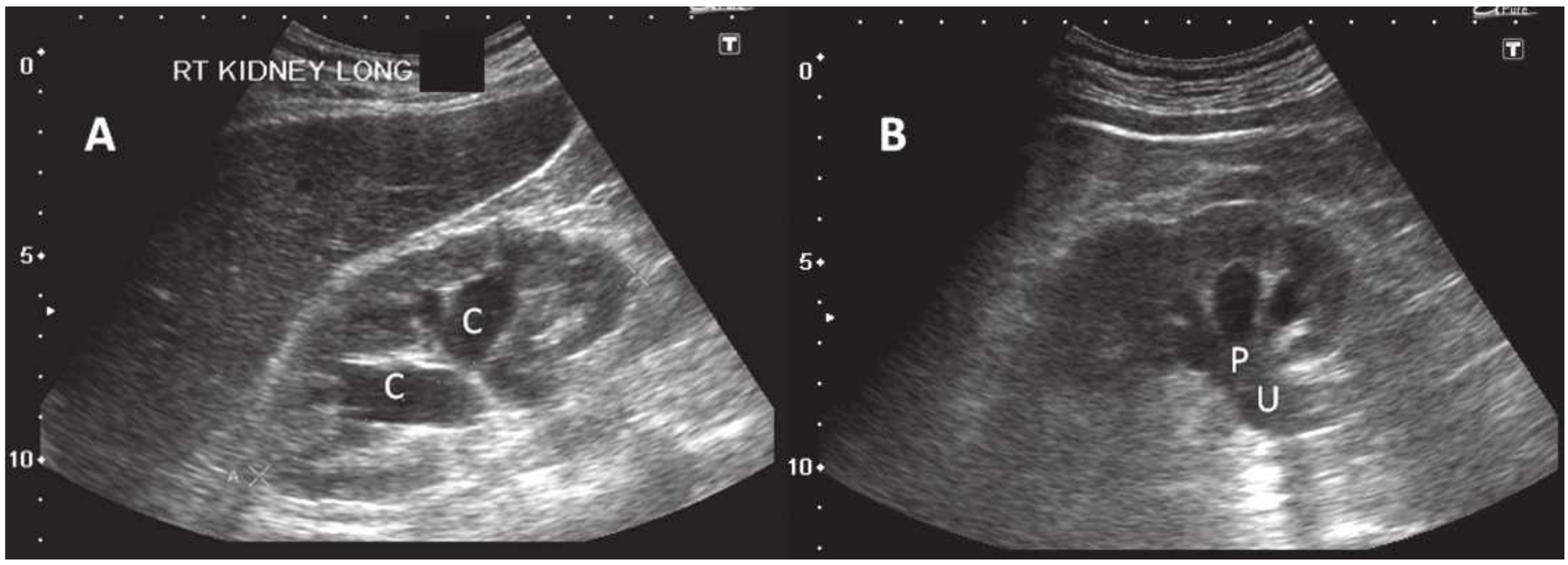

FIGURE 10.16 Acute hydronephrosis with hydroureter. Longitudinal image of the right kidney showing dilatation primarily of the major calyces (*C*) with some enlargement of the minor calyces and with conserved parenchymal thickness. The dilatation of the pelvis (*P*) and ureter (*U*) is easily visualized.

use of Doppler sonography, can differentiate blood vessels from the urinary tract. Occasionally, the renal pelvis is situated outside the sinus (extrarenal pelvis) appearing as a dilated proximal ureter but without any calyceal enlargement (Fig. 10.21).

The urinary bladder should be carefully examined by sonography in all patients with hydronephrosis. Additional indications are anuria, hematuria, pain, and urinary tract infections. The bladder is located in the midline, posterior to the symphysis pubis, and contains no luminal structures. When full, it appears as an anechoic fluid collection that is oval in transverse plane and becomes more elongated in the sagittal plane. The bladder volume is calculated by using the following formula for ellipsoid structures[65]:

$$\text{Volume} = 0.523 \times \text{length} \times \text{width} \times \text{depth}$$

A normal bladder is usually empty after a complete void and should not contain more than 10 mL of urine. A postvoid residual volume of more than 50 mL is associated with a threefold risk of urinary retention in males and is often used as a threshold for the diagnosis of urinary retention.[66] Hyperechoic structures such as stents, Foley catheters, bladder stones (Fig. 10.22), tumors, and blood

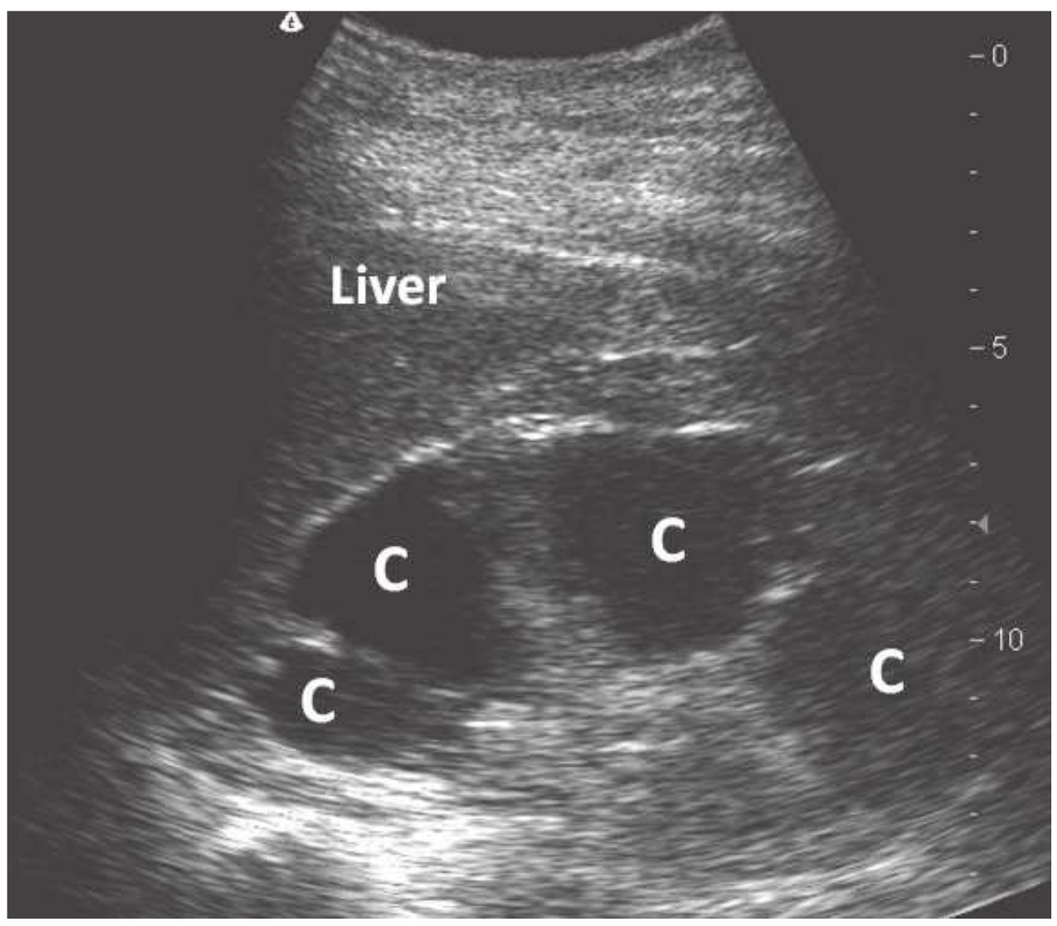

FIGURE 10.17 Chronic hydronephrosis. Longitudinal view of the right kidney showing dilated calyces that extend to the renal capsule, indicative of an extremely thin cortex.

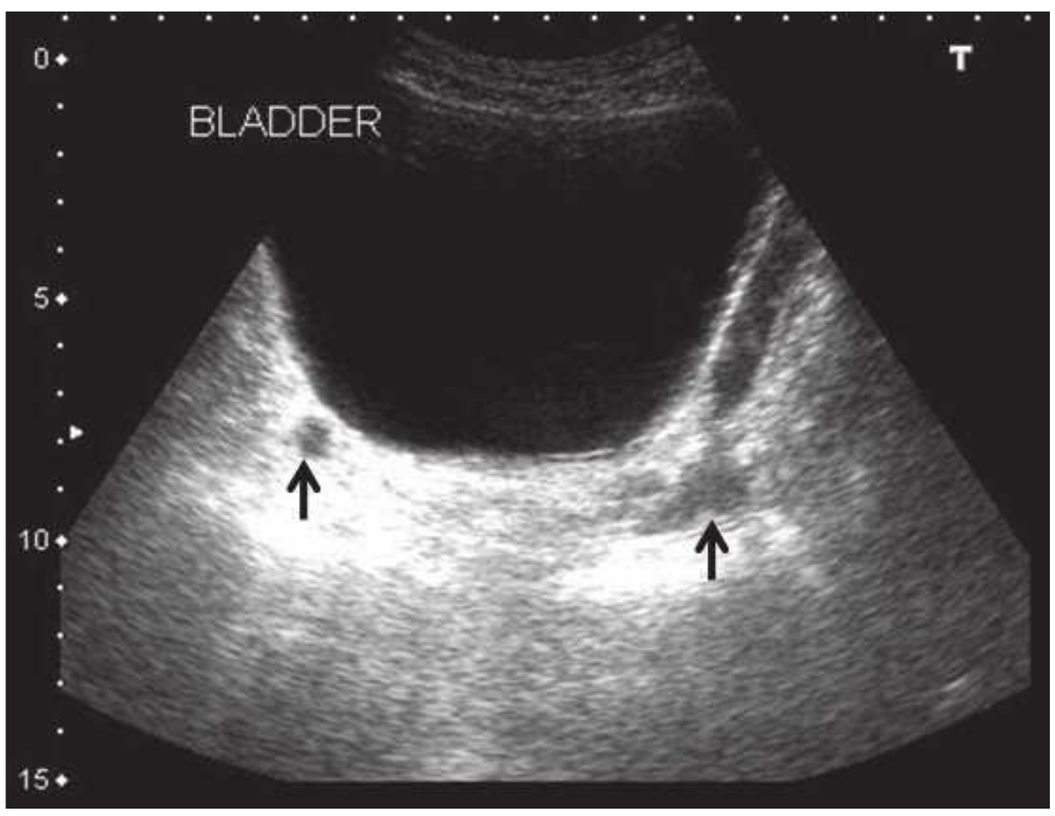

FIGURE 10.18 Urinary bladder retention. Transverse view showing an extremely dilated bladder. The distal ureters (*arrows*) are visible posterior to the bladder.

FIGURE 10.19 Hydronephrosis in autosomal dominant polycystic kidney disease. Converging dilated calyces (*C*) are apparent in this young patient who presented with major hemorrhagic cyst rupture and acute renal failure due to ureteral clots. Hydronephrosis resolved after ureteral stent placement. The multitude of cysts and disruption of the normal anatomy often make detection of hydronephrosis difficult.

clots (Fig. 10.23) may be visible in the bladder. The presence of urinary jets from a ureter proves its patency. Ureteral stents may transmit bladder pressure back to the kidney, resulting in hydronephrosis. Thus, the diagnosis of stent obstruction requires an empty bladder.

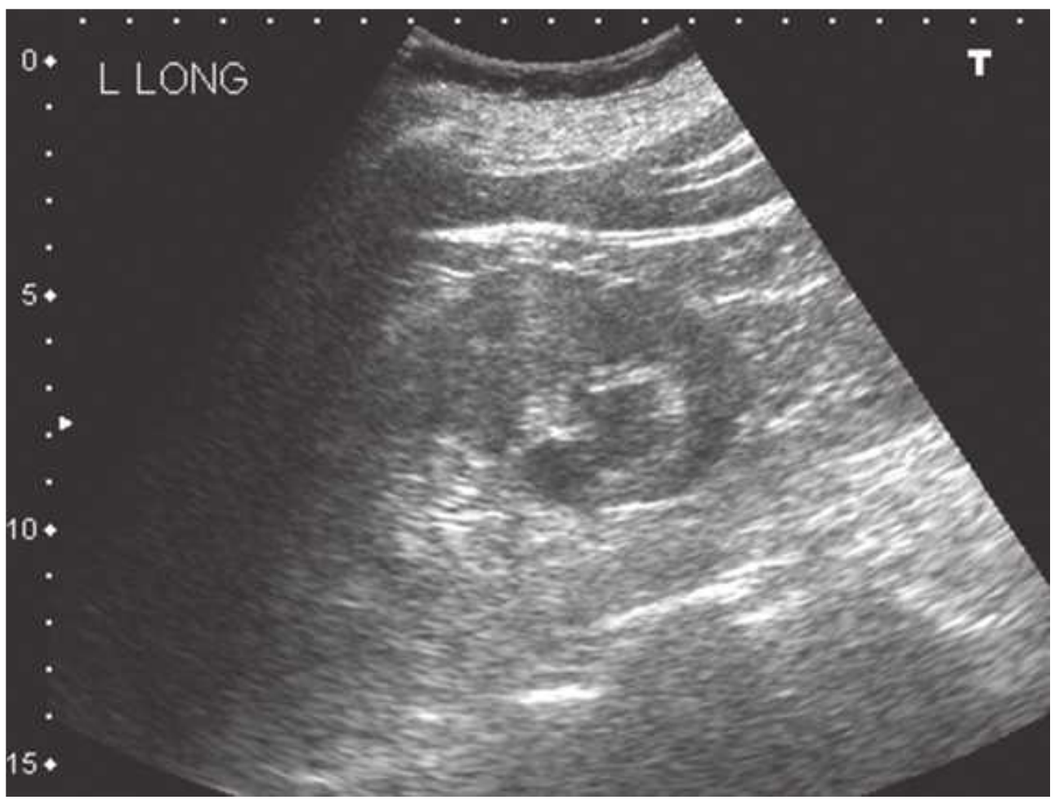

FIGURE 10.20 Peripelvic cyst. Longitudinal view of the left kidney showing a hypoechoic structure where the renal pelvis is expected to be seen. The absence of calyceal dilatation and presence of the echogenic sinus fat interposed between the cyst and the parenchyma are indicative of peripelvic cysts rather than hydronephrosis.

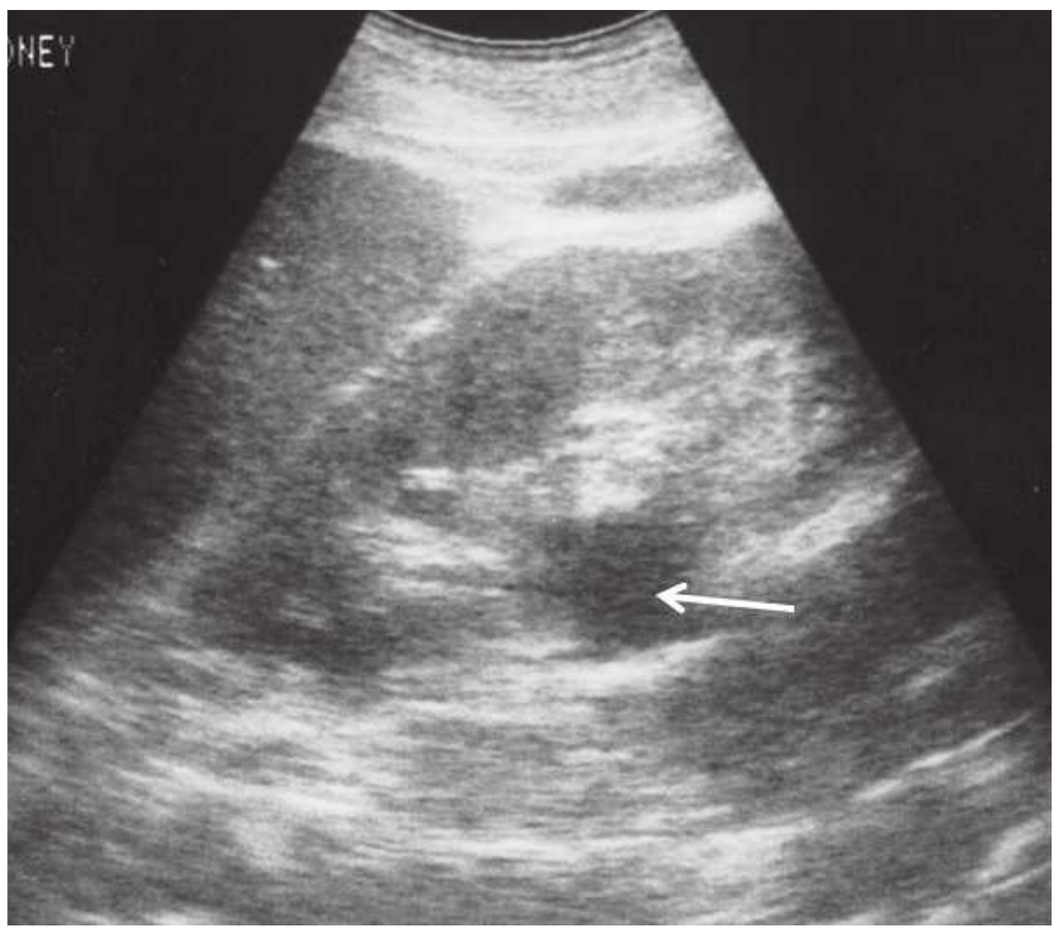

FIGURE 10.21 Extrarenal pelvis. Longitudinal view of the left kidney. There is apparent dilatation of the initial proximal ureter with no further hydroureter. Although the major calyces can be seen converging into the extrarenal renal pelvis, there is no enlargement of the minor calyces.

Kidney Stones and Calcifications

Stones typically reflect most of the sound, rendering them echogenic with a distal shadow and very easily discernible by ultrasonography no matter what the composition. However, both findings may not be present and small kidney stones

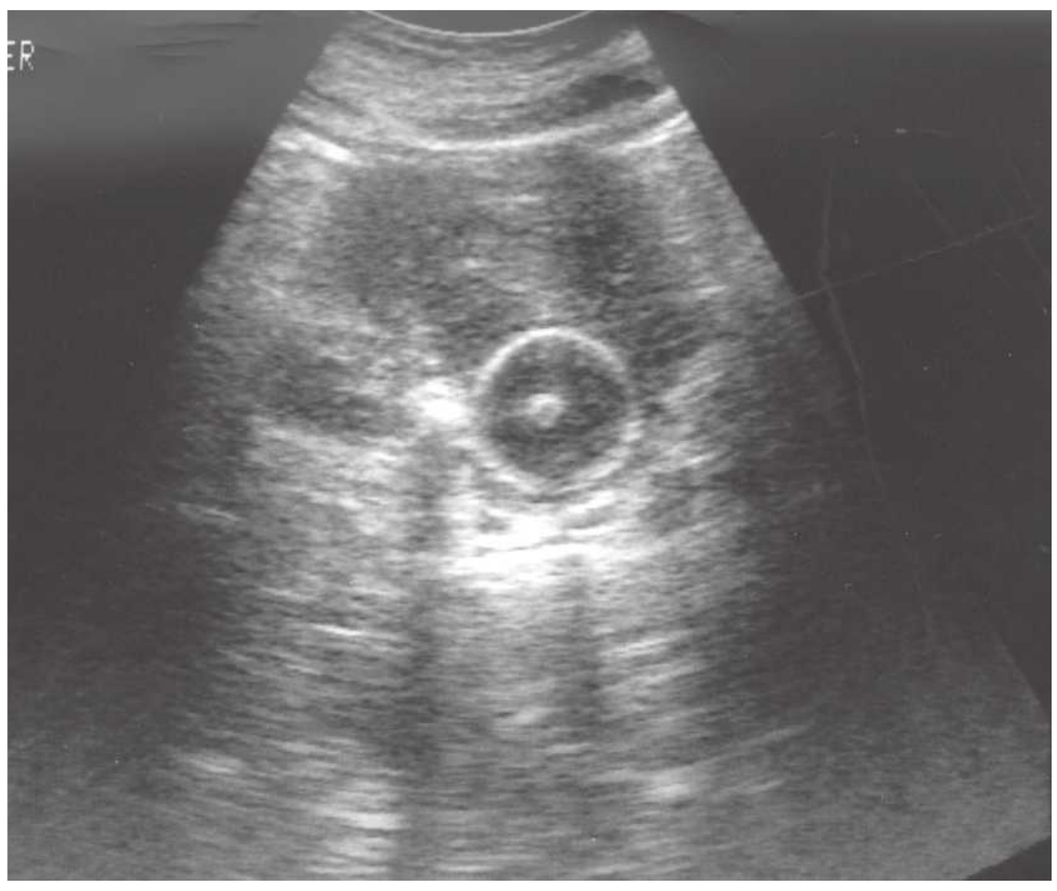

FIGURE 10.22 Foley catheter and bladder stone. Transverse view of the bladder shows a perfectly round shaped circle with echogenic walls (inflated balloon) surrounding the central echogenic catheter. Adjacent to the left side of the Foley catheter, a small opacity with a posterior shadow represents a bladder stone.

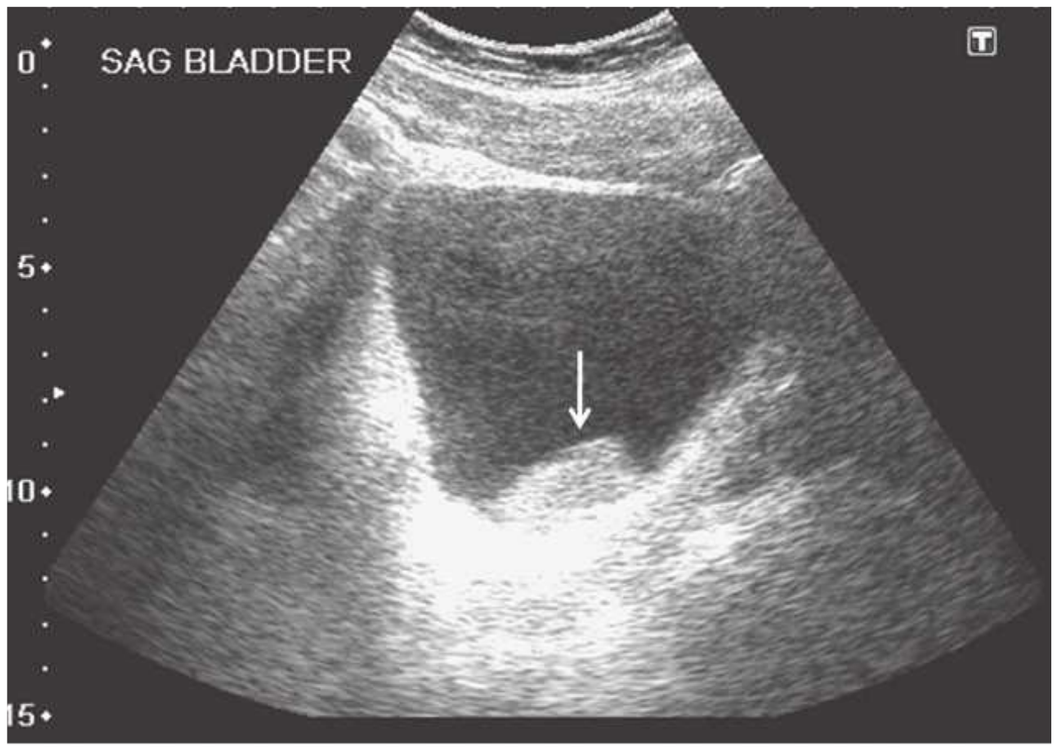

FIGURE 10.23 Clot in the bladder. Sagittal view of a distended bladder containing a hyperechoic mass, representing a blood clot (*arrow*).

and ureteral stones may not be visible. Stones are seen in the urinary space (Fig. 10.24) and may be associated with urinary obstruction, hydronephrosis, and urinary tract infection. Staghorn calculi typically fill the entire calyceal system but can appear as multiple stones on single images (Fig. 10.25).

In nephrocalcinosis (Fig. 10.9) and papillary necrosis, the calcification is in the renal medulla and not the urinary space but this distinction can sometimes be difficult. The differential diagnosis also includes ureteral stents, which typically are not as echogenic and yield less distinct shadows.

Neoplasms

Renal neoplasms are usually discovered incidentally or during the workup for pain or hematuria. Special attention

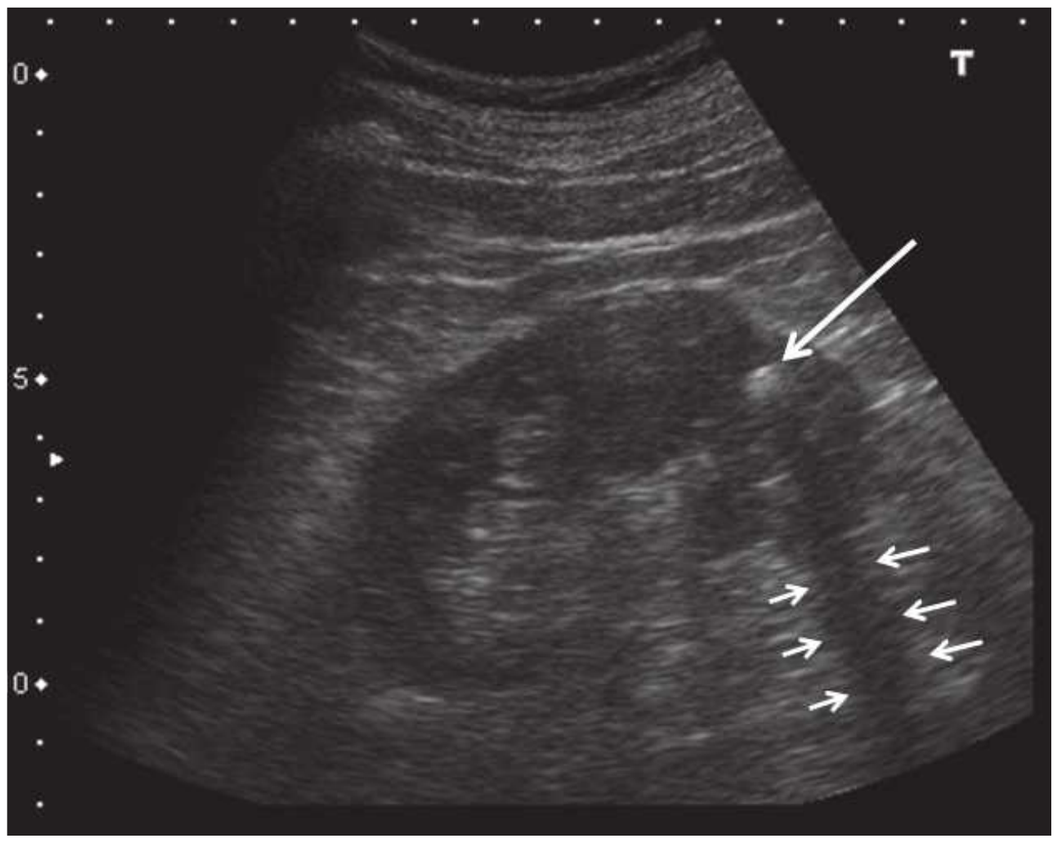

FIGURE 10.24 Kidney stone. Longitudinal view showing a hyperechoic stone (*large arrow*) in the lower pole that casts an acoustic shadow (*small arrows*).

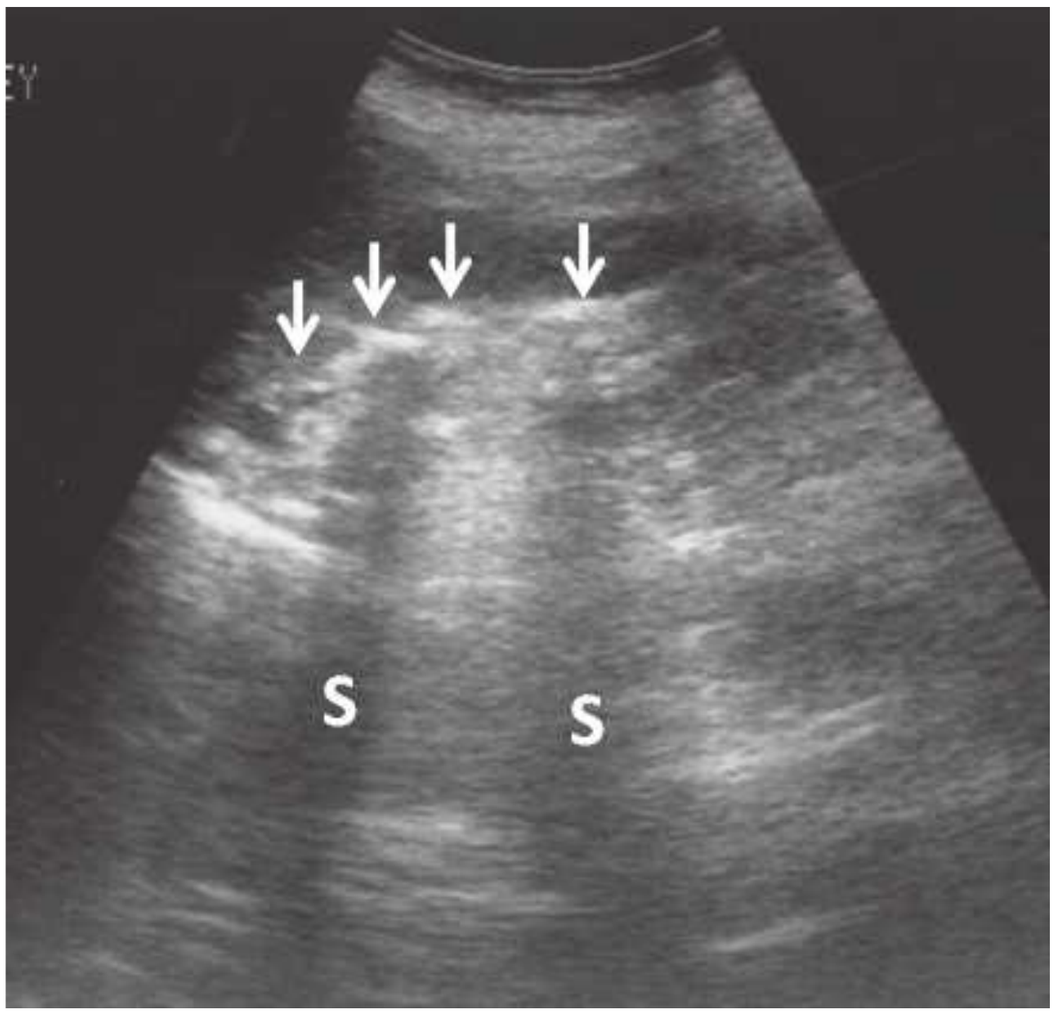

FIGURE 10.25 Staghorn calculus. Longitudinal image of the right kidney showing a long curvilinear echogenicity in the renal sinus with dense acoustic shadows (*S*).

should be given to rule out cysts, transmission artifacts, and normal variants such as lobulation and hypertrophied columns of Bertin.[67] Although the absence of blood flow by Doppler ultrasound may point to a cyst, additional imaging is almost always indicated because sonography can rarely identify the cause of a solid lesion.

Renal Cell Carcinoma

The typical sonographic appearance of renal cell carcinoma is of a well-demarcated hypoechoic mass that distorts the renal contour (Fig. 10.26), but tumors can be isoechoic (and more difficult to visualize) and can be hyperechoic when small (<3 cm). About 10% of renal cell carcinomas have a cystic appearance.[68]

Transitional cell carcinoma is a tumor of the renal pelvis that typically presents as a relatively hypoechoic mass within the renal sinus, separated from parenchyma by fat tissue.[69–71] They can also contain echogenic areas and occasionally can be diffusely infiltrative.

Angiomyolipoma

Sporadic angiomyolipomas (AMLs) are the most commonly encountered tumors in kidneys (autopsy incidence of 11%, more commonly seen in middle-aged women)[72] but multiple AMLs can be observed in tuberous sclerosis. They are not malignant but may cause hemorrhage. The typical presentation is of a very echogenic parenchymal mass (due to the high fat content) with an acoustic shadow in 33% of cases[73] (Fig. 10.27).

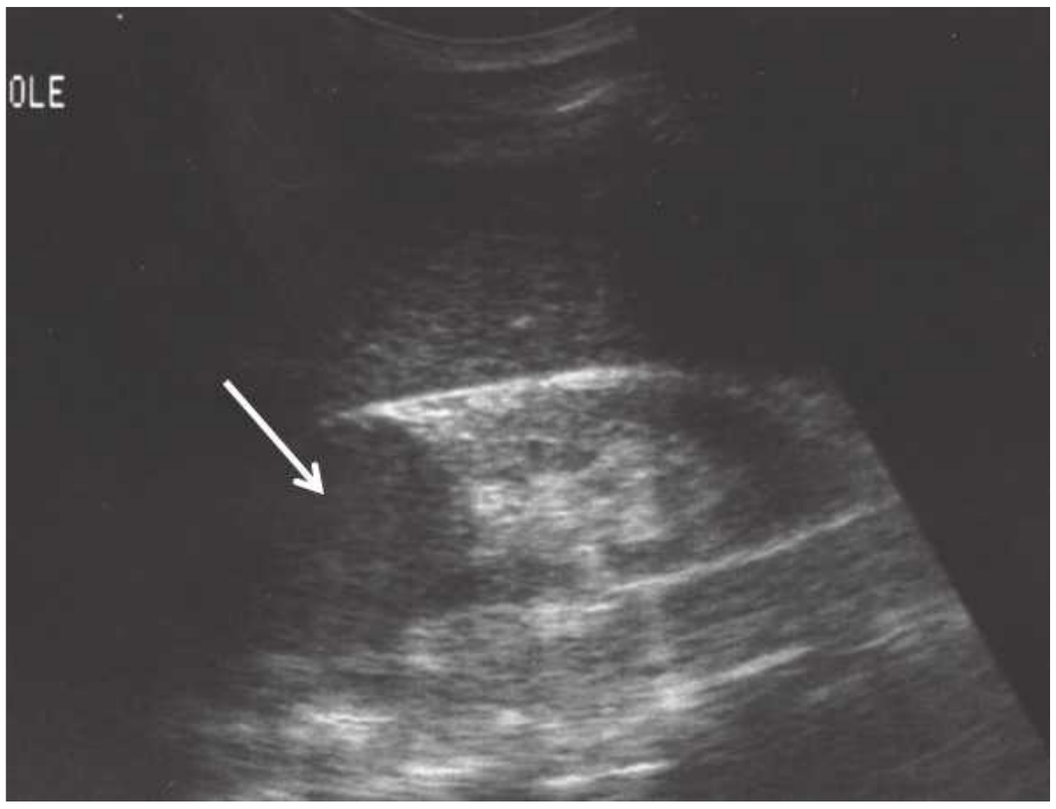

FIGURE 10.26. Renal cell carcinoma. Longitudinal view of the left kidney shows a hypoechoic mass (*arrow*) in the upper pole which was confirmed to be a renal cell carcinoma.

FIGURE 10.27 Angiomyolipoma. Longitudinal view of the left kidney shows a small, brightly echogenic mass in the cortex (*arrowhead*) without any distal shadowing.

Metastasis and Infiltrative Neoplastic Diseases

Infiltration of the kidneys is common in lymphomas (20% on CT scan,[74] 50% on autopsies[75]). They can cause acute renal failure by obstruction or diffuse infiltration.[76] The typical appearance is of multiple hypoechoic masses but a "perirenal halo" is also a classic but more unusual occurrence.[77] Leukemias can also infiltrate the kidney. Other solid tumors (e.g., lung cancer) may metastasize to the kidney, in which case they tend to be focal and nodular and are not distinguishable from other tumors.

Infections

Sonography is not indicated in most routine cases of pyelonephritis. Indications include male gender, children, failure to resolve, complications, and frequent recurrence. Pyelonephritis is usually lobular, appearing as a poorly defined hypoechoic area corresponding to a lobule, but it occasionally is diffuse. This can progress to abscesses which are usually single or multiple, heterogenous masses. The differential diagnosis includes complex cysts and neoplasms, which may require CT or MR for diagnosis.

Hemorrhage

Renal hemorrhage usually appears as perirenal or subcapsular hematomas and usually results from percutaneous kidney biopsy, surgery, or trauma. Initially they may appear as anechoic fluid collections but typically they are heterogeneous with fluid and solid components.

Transplanted Kidneys

Although many aspects of sonography are similar in native and transplanted kidneys, important differences exist due to anatomic considerations. The allograft is usually placed in the right pelvic fossa, aligned along the incision with the hilum oriented inferiorly and posteriorly, but a variety of other orientations can be encountered especially in obese patients, repeat transplantations, and combined kidney-pancreas transplantation. The donor artery and vein are anastomosed to the external iliac (or the common iliac) vessels and the ureter is anastomosed to the superolateral wall of the bladder (Fig. 10.28). When two kidneys are transplanted en bloc, portions of the donor aorta and vena cava are retained and anastomosed to the recipient vessels.[78,79] The kidney is often placed within the peritoneum when combined with a pancreas transplant. In very young children, the kidney may be placed posterior to the cecum with anastomosis of the donor vessels to the great vessels.[79] The anatomic relationships are readily apparent on sonograms. The psoas muscle and iliac vessels lie posteriorly and are usually imaged transversely on longitudinal scans of the allograft. The former can be identified by its contraction when the leg is flexed at the hip, and the latter are frequently pulsatile. The ureter and renal vessels are often visible even in normal allografts. The ureter courses medially, usually lying directly under the lower (medial) pole, whereas the renal vein travels posteriorly. The bladder lies medially and can easily be mistaken for a perirenal fluid collection. The peritoneum is superior and occasionally anterior to the allograft, typically appearing as a

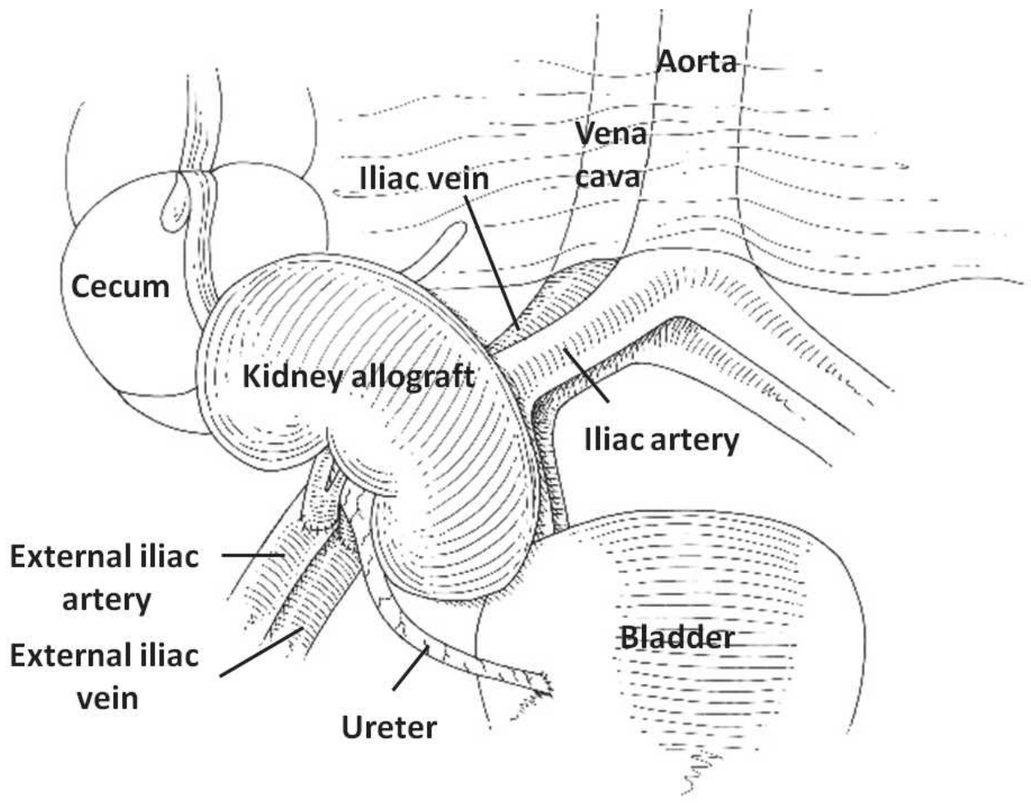

FIGURE 10.28 Anatomic relationships of the kidney. (Adapted from O'Neill WC. *Atlas of Renal Ultrasonography*. Philadelphia: WB Saunders; 2011, with permission.)

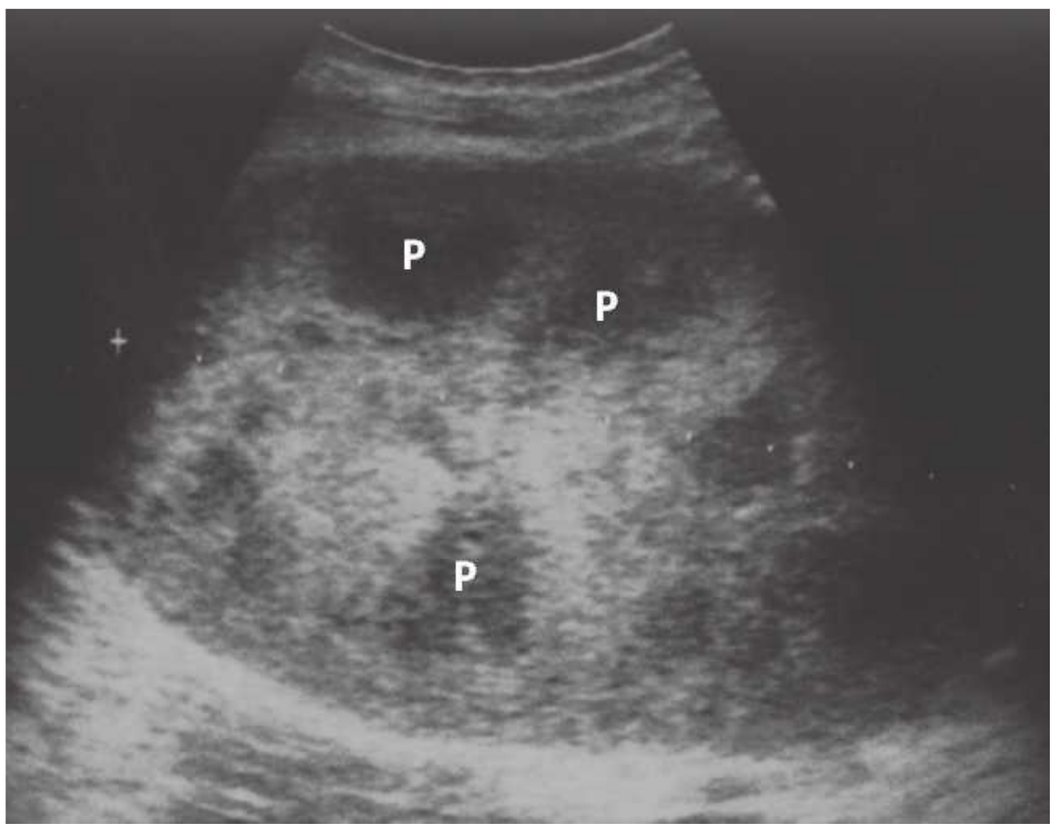

FIGURE 10.29 Acute rejection, longitudinal scan. The kidney is swollen and globular and the cortex is brightly echogenic, rendering medullary pyramids (*P*) very prominent.

beaklike projection over the allograft, and is easily identified by the peristalsis of the bowel loops.

Sonography of the transplanted kidney is indicated in most cases of acute renal failure[80] and can easily diagnose thrombosis of the renal artery or vein, urinary obstruction, and urine leaks in the immediate postoperative period. Other, nonspecific findings can suggest acute rejection. Sonography can be helpful in guiding percutaneous biopsy, diagnosing fluid collections, measuring residual bladder volume, and identifying ureteral stents.

Allograft Parenchymal Disease

The visualization of renal allografts is easier than native kidneys but suffers from the inability to evaluate two important parameters: renal size and echogenicity. Measurement of renal length is problematic due to the frequent inability to capture the entire length of the kidney in one view and the uncertainty of its significance due to both donor-dependent and recipient-dependent variables. Renal size can increase up to 40% during the 6 first months after transplantation.[81–83] Evaluation of echogenicity is difficult due to the lack of an adjacent reference organ. The only useful clues are prominence of the medullary pyramids and, when echogenicity is markedly increased, blending of the allograft with the surrounding tissue. Because of these limitations and also the simplicity of allograft kidney biopsy, size and echogenicity are usually not considered in clinical decisions.

The most common causes of allograft failure are acute tubular necrosis (related to harvesting or storage), acute rejection, drug toxicity, chronic allograft nephropathy, and recurrent disease, but sonographic findings lack sensitivity and specificity in diagnosing any of these. In particular, kidneys often appear normal in mild and even moderate cases of rejection. When present, findings consist of cortical swelling and increased echogenicity (due to cellular infiltration). Allograft enlargement is fairly specific for acute rejection[83–90] but can occur with ATN and recurrent nephritis (Fig. 10.29). Infections (pyelonephritis and BK virus) can also cause allograft failure but sonographic findings are nonspecific.

Urinary Obstruction of the Allograft

The frequent occurrence of urinary tract obstruction is the principal reason for performing sonography in most transplant patients presenting with acute renal failure. In the immediate postoperative period, the ureter may be obstructed by intraluminal blood clots, kinking, or external compression by edema or hematomas. Urinary retention, lymphoceles, and ureteral strictures are responsible for most other cases,[91,92] but are rarely seen when ureteral stents are routinely placed during transplantation. Acute rejection within the ureter may also obstruct urine flow.[93,94] Ultrasonography is an excellent test to diagnose obstruction in allografts with a sensitivity of almost 100%.[95] Specificity is lower because hydronephrosis is not always an indication of obstruction because small degrees of calyceal dilatation are easily and commonly seen in otherwise normal allografts. Mild, and even moderate, dilatation may not be a manifestation of urinary obstruction,[92,96] but dilatation of the minor calyces and ureter are usually indicative of obstruction (Fig. 10.30). Sonography is also very useful in pinpointing the site of obstruction. Hydronephrosis without dilatation of the proximal ureter indicates obstruction at the ureteropelvic junction, which may be caused by extrinsic compression by a lymphocele or ureteral strictures.[97] In both cases, there is usually abrupt tapering of the renal pelvis. A common site for strictures is in the distal segment or near the anastomosis

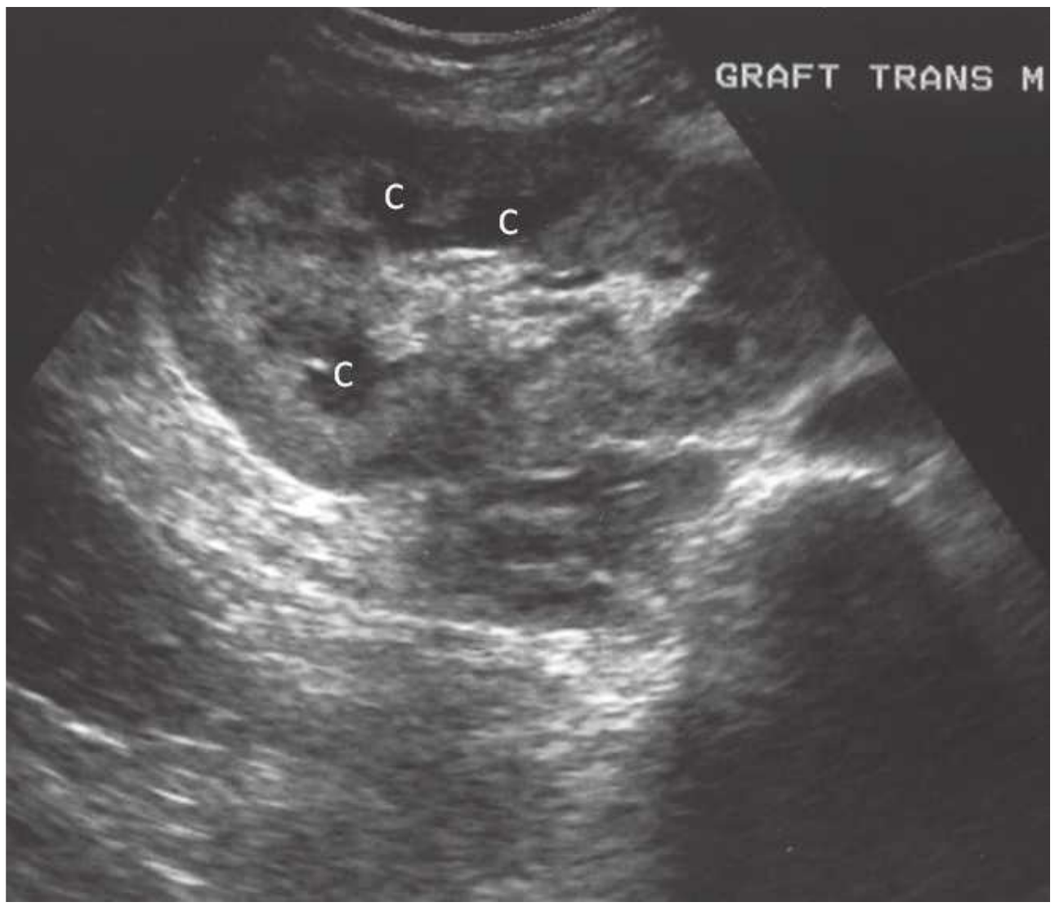

FIGURE 10.30 Mild hydronephrosis of the allograft kidney. Transverse view of the allograft shows mild dilatation of the calyces (*C*), consistent with mild hydronephrosis.

with the bladder.[91,97] In this setting the dilated ureter can be followed to the bladder and remains dilated when the bladder is emptied.

Thickening of the calyceal or ureteral walls is not uncommon and can be mistaken for luminal dilatation. This is usually caused by edema (Fig. 10.31) and has a fine echo pattern as opposed to anechoic urine. A fine central line presumably representing apposition of the luminal surfaces is occasionally seen.[98] Edema is frequently associated with stents and may also be caused by ureteral rejection.[93] Calyceal thickening was initially thought to be a sign of acute rejection but is now known to be nonspecific.[99,100] Additional causes of echogenicity within the collecting system are stents, hemorrhage, stones, and infection.

Fluid Collections and the Kidney Allograft

Fluid collections consisting of blood, urine, or lymph can be complications of transplant surgery.[95] Sonography cannot distinguish different types of fluid but the location, shape, internal structure, and the clinical presentation can all help in making the correct diagnosis. Additional studies such as examination of aspirated fluid and pyelography or radionuclide scanning to detect extravasation of urine may be needed. Care must be taken to distinguish fluid collections from the bladder or ascites.

Lymphoceles are the most common fluid collections encountered near renal allografts, with a frequency as high as 20%.[91,101] Half occur in the first 10 months after surgery but they can occur as late as 4 years.[101] They are usually not diagnosed unless they compress the ureter or the iliac vein and spontaneous resolution is a common feature.[101] In general, two types of lymphoceles are observed, consistent with different origins.[91,92,101] Most commonly they arise from donor lymphatics and are seen immediately adjacent to the allograft and have a propensity to obstruct the proximal ureter. They often appear as triangular-shaped fluid collections adjacent to the normal pelvis (Fig. 10.32) but can attain any shape and even surround the allograft when large. Less commonly, lymphoceles arise from native lymphatics disrupted during anastomosis of the donor vessels. They are in proximity to the iliac vein and have a tendency to obstruct the venous drainage of the leg, producing ipsilateral edema.[92,102]

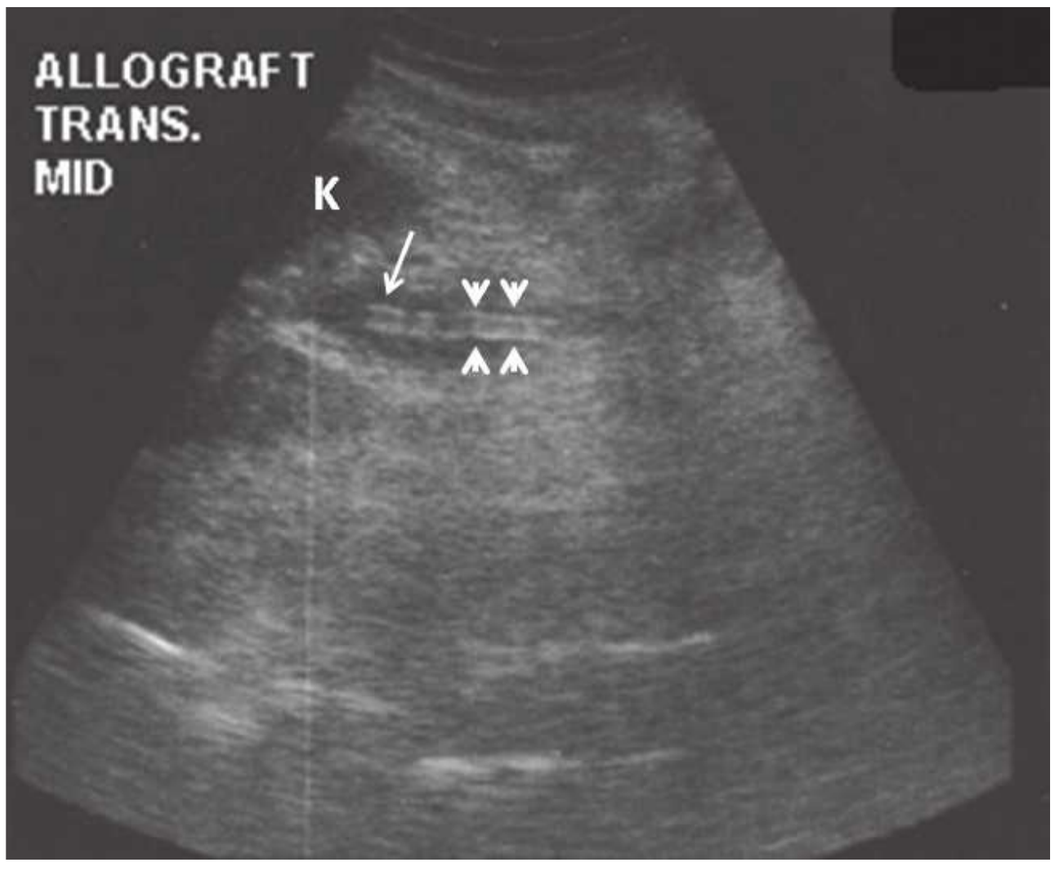

FIGURE 10.31 Urinary leak and ureteral stent. Transverse view of the allograft kidney (*K*) shows a small urine leak (*arrow*) surrounding a ureteral stent (*arrowheads*), medial to the allograft.

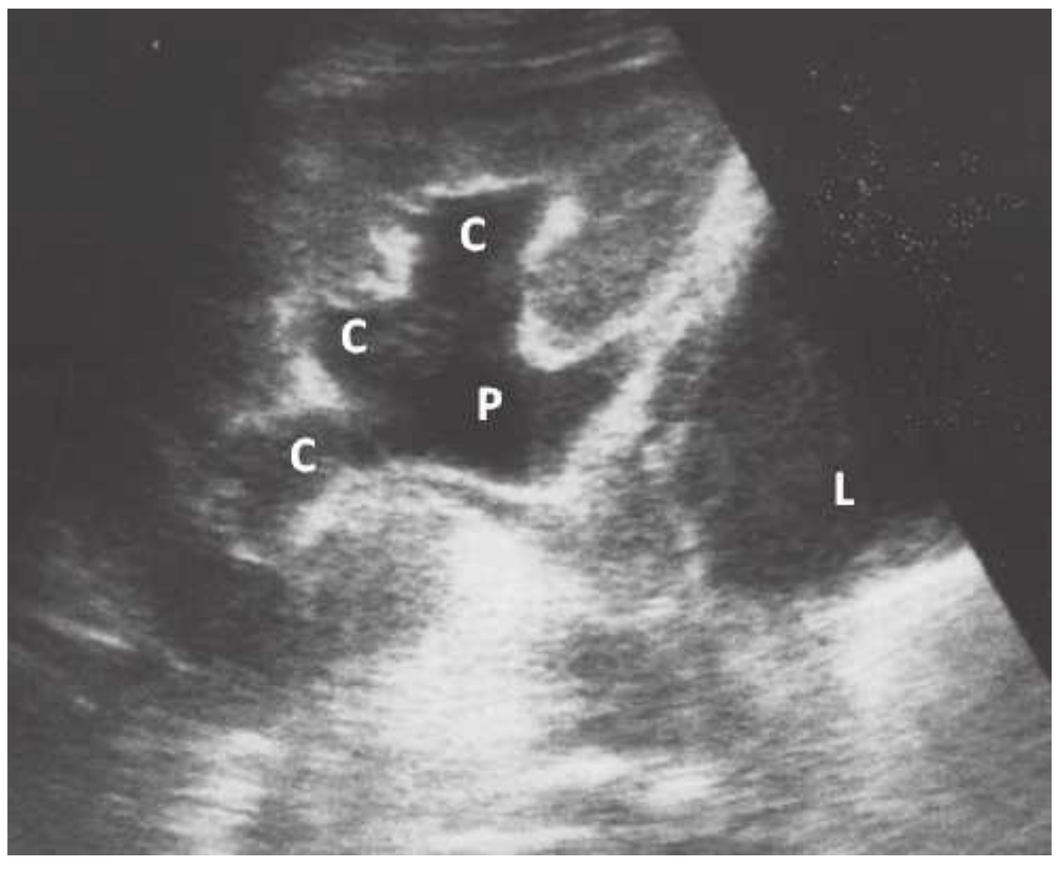

FIGURE 10.32 Large lymphocele with hydronephrosis. The lymphocele (*L*) presents as a hypoechoic collection medially situated vis-à-vis the allograft and causing obstruction of the ureter resulting in dilatation of calyces (*C*) and renal pelvis (*P*).

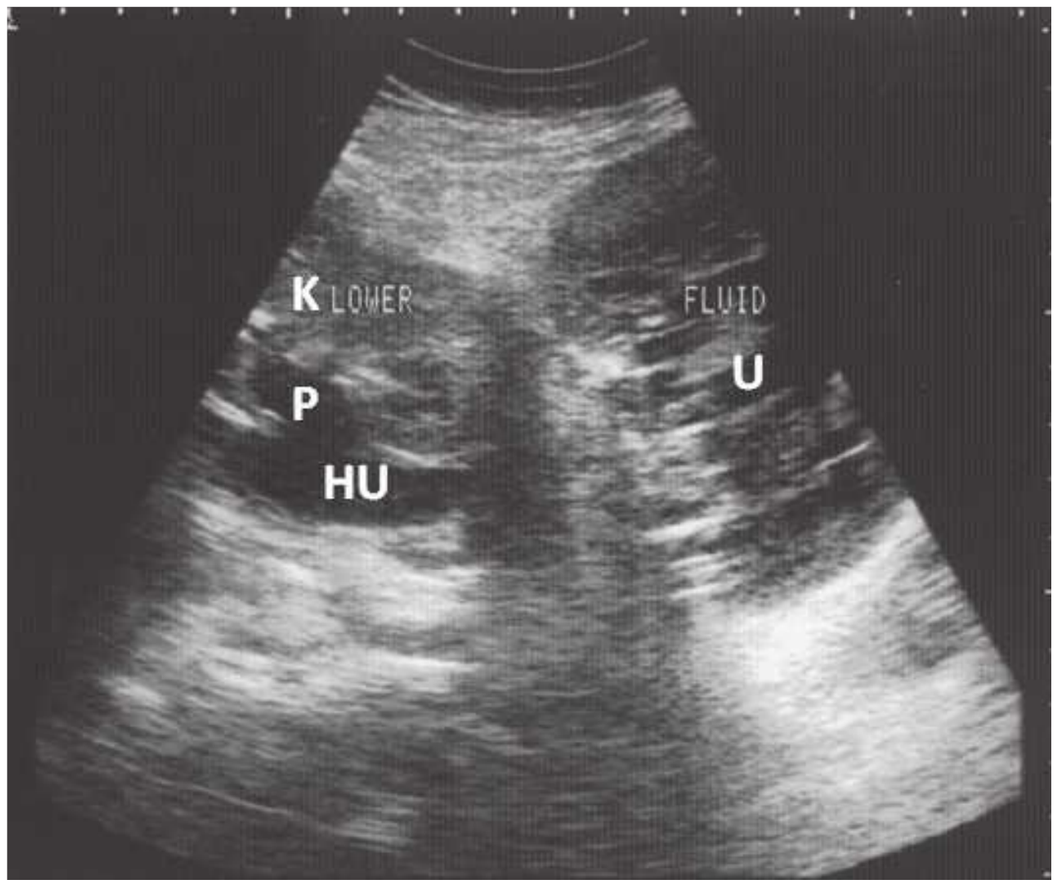

FIGURE 10.33 Large urinoma, longitudinal scan. The urinoma (*U*) appears as a large, complex fluid collection medial to the allograft (*K*). Hydroureter (*HU*) and renal pelvis dilatation (*P*) are common with urine leaks.

FIGURE 10.34 Seroma (*S*) appears as a complex fluid collection containing echogenic material in the subcutaneous tissue anterior to the allograft (*K*).

Urinomas, arising from urine leaks, need to be considered when fluid collections are seen within several weeks after surgery.[91] Tenderness and fever occur in one half and one quarter of patients, respectively,[103] but acute renal failure or delayed graft function can also be seen. Urinomas are usually adjacent to the ureter, but they can dissect along tissue planes and form seemingly separate collections, usually medial or anterior to the allograft and even surrounding it (Fig. 10.33). The appearance can be identical to that of a lymphocele, but often the margins are irregular and indistinct. Dilatation of the collecting system proximal to the leak is common.[102,103]

Hematomas are commonly seen in sonograms performed in the first few weeks after transplantation[91,92] but can also be seen after percutaneous biopsy. The typical appearance is of a heterogeneous mass containing both liquid (anechoic) and solid (echogenic) components. Echogenicity may increase with the level of organization of the clot.

Seromas are related fluid collections that are extremely common in the immediate postoperative period. These serosanguineous collections usually follow tissue planes anterior to the allograft and thus appear linear, often with septations (Fig. 10.34). They generally have little clinical significance and resolve spontaneously, and are important only in the differential diagnosis of other types of fluid collections.

Doppler Ultrasonography of the Kidneys

Doppler ultrasound measures the shift in frequency when sound strikes a moving object. This shift is dependent on the angle of the sound beam relative to the direction of flow, so that it is maximal when the sound is parallel to the flow and absent when the sound is perpendicular. In practice, the scanning angle should ideally be no greater than 60 degrees because large errors in velocity occur above this. This becomes critically important in evaluating the renal artery. The Doppler signal can be displayed in several formats. A small region can be selected (e.g., the lumen of a blood vessel) and velocity versus time displayed as a graph (pulse wave Doppler). Alternatively, a larger region can be selected and the velocities displayed on a color scale superimposed on the B-mode image (color flow Doppler). These modes can be combined (duplex Doppler). Lastly, the signal can be displayed in a vectorless form (power Doppler) where the color scale indicates the speed but not the direction. This last mode is useful for demonstrating the presence or absence of flow, and has the advantage of being less dependent on the angle of insonation.

In the kidney, Doppler sonography is used primarily to determine whether masses are vascular and to diagnose vascular disorders, particularly renal artery stenosis. The main renal artery and vein branch into segmental (also called interlobular) vessels at the renal hilum, which is located just outside of the medial aspect of the mid kidney. The segmental vessels travel through the renal sinus directly to the parenchyma, usually without further branching. They course through the columns of Bertin between the medullary pyramids, branching into the arcuate vessels at the corticomedullary junction. Evaluation of the renal vasculature usually consists of two separate examinations: (1) direct visualization and measurement of velocity in the renal artery or vein; and (2) analysis of wave forms in intrarenal arteries.

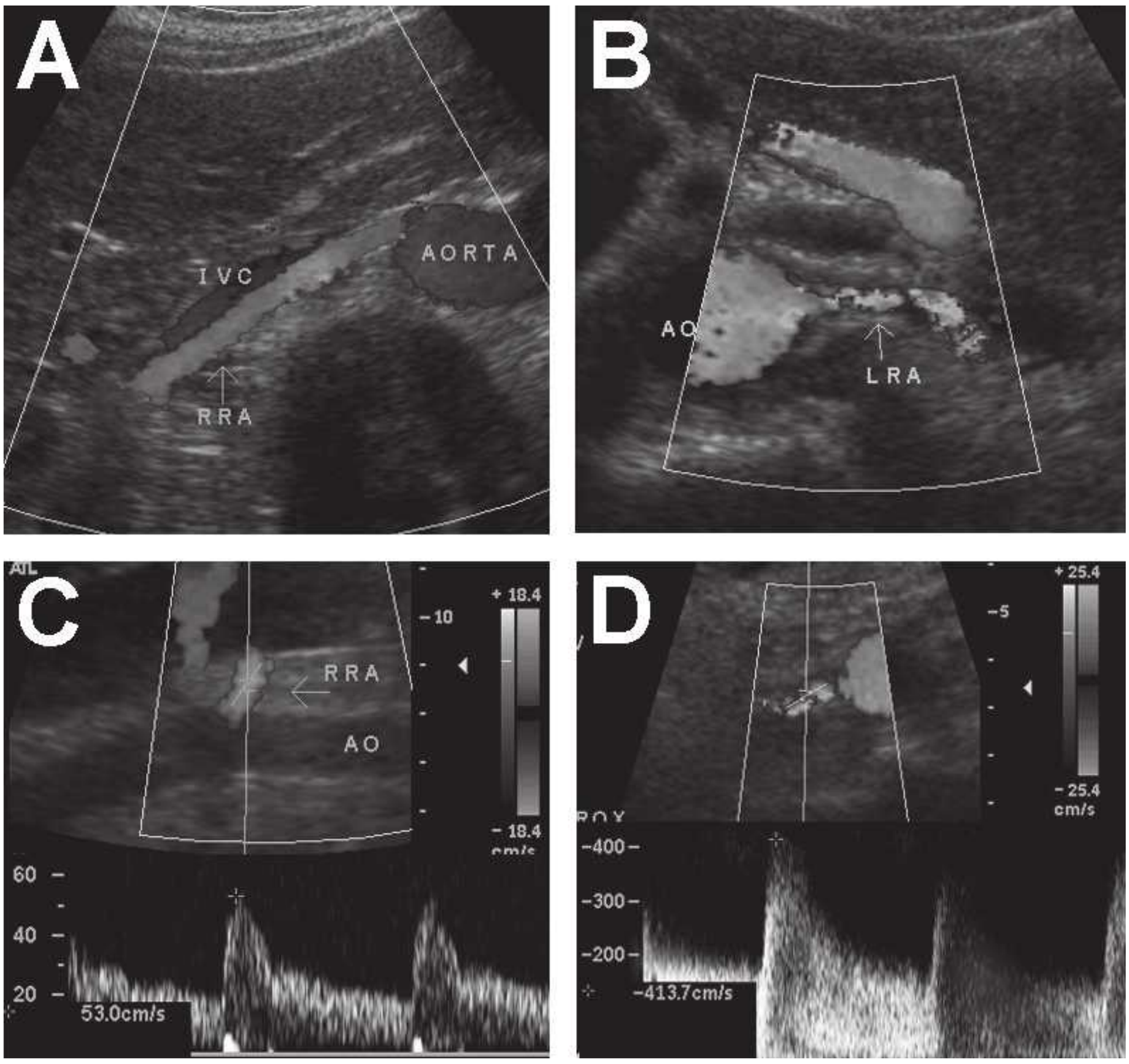

FIGURE 10.35 Renal artery Doppler. **A:** Normal right renal artery, midline transverse image. **B:** Stenotic left renal artery, midline transverse image. Note the turbulent flow (speckled color pattern) and the poststenotic dilatation. **C:** Normal right renal artery, coronal view, with a peak systolic velocity of 53 m per second. **D:** Stenotic right renal artery, midline transverse view. The peak systolic velocity averages well over 300 m per second. (Images courtesy of Sue Zellman, RDMS, RVT.)

Renal Artery Doppler

Examination of the renal artery is usually performed to rule out stenosis but should be reserved for patients with a high index of suspicion due to the poor performance of Doppler ultrasound. This can be a challenging examination in many patients because of overlying bowel gas, difficulty in achieving an angle less than 60 degrees, and the presence of multiple renal arteries in 30% of individuals. As many as a third of examinations may be inadequate.[104] The artery is examined by color flow Doppler from the aorta to the renal hilum, looking for narrowing, poststenotic dilatation, and turbulent, high velocity flow (Fig. 10.35). The diagnosis of significant renal artery stenosis is suggested by peak blood velocities greater than 2.0 meters per second (Fig. 10.36), and/or a ratio of peak systolic velocities in the renal artery and aorta above 3.5.

Intrarenal Arteries

Examination of the intrarenal arteries (segmental or interlobular) is limited to analysis of the waveforms, which can provide information on blood flow in the larger vessels. In renal artery stenosis, systolic flow can be dampened, leading to a delay in the peak flow (Fig. 10.36). In renal vein thrombosis, increased distal resistance can reduce diastolic flow. There may even be reversal of diastolic flow, which is virtually pathognomonic for renal vein thrombosis. Because most waveform analysis is based on indices (one portion of the wave compared to another) or on time, rather than on absolute velocity, it is independent of the angle of insonation. It is therefore a far easier study to perform but the evidence obtained is indirect.

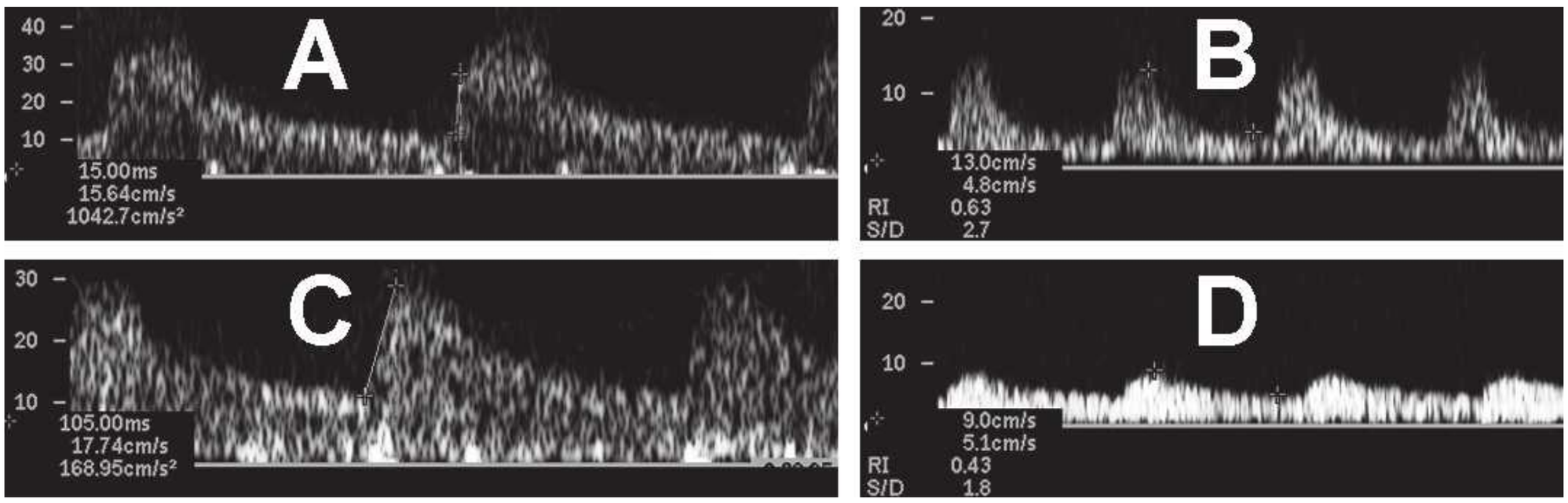

FIGURE 10.36 Intrarenal Doppler waveforms. **A:** Normal segmental artery with maximum systolic acceleration of approximately 1000 m per sec^2. **B:** Normal intraparenchymal artery. **C:** Segmental artery with maximum systolic acceleration less than 200 m per sec^2, indicative of renal artery stenosis. **D:** Intraparenchymal artery showing marked delay and blunting (tardus-parvus) of the systolic peak consistent with severe renal artery stenosis. (Images courtesy of Sue Zellman, RDMS, RVT.)

Renal Artery Stenosis

A number of Doppler parameters have been applied to the diagnosis of renal artery stenosis including direct measurements and indices of velocity and acceleration, indices of resistance and pulsatility, or combinations of these.[105] Although good results have been published using renal artery Doppler as a screening test for renal artery stenosis, a large meta-analysis showed that CT angiography and MR angiography performed significantly better.[106]

Parenchymal Disease

Much attention has been focused on duplex Doppler as a diagnostic tool for renal disease but the findings are nonspecific. Resistive index has been proposed as a parameter to predict outcomes after revascularization of stenotic kidneys,[107] but this approach is flawed because the resistive index is influenced by systemic parameters such as heart rate and pulse wave velocity.[108,109] Doppler indices are of no utility in the diagnosis of acute rejection in transplanted kidneys.[110,111]

Renal Vein Doppler

The main renal veins are often visible in adults and can be prominent in children or young adults, in patients with heart failure, and in inflamed kidneys. The right renal vein tracks directly from the inferior vena cava to the right kidney whereas the left renal vein has a longer course, passing just underneath the origin of the superior mesenteric artery. Renal vein thrombosis presents as enlarged, echogenic kidneys with clot sometimes visible within the lumen of the renal vein, best detected by power Doppler. When limited to the intrarenal vessels, the thrombus may not be visible. Duplex Doppler may reveal absent flow in the renal vein although this can be difficult to determine due to the lack of pulsatility in venous flow.

The Role of the Nephrologist

Because sonography is the most common imaging modality in patients with kidney disease and is essential to their management, nephrologists should consider incorporating this tool into their practice. The simplicity, the low cost and portability of the equipment, and the availability of training all make this a realistic goal. Certification in the performance and interpretation of renal sonograms can be obtained from the American Society of Diagnostic and Interventional Nephrology (www.ASDIN.org). Even if they are not performing the procedure themselves, nephrologists must have a comprehensive understanding of sonography of the kidneys and the urinary tract because interpretation frequently requires clinical input and correlation.

NUCLEAR MEDICINE IMAGING OF THE KIDNEYS

Radionuclide renal scintigraphy provides important functional data to assist in the diagnosis and management of patients with a variety of suspected genitourinary problems. Requesting a renal scan, however, is not always straightforward because there are five different renal radiopharmaceuticals and several imaging protocols. Renal scintigraphy is also complicated by the fact that there can be marked differences in scan quality at different institutions despite using the same radiopharmaceutical, the same equipment, and identical billing. To ensure that the patient receives the most appropriate study, the clinical question must be clearly specified. In addition, referring physicians should be familiar with the elements that make up a quality study, the different procedures and their limitations, the principal radiopharmaceuticals and the rationale for their use, as well as the terminology and quantitative parameters often included in the report. To achieve these goals, this section describes the available radiopharmaceuticals, the basic renal scan, and the quantitative indices used to interpret the study; it also reviews clearance measurements, the primary scan indications (Table 10.2), essential information needed by patients, radiation exposure, and includes a short discussion of renal scan applications in selected clinical settings.

10.2 Scans and Primary Clinical Indications

I. Basic Renogram
- To assess renal function and urodynamics
- To determine the percent of total renal function contributed by each kidney

II. Diuresis Renogram
- To diagnose or exclude urinary tract obstruction

III. ACE Inhibition (RVH or Captopril) Renogram
- To diagnose or exclude renovascular hypertension

IV. Renal Transplant Scintigraphy
- To evaluate arterial flow and function
- To help diagnose rejection and acute tubular necrosis
- To detect urinary leak, infarct, or outflow obstruction

V. Renal Cortical Scintigraphy
- To detect or exclude pyelonephritis
- To determine the percent of the total renal function contributed by each kidney

VI. Radionuclide Cystography
- To detect, quantitate, and monitor reflux
- To evaluate asymptomatic siblings of children with reflux

ACE, angiotensin-converting enzyme; RVH, renovascular hypertension.

Radiopharmaceuticals

The radiopharmaceuticals available for assessment of renal function and anatomy can be grouped into three broad categories: radiopharmaceuticals filtered by the glomerulus, tracers primarily secreted by the renal tubules, and those retained in the renal tubules for long periods of time.

^{99m}Tc-DTPA (Glomerular Filtration)

^{99m}Tc-DTPA (technetium-99m diethylenetriamine pentaacetic acid) is the only renal radiopharmaceutical available for routine imaging that is purely filtered by the glomerulus; consequently, it is the only imaging radiopharmaceutical that can be used to measure glomerular filtration rate (GFR).[112] In normal subjects, the extraction fraction of DTPA (the percentage of the tracer extracted with each pass through the kidney) is approximately 20%; this extraction fraction is relatively low compared to the extraction fraction of tubular tracers (40%–50%).

^{51}Cr-EDTA (Glomerular Filtration)

^{51}Cr-EDTA (chromium-51 ethylenediamine-tetraacetic acid) is used to measure GFR.[112] Chromium-51 does not emit enough photons to be used for imaging and the tracer is not available in the United States.

^{125}I-iothalamate (Glomerular Filtration)

^{125}I-iothalamate is used to measure GFR.[112] Iodine-125 does not emit a photon of sufficient energy to be useful for renal imaging.

^{99m}Tc-MDP (Glomerular Filtration)

^{99m}Tc-MDP (methylene diphosphonate) is a bone imaging tracer but it is cleared by glomerular filtration. Measurements of relative renal uptake (relative GFR) can be obtained at the time of a bone scan using standard renal software.

^{123}I- and ^{131}I-OIH (Tubular Secretion)

Iodine-123 and iodine-131 orthoiodohippurate (OIH) are cleared primarily by the proximal tubules although a small component is filtered by the glomeruli. The clearance of OIH is approximately 500–600 mL per minute in subjects with normal kidneys; this clearance is often described as the effective renal plasma flow (ERPF).[113] There is a common misconception that the ERPF (OIH clearance) is equivalent to renal plasma flow or, at least, proportional to renal plasma flow. The clearance of OIH and the clearance of ^{99m}Tc tubular tracers have two components: (1) delivery to the kidney (renal plasma flow) and (2) extraction from the plasma and transport to the tubular lumen (tubular function). These parameters do not always change in a proportional fashion. Because of poor imaging characteristics, the potential for delivering a high radiation dose, and/or unfavorable logistics, ^{123}I- and ^{131}I-OIH are no longer commercially available in the United States.[114,115]

^{99m}Tc-MAG3 (Tubular Secretion)

^{99m}Tc-mercaptoacetyltriglycine (MAG3) is highly protein-bound and is removed from the plasma almost exclusively by the organic anion transporter 1 (OAT1) located on the basolateral membrane of the proximal renal tubules.[113,116,117] The extraction fraction is 40% to 50%,[116] more than twice that of DTPA. Because of its more efficient extraction, MAG3 is preferred over DTPA in patients with suspected obstruction and impaired renal function and is used in approximately 70% of the renal scans performed in the United States.[118–122]

The MAG3 clearance averages about 320 mL/min/1.73 m^2 in adults under age 40 and decreases by approximately 1% per year after age 40.[123,124] The clearance of MAG3 is highly correlated with the clearance of OIH, and MAG3 clearance can be used as an independent measure of renal function.[112,113]

^{99m}Tc-L,L and D,D-EC (Tubular Secretion)

^{99m}Tc-L,L and D,D ethylene dicysteine (EC) are enantiomers—both are excellent renal radiopharmaceuticals with clearances

slightly higher than MAG3.[125,126] Although D,D-EC is cleared more rapidly than LL-EC,[127] LL-EC was first described and is available in several countries as a kit formulation.

^{99m}Tc-DMSA (Cortical Retention)

^{99m}Tc-DMSA (dimercaptosuccinic acid) is an excellent cortical imaging agent that is used primarily in pediatrics to evaluate relative function, pyelonephritis, and renal scarring.[128,129] Approximately 40% of the injected dose is retained by the renal tubules within 1 hour after injection; the remainder is slowly excreted in the urine over the subsequent 24 hours.

^{99m}Tc-GH (Cortical Retention and GFR)

^{99m}Tc-GH (glucoheptonate) is cleared both by glomerular filtration and tubular secretion. Most of the dose is rapidly excreted but 10% to 15% of the injected dose remains in the renal tubules allowing delayed, high-resolution static images to be obtained. GH tends to be used if DMSA is unavailable.

Basic Renal Scan and Renogram Curve

The basic renal scan is performed by injecting 1 to 10 mCi (37–370 MBq) of ^{99m}Tc-MAG3 or ^{99m}Tc-DTPA into a peripheral vein with the patient supine. Images are acquired dynamically for 20 to 30 min and postvoid views of the kidneys and bladder are often obtained at the conclusion of the study. Images are usually displayed at 1-, 2-, or 3-minute intervals as the radioactive tracer is removed from the blood, transits the kidney, and enters the bladder (Fig. 10.37A). Data are recorded on the computer for subsequent analysis, and renogram curves are obtained by placing a region of interest (ROI) over each kidney and generating time-activity curves for each ROI from the time of injection to end of the study.

Quantitative Indices

The more common quantitative indices and their clinical relevance are discussed here.

1. Relative function: The relative uptake of the radiopharmaceutical provides a measure of differential renal function (the specific function depends on the radiopharmaceutical) and should be reported. For MAG3 and DTPA, the measurement is usually made by placing an ROI over each kidney and measuring the radioactivity during the 1 to 2, 1 to 2.5, or 2 to 3 minute period postinjection. Because of radiotracer present in blood and the interstitial space of the kidney, as well as in the tissues anterior and posterior to the kidney, a background correction needs to be performed to correct for nonrenal counts present in the renal region of interest. Automated perirenal backgrounds (see Fig. 10.37A,B) and C-shaped backgrounds are preferred over background regions placed inferior to the kidney.[119,130] The 95% confidence interval for the relative uptake of MAG3 in the presence of normal renal function ranges from 42% to 58%.[123]
2. GFR, ERPF, and MAG3 clearance measurements: Measurement of GFR, effective renal plasma flow (ERPF), or MAG3 clearance may be obtained, depending on available software, protocols, and expertise (see discussion of clearance measurements).
3. Whole kidney versus cortical ROIs: The whole kidney ROI consists of an ROI placed around the entire kidney including the renal pelvis. Quantitative values generated using this ROI will be affected by retention of tracer in both the kidney parenchyma and renal pelvis. Thus retention may be due to pathologic states such as diabetic nephropathy or obstruction but may also occur in nonpathologic states such as a nonobstructed dilated collecting system or mild dehydration. To obtain a better assessment of parenchymal function, ROIs can be limited to the renal cortex (parenchyma), thereby excluding any activity retained in the pelvis or calyces (Fig. 10.37).
4. Time-to- peak or T_{max}: The time-to-peak or T_{max} simply refers to the time from radiopharmaceutical injection to the peak height of the renogram curve. MAG3 and DTPA renograms normally peak by 5 minutes and decline to half-peak height by 15 minutes postinjection; however, physiologic retention of the tracer in the renal calyces or pelvis can alter the shape of the whole kidney renogram curve in normal kidneys and lead to prolonged values for the time-to-peak, 20 min/max count ratio, and T1/2.
5. The T1/2: The T1/2 refers to the time it takes for the activity in the kidney to fall to 50% of its maximum value (see suspected obstruction).
6. Postvoid kidney counts/maximum or 1 to 2 minute kidney counts: In evaluating suspected obstruction, simple ratios that incorporate gravity-facilitated drainage from the kidneys such as counts in the postvoid kidney divided by the maximum counts in the kidney or counts at 1 to 2 minutes appear to provide more robust measurements of drainage than the T1/2.[131–134]
7. 20 min/max count ratio: The 20 min/max count ratio is the ratio of the kidney counts at 20 minutes to the maximum (peak) counts; this measurement provides an index of the transit time and parenchymal function and is often obtained for both whole kidney and cortical (parenchymal) ROIs. For MAG3, the normal 20 min/max count ratio for cortical ROIs averages 0.19 with standard deviations of 0.07 and 0.04 for the right and left kidneys, respectively.[123] If the patient is not dehydrated and the 20 min/max count ratio for the cortical ROI exceeds 0.35 (greater than two to three standard deviations above the mean), the kidney is likely to be abnormal. With the tubular agents, this index can be useful in monitoring patients with suspected urinary tract obstruction and renovascular hypertension.[135–137]

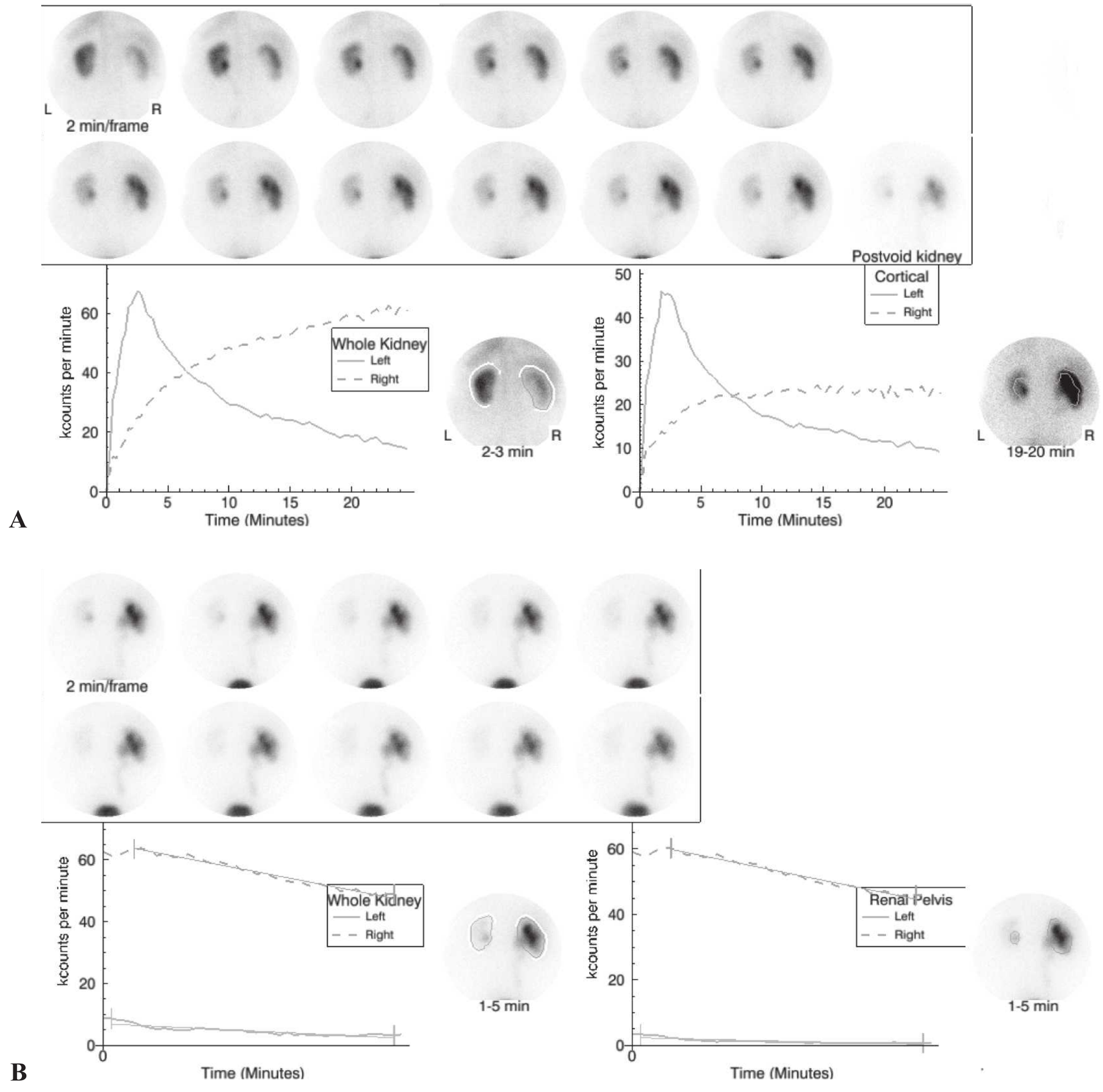

FIGURE 10.37 A 70-year-old man was referred for a renal scan because of suspected obstruction of the right kidney. The patient received an intravenous injection of 9.2 mCi (340 MBq) of ^{99m}Tc MAG3. **A:** The upper panel shows sequential 2-minute MAG3 images in a posterior projection; the final image in the series is a postvoid image. The lower left panel shows the whole kidney renogram curves (*blue*, left kidney; *green*, right kidney); the lower right panel shows cortical renogram curves. The relative uptake was 74% in the left kidney, 24% in the right kidney; the MAG3 clearance was 231 mL/min/1.73 m^2. The images and renogram curve for the left kidney are normal. There is retention of the MAG3 in the right renal collecting system with a rising renogram curve. **B:** To further investigate the possibility of obstruction in the right kidney, the patient received an intravenous injection of 40 mg furosemide followed by an additional 20 minutes of imaging. The upper panel shows sequential 2-minute images following furosemide administration. The lower left panel shows the whole kidney renogram curve and the lower right panel shows the renogram curve with the regions of interest placed around the retained tracer in the collecting system. There is very little MAG3 remaining in the left kidney (*blue*); the post-furosemide images show continuing retention in the right renal collecting system with very slow washout (T1/2 = 36 minutes for the region of interest over the collecting system) consistent with obstruction. (See Color Plate.)

8. Residual urine volume: Residual urine volume can be measured based on the counts in pre- and postvoid ROIs over the bladder and a measurement of the voided volume.[138] This is a relatively easy measurement to perform, is routine at some institutions, and may detect unsuspected urinary retention. The main source of error is tracer remaining in the renal pelvis which subsequently drains into the bladder after voiding; this problem can be detected by looking at the last kidney image in the study.
9. Urine flow rate: The rate of urine flow can be useful in assessing the adequacy of hydration and the adequacy of diuresis following furosemide administration. Assuming a constant postvoid volume, urine flow

rate can be calculated by dividing the voided volume at the conclusion of the study by the time interval between voiding prior to and at the conclusion of the study.

Renal Function and Clearance Measurements

Because of inaccuracies associated with estimation of GFR based on serum creatinine or creatinine clearance, a more accurate measurement of renal function may be needed in patients at the extremes of age and body mass and in patients with severe malnutrition, grossly abnormal muscle mass (amputation, paralysis), high or low intake of creatinine or creatine (vegetarian diet, dietary supplements), rapidly changing renal function, prior to kidney donation, and prior to dosing with toxic drugs excreted by the kidney. Measurement of renal function at the time of the scan can aid in the interpretation of a radionuclide study, provide a measurement of renal function independent of serum creatinine, and serve as a baseline for monitoring changes. The two most widely used techniques to measure clearances are plasma sampling and camera-based techniques.

Multisample Plasma Clearances. The gold standard for measuring renal clearances is a constant infusion technique where the plasma concentration of the tracer remains constant.[112] A variant of this technique uses a subcutaneous injection; however, both of these methods are cumbersome, time consuming, expensive, and limited to research applications. An alternative approach that does not require urine collections is the plasma clearance obtained using the single injection, two-compartment model.[139] For tubular tracers, the plasma disappearance curve can be determined from multiple blood samples obtained over 90 minutes. Because GFR tracers have a much lower extraction fraction and a lower clearance, plasma samples typically need to be obtained for 4 hours to adequately characterize the curve.

Single and Dual Plasma Sample Clearances. Simplified techniques based on one or two plasma samples have been developed to estimate the multisample clearance.[112] The MAG3 clearance can be estimated from the dose injected and the amount of radioactivity in a single blood sample obtained approximately 45 minutes after injection[112,124,140] and the GFR can be estimated from the dose injected and the activity in one or two plasma samples obtained 1 to 4 hours after injection.[112,141–143] These techniques provide reliable results and can be performed at the time of a standard renal scan using MAG3 or DTPA.

Plasma Sample Techniques: Sources of Error and Availability. Plasma sampling techniques assume a normal volume of distribution. If a patient has ascites, marked edema, or a large effusion, the tracer can diffuse into these extra fluid spaces and the plasma clearance will not provide an accurate measure of renal function. Plasma sample clearances require meticulous technique and attention to detail. If the measurement is performed by a poorly trained or inexperienced individual, technical errors are often made and the results are spurious. Because of the need for specialized training, the necessity of handling plasma samples, extra effort, and lack of reimbursement, plasma sample clearances are not widely available in the United States.

Camera-Based Clearances. Camera clearance methods have been developed for DTPA, OIH, and MAG3 that do not require blood or urine samples.[141–145] The principle is based on the fact that the initial tracer accumulation by the kidneys is proportional to the clearance. Camera-based techniques determine the tracer accumulation (counts) in the kidneys at a defined period shortly after injection and divided by the counts injected to obtain a percent injected dose in the kidneys. The percent injected dose is converted to a clearance measurement using a validated nomogram.[145]

Camera-based clearances appear to be reproducible and have been reported to be superior to creatinine clearance for monitoring changes in renal function.[146] Although camera-based clearances are considered to be less accurate than plasma sample clearances,[112] they avoid sources of error (timing of plasma samples, correction for radioactive decay, dilution of standards, pipetting small volumes) inherent in plasma sample techniques.

Camera-based Clearances: Sources of Error. To obtain the percent injected dose in each kidney, kidney counts have to be corrected for background, infiltration, attenuation, and renal depth. Two common sources of error are background subtraction and the estimation of renal depth. Because MAG3 is extracted more than twice as efficiently as DTPA, the kidney-to-background ratio will be much higher for MAG3 than DTPA and any potential error introduced by background subtraction will be minimized.

Renal depth is usually estimated from a nomogram based on height and weight.[147,148] To the degree that a population-derived nomogram fails to fit a particular individual, the clearance measurement will vary from the true clearance. The sources of error due to background, self-attenuation, and renal depth tend to be reflected in a wider confidence interval associated with the accuracy of camera-based clearance compared to plasma sample clearances; however, these parameters tend to be constant on sequential studies and have less effect on reproducibility. Commercial camera-based techniques are currently available for measuring GFR (DTPA), effective renal plasma flow (OIH), and the MAG3 clearance. In evaluating the reliability of commercial software, it is important to confirm that the vendor has (1) incorporated the appropriate quality control features and (2) provided citable validation studies to confirm that the software is performing as claimed.

General Patient Preparation and Information

Patients appreciate knowing what to expect when they are referred for an unfamiliar test. The following information should be communicated to the patient.

Procedure and Time Required for the Study

The patient will receive an intravenous injection of the radiopharmaceutical and will lie quietly on an imaging table for 20 to 30 minutes. Depending on the protocol, there may be two imaging sessions. Unlike radiographic contrast, there is essentially no risk of an allergic or anaphylactic reaction.

Hydration

The patient should be told to arrive well hydrated because good hydration minimizes the radiation dose to the bladder and facilitates interpretation of the exam.

Diet and Medication

For a basic renogram, there are no medication or dietary restrictions. Medication and dietary restriction for angiotensin-converting enzyme (ACE) inhibition renography are discussed later.

Radiation Exposure

Depending on the radiopharmaceutical and the amount administered, the radiation exposure from a typical MAG3 or DTPA scan ranges from 5% to 70% of the background radiation a patient receives each year from cosmic rays and naturally occurring radioactive sources in the environment; it is less than 5% of the yearly radiation dose considered safe for doctors and technologists who work with radiation. In patients with normal kidney function, over 95% of the radiation leaves the body by 3 hours. Patients can go to public places and use a bathroom without risk to others (see later text for a more detailed discussion of radiation).

Pregnancy

If the patient is pregnant or thinks she may be pregnant, she should discuss this possibility with the nuclear medicine physician prior to arrival for the test.

Radiation Exposure to the Nuclear Medicine Patient

Radiopharmaceuticals are designed to target specific organs, tumors, or pathways and to avoid others; consequently, they do not distribute uniformly throughout the body. Different tissues receive different exposures depending on the isotope, its half-life, its tissue distribution, and its retention time. For example, ^{99m}Tc has a half-life of about 6 hours; even if none of a ^{99m}Tc tracer was eliminated from the body after intravenous administration, the amount remaining in the body 24 hours later (four half-lives) would be only about 6% of the administered dose.

The concept of effective radiation dose has been developed to define a single quantity that could express the overall potential deleterious effect of radiation exposures. This concept allows the risk of the different radiation doses to different tissues throughout the body to be expressed in a single measurement. The effective radiation dose equivalent is the whole-body radiation dose that would have to be given to produce a risk equivalent to the sum of the risks from the individual radiation doses to the various organs. The effective dose from a MAG3 or DTPA scan ranges from 15 to 20 mrem (0.15–0.2 mSv) per millicurie injected. The typical administered dose is 1 to 10 millicuries (37–370 MBq); consequently, the effective dose for a renal scan ranges from 15 to 200 mrem (0.15–2.0 mSv).[115] For comparison, background radiation is estimated to be approximately 300 mrem (3.0 mSv) per year.

Suspected Obstruction (Diuresis Renography)

Obstruction to urinary outflow may lead to obstructive uropathy (dilatation of the calices, pelvis, or ureters) and obstructive nephropathy (damage to the parenchyma). Urine outflow obstruction may be suspected based on clinical findings, the incidental detection of a dilated renal collecting system, or diagnosis of previous obstruction in a patient referred for follow-up. Diuresis renography is noninvasive, widely available, and can evaluate renal function and urodynamics in a single test. This noninvasive test is based on a high endogenous rate of urine flow stimulated by the administration of furosemide. Interpretation of the test is based on the washout of the radiopharmaceutical from the collecting system in the upper urinary tract.

Acquisition Protocols, Radiopharmaceutical Choice, and the Timing of Furosemide

The patient should arrive well hydrated and void immediately prior to the examination because a full bladder may affect upper tract emptying and give false-positive results.[120] Adult and pediatric consensus groups recommend tubular agents for diuresis renography because tubular tracers are much more efficiently extracted by the kidney than DTPA.[120,122,134,149] Several protocols are available for diuretic renography that differ mainly in the timing of furosemide administration and in the use of a single acquisition or a baseline scan followed by post-furosemide acquisitions if the baseline scan does not exclude obstruction.[120,122] Typical times for furosemide administration are the F – 15, F = 0, and F + 20 protocols where the furosemide is administered 15 minutes before, simultaneously with, or 20 minutes after the tracer administration. Each protocol has its advocates but all are acceptable and appear to give comparable results in the majority of patients.[134,150–153]

Dose of Furosemide

Furosemide is secreted by the proximal tubule and reaches its site of action in the tubular lumen of the thick ascending loop of Henle via the tubular fluid.[154] Secretion of

furosemide is reduced in patients with impaired renal function; consequently, the standard 40-mg adult dose may not be sufficient to induce an adequate diuretic response in a kidney with moderate or severely impaired renal function and a larger dose of furosemide may be required.[154,155]

Diagnostic Criteria, the T1/2, Gravity-Assisted Drainage, and Postvoid Images

Drainage is often assessed quantitatively by measurement of the T1/2 following furosemide administration. Although the T1/2 calculated from an ROI placed around retained activity in the collecting system rather than around the whole kidney provides a better assessment of drainage, T1/2 measurements are not standardized and they vary depending on timing, ROI assignment, and method of calculation.[120,122,156,157] There is general agreement that prompt clearance of the radiopharmaceutical from the renal collecting system with a T1/2 under 10 minutes excludes obstruction. On the other hand, a prolonged T1/2 should never be the sole criterion for determining the presence of obstruction and must be interpreted in the context of the whole set of images, curves, and quantitative indices as well as any clinical information or diagnostic studies that may be available. Techniques that consider renal function, utilize gravity-assisted drainage, and incorporate postvoid images appear to provide more robust alternatives to the T1/2.[131,133,134,136,158,159]

False-Positive and Indeterminate Studies

A poor diuretic response due to dehydration or impaired renal function may result in false-positive or indeterminate findings. Measuring the urine flow rate alerts the nuclear medicine physician to an inadequate diuresis.

Relative Renal Function

Unless obstruction is acute, it usually causes a loss of function in the affected kidney. If the relative renal function is approximately the same in both kidneys in a patient with suspected unilateral obstruction, the likelihood of obstruction is reduced even if the quantitative data such as the T1/2 are abnormal. In these cases, it may be appropriate to observe the patient and repeat the study at a later date or to combine the study with sonography to determine if the size of the renal pelvis is increasing.

Does a Patient Presenting with Flank Pain have Acute Renal Colic? If so, Can He be Managed Conservatively?

Knowledge of the size of the obstructing calculus is important because calculi less than 5 mm generally pass spontaneously; as the size of the calculus increases, spontaneous passage becomes less likely. Unenhanced (noncontrast) helical CT (UHCT) has rapidly gained acceptance as the procedure of choice for patients presenting with acute renal colic. UHCT avoids the risk of contrast, which is particularly important for patients with renal insufficiency, diabetes, dehydration, or allergy to iodinated contrast agents; moreover, stone size can be accurately ascertained, and the correct diagnosis can be made in approximately 50% of patients whose symptoms are not caused by a renal stone.

Many calculi between 3 to 8 mm in size are followed conservatively in the hope of spontaneous passage, and patients may be managed on an outpatient basis. In spite of its advantages, UHCT cannot determine the functional status of the kidney. Larger stones (5–8 mm) may not be associated with high-grade obstruction and can be managed conservatively, whereas some small stones (3–5 mm) do result in high-grade obstruction and may need more aggressive management. The addition of a diuretic renal scan can determine the presence or absence of obstruction and has been shown to direct patient management; in one study, the scan changed the decision to admit or discharge the patient in 30% of cases.[160–162] Data have not yet been collected to determine if the addition of the scan and resulting change in practice leads to better patient outcomes and/or reduced medical costs.

Ultrasound or CT Show a Dilated Collecting System. Is There Ureteral Obstruction?

Dilatation of the urinary tract with no apparent cause may be incidentally detected by ultrasound, CT, or MRI in a patient with no symptoms of acute obstruction. If the dilated collecting system represents chronic obstruction, an intervention may be required to preserve renal function; if there is simply dilatation of a nonobstructed collecting system, no further workup is required. Diuresis renography is preferred in the evaluation of the nonacute dilated collecting system because it is noninvasive, relatively inexpensive compared to CT or MR urography, and allows the clinician to quantitate the physiologic significance of the anatomic abnormality by measuring both the relative renal function and the diuretic stimulated washout of the tracer from the dilated system. Contrast is avoided, and the gonadal radiation dose is substantially reduced compared to CT urography.

A Patient with Previous Obstruction has Recurrent Symptoms. Has Obstruction Recurred? Has Surgery Successfully Relieved a Documented Obstruction?

A patient with previous documented and treated obstruction may present with symptoms suggesting recurrent obstruction; sonography is often not helpful in this setting because the urinary tract can be dilated secondary to the previous episode of obstruction. Diuresis renography is the preferred examination.

Antenatal Sonography Shows a Dilated Pelvis or Ureter. Is There Obstruction or Loss of Renal Function?

The significance of an abnormal antenatal renal sonogram can be readily evaluated by MAG3 diuresis renal scintigraphy in

the newborn. Relative function can be quantitated and drainage assessed. If the diagnosis of obstruction is uncertain, sequential studies can be obtained with sonography to determine if the renal pelvis is enlarging or with sequential MAG3 scans to evaluate drainage and to determine if function is decreasing in the affected kidney.

Suspected Renovascular Hypertension (ACE Inhibition Renography)

The diagnostic and therapeutic approach to patients with suspected renal artery stenosis (RAS) remains uncertain and controversial. Atherosclerotic renal artery stenosis (ARAS) is the most common cause of secondary hypertension[163]; however, it may be present in as many as 25% of normotensive patients over age 50[164] and is often present as an incidental or secondary finding in hypertensive patients.[164,165] ARAS is far more common than renovascular hypertension (RVH), whose classical definition is based on cure or amelioration of the hypertension after revascularization. Consequently, it comes as no surprise that the Scottish, EMMA, and DRASTIC studies, and the more recent STAR and ASTRAL trials, indicate that the indiscriminate revascularization of an atherosclerotic RAS appears to have little advantage over optimal medical therapy and is no longer justified.[166–170] These five trials, however, did not distinguish between the impact of revascularization in a hypertensive patient with RAS and the impact of revascularization in a hypertensive patient with a functionally significant stenosis. Although indiscriminate revascularization of a stenotic renal artery in hypertensive patients is no longer justified, more focused selection criteria that evaluate the functional significance of the stenosis may lead to improved outcomes.

Spiral computed tomography (CTA) and magnetic resonance angiography (MRA) provide detailed images of the aorta and renal arteries and have high sensitivity and specificity for detecting RAS.[163,171] The main limitation of CTA and MRA is the lack of information on renal blood flow or pressure distal to the stenosis.[171] In azotemic patients, CTA carries the risk of contrast nephrotoxicity, and the use of MR contrast in patients with a low GFR is associated with nephrogenic systemic fibrosis.[172] Doppler ultrasound is reported to provide reliable hemodynamic assessment of renal artery lesions in selected centers but others have found it to be time consuming, operator dependent, lacking diagnostic uniformity, and too unreliable in obese individuals to be an efficient tool to screen hypertensive patients for a functionally significant RAS.[171,173] This introduction underscores the need for diagnostic procedures that can accurately select those hypertensive patients with RAS most likely to be cured or improved after revascularization.

ACE Inhibition Renography and Scan Interpretation

A functionally significant stenosis leads to a decrease in the perfusion pressure distal to the stenosis resulting in a decrease in the transglomerular pressure gradient and a decrease in GFR. The reduction in perfusion pressure stimulates the release of renin and increased production of angiotensin I which is converted to angiotensin II by ACE. Angiotensin II preferentially constricts the efferent arteriole of the glomerulus and raises the transglomerular pressure gradient—a process that maintains GFR in the face of a moderate reduction in perfusion pressure.

In patients with a functionally significant renal artery stenosis, the blockade of angiotensin II production by ACE inhibition leads to a reduction in GFR that can be detected by renography. ACE inhibitors also inhibit kininase II, a dipeptidyl carboxy-peptidase that inactivates bradykinin, a potent vasodilator that causes selective efferent arteriolar dilation; this mechanism also contributes to the ACE-induced reduction in GFR.[174–176]

The reduction in GFR in patients with a functionally significant RAS following ACE inhibition can be detected by a decrease in renal uptake of DTPA by the affected kidney compared to the baseline scan; tubular tracers such as MAG3 demonstrate cortical retention (Fig. 10.38, right kidney)[135,137,159,177,178] which is also secondary to the decrease in GFR and results from a decreased flow of primitive urine through the renal tubules.[179]

Consensus panels have recommended that the test be interpreted as high, low, or indeterminate probability for renovascular hypertension.[135,177] A normal or near normal renogram that is unchanged or improves following ACE inhibition is low probability for renovascular hypertension and indicates that revascularization is unlikely to ameliorate the hypertension (Fig. 10.38, left kidney). Abnormal baseline renograms that are unchanged following ACE inhibition are indeterminate and are not predictive of the response to revascularization. Unilateral deterioration of the renogram curve and/or of the relative function following ACE inhibition compared to the baseline study represents a high probability scan for renovascular hypertension and indicates a high likelihood that blood pressure will be normalized or ameliorated by revascularization.

Sensitivity and Specificity of ACE Inhibition Renography

ACE inhibition renography in an appropriately screened hypertensive patient with preserved renal function can detect renovascular hypertension with a sensitivity approximating 90%.[137,175,178,180–188] Using the criterion of ACE inhibition-induced changes between baseline and ACE inhibition scans to define a positive test, the test has a specificity ≥90% and consequently has a high positive predictive value.[178,187] The sensitivity and specificity of ACE inhibition renography, however, are affected by several factors that have contributed to confusion in the literature.

1. Use of the anatomic presence of a renal artery stenosis as a surrogate for renovascular hypertension. ACE inhibition renography is a test to detect a functionally significant RAS, NOT a test to detect the presence of RAS.[135,177] Nevertheless, many investigators have used the angiographic

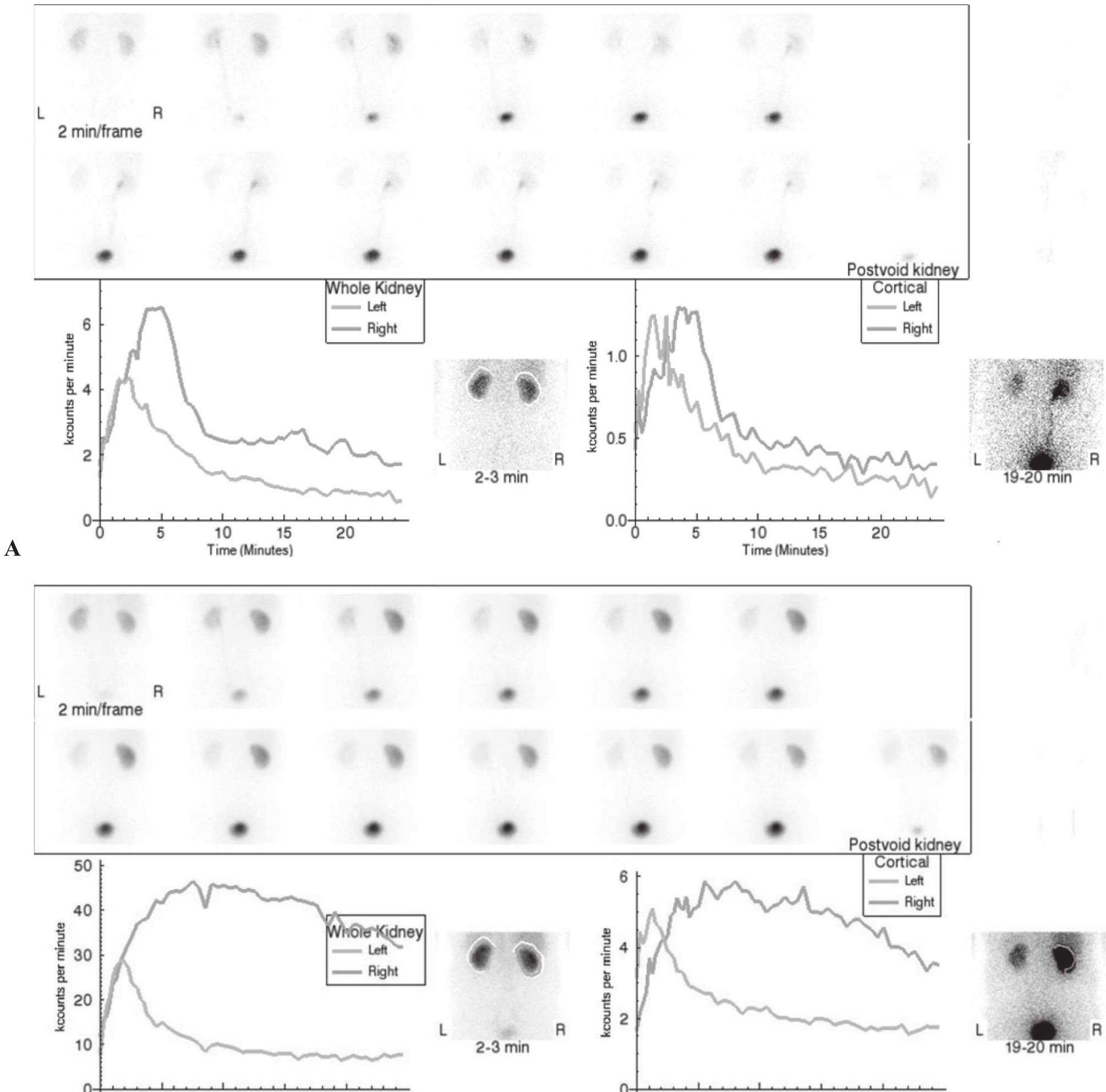

FIGURE 10.38 A 52-year-old patient with hypertension with a normal serum creatinine had a computed tomography (CT) scan for a possible incarcerated abdominal hernia. The CT scan revealed a heavily calcified right renal artery. A subsequent CT angiogram confirmed a renal artery stenosis and an angiotensin-converting enzyme (ACE) inhibition renal scan was requested to determine its functional significance. **A:** A baseline scan was obtained following the injection of 1.4 mCi of ^{99m}Tc MAG3 (52 MBq). The upper panel shows sequential 2-minute MAG3 images. The lower left panel shows the whole kidney renogram curves (*blue*, left kidney; *green*, right kidney); the lower right panel shows cortical renogram curves. The relative uptake was 51% (*left*) and 49% (*right*) with a MAG3 clearance of 295 mL/min/1.73 m^2. The images appear normal with time to maximum counts (T_{max}) and 20 min/max count ratios in the normal range for both kidneys although there was asymmetry with the T_{max} for the right kidney (4.8 min) more delayed than the T_{max} for the left kidney (1.8 minutes); in addition, the 20 min/max ratio for the right kidney, 0.30, was higher than that of the left (0.19). **B:** The patient received an intravenous injection of 2.5 mg of enalaprilat followed 20 minutes later with a second MAG3 injection of 9.0 mCi of MAG3 (333 MBq). The left kidney is normal. The relative function was essentially unchanged, 49% left, 51% right but the sequential 2-minute images show marked parenchymal retention of the tracer in the right kidney with a correspondingly abnormal whole kidney and cortical renogram curves. The marked change in the right kidney from the baseline to the ACE study indicates a high probability scan for renovascular hypertension. (See Color Plate.)

presence of a stenosis >50% as a surrogate for renovascular hypertension in spite of the fact that many of these stenotic lesions will not be hemodynamically significant.[106,177,178,189] In an attempt to circumvent this problem, other investigators have used the more stringent standard of >70% stenosis. Although good results have been obtained using RAS as the gold standard,[190] not surprisingly, the sensitivity and specificity of ACE inhibition renography is improved when the gold standard is the response to revascularization rather than the anatomic presence of RAS.[178,184,185,187,188]

2. Patient selection: test performance in azotemic and nonazotemic populations. Current data indicate that the test is not as accurate in azotemic patients with RAS. Although some studies report good results in azotemic patients,[183,191,192] most investigators have found ACE inhibition renography to be less accurate in azotemic patients.[135,137,177,178,181] In this population, a positive test retains a high specificity indicating a high likelihood that the hypertension will be ameliorated by revascularization,[193] but one study reported as many as 50% of tests in this population were intermediate probability.[137] Intermediate probability outcomes result from an abnormal baseline scan which is unchanged following ACE inhibition and are not predictive of the response to revascularization.
3. Analysis of the "intermediate probability" or indeterminate scan. To calculate sensitivity and specificity, indeterminate results must be placed with the high or low probability results. Intermediate probability studies placed in the "high probability" category increase sensitivity at the expense of specificity and, conversely, intermediate probability studies placed in the "low probability" category increase specificity at the expense of sensitivity.[194] The reported values for sensitivity and specificity vary depending on the frequency of azotemic patients in the study population and how intermediate probability results are handled in the data analysis.
4. Inconsistent use of recommended criteria for interpreting ACE inhibition renograms. Interpretative criteria for ACE inhibition renography have been published as an international consensus report in 1996; this report has subsequently been updated by the Society of Nuclear Medicine and published on its website.[135,177] Studies performed after 1996 should include an analysis based on these criteria especially because data show that strict adherence to these criteria improves the performance of ACE inhibition renography.[195]

Performance of the Examination

Detailed recommendations for performance of ACE inhibition renography are described in consensus reports[135,177] but several points should be emphasized.

1. Blood pressure must be monitored. Asymptomatic hypotension secondary to ACE inhibition can result in bilateral symmetrical abnormalities in the renogram curves.[194,196] This phenomenon is relatively uncommon but may occur in as many as 3% of patients referred for ACE inhibition renography, usually in patients who are volume or salt depleted.[196,197]
2. ACE inhibitors and angiotensin II receptor blockers (ARBs). The majority of ACE inhibition studies have been performed with captopril (25–50 mg) but enalaprilat (Vasotec, 40 μg per kg IV over 3–5 minutes, maximum dose of 2.5 mg) administered at least 15 minutes prior to tracer administration is an acceptable alternative.[177,183] Intravenous injection of enalaprilat avoids the possibility of a false-negative test due to delayed gastric emptying or poor absorption—a potential disadvantage is the possibility of a greater risk of a hypotensive response. Chronic ACE inhibition may reduce the sensitivity of the test[179,192] and, for this reason, guidelines recommend that captopril be discontinued for 4 days prior to the study and ACE inhibitors with a longer half-life be discontinued for 7 days. Data are limited regarding the impact of chronic ARB administration on the sensitivity and specificity of ACE inhibition renography.[175]
3. Diuretics. Chronic diuretic administration increases the likelihood of volume depletion which may lead to renal retention of the radiopharmaceutical, reduce the specificity of the test, and increase the risk of a hypotensive response. These concerns can be minimized if diuretics are discontinued for several days prior to the study.
4. Choice of radionuclide. In patients with azotemia, tubular agents such as MAG3 or I-123 are the agents of choice.[137,177] In patients with normal function, MAG3 and DTPA appear to give comparable results.
5. One-day versus two-day protocol. The traditional approach is a one-day protocol; a baseline study is performed, the ACE inhibitor is administered, and a second study is obtained allowing an immediate comparison between the baseline and ACE inhibition results. An alternative approach is to begin with ACE inhibition renography because a normal study is low probability for renovascular hypertension and obviates the need for a baseline study. If the ACE inhibition study is abnormal, the specificity can be improved by obtaining a baseline renogram; however, the patient will have to return for the baseline study on another day because of the earlier administration of the ACE inhibitor.

Does a Hypertensive Patient Have Renovascular Hypertension?

Risk factors for renovascular hypertension (RVH) include abrupt or severe hypertension, hypertension resistant to medical therapy, abdominal or flank bruits, unexplained azotemia in an elderly hypertensive patient, worsening renal function during ACE inhibition therapy, grade 3 or 4 hypertensive retinopathy, a history of heavy smoking, occlusive

disease in other vascular beds, and onset of hypertension under age 30 or over age 55. To determine the most appropriate test, patients need to be categorized into (1) those with low likelihood of RVH, (2) those with moderate to high likelihood of RVH and normal renal function, and (3) those with moderate to high likelihood of RVH and azotemia.

Technologies are evolving and multiple diagnostic imaging strategies have been proposed, but, to date, there is no generally accepted approach. Costs need to be considered in determining the clinical approach but costs are a moving target and hard to ascertain. Patients with a low likelihood of RVH can be treated medically without additional imaging studies. For the patient with one or more risk factors for RVH, normal renal function, and no known unilateral kidney disease, ACE inhibition renography provides a logical and cost-effective diagnostic approach. In this patient population, a recent analysis showed that ACE inhibition renogram as the first test was more cost effective than CT or MRA.[194]

The evaluation of the patient with azotemia or a patient known to have a small, poorly functioning kidney is more problematic. In this patient population, a positive ACE inhibition renogram still has a high predictive value for amelioration of the hypertension, but as many as half of the tests may be indeterminate for RVH, and the specificity of the test probably falls to about 80%. The advantages and disadvantages of other diagnostic approaches have been described, and test selection should be based on local expertise, cost, and how the test result will influence patient management.

Renal Transplant Scintigraphy

Donor Evaluation

Renal scintigraphy can evaluate global and individual renal function in potential donors as well as help determine which kidney to select for donation. Use of renal scintigraphy in donor evaluation, however, varies widely between centers.

Transplant Evaluation

Complications of renal transplantation can be divided into parenchymal failure (acute tubular necrosis [ATN], acute and chronic rejection, and calcineurin inhibitor toxicity) and mechanical failure (injury to the renal artery or vein, ureteral obstruction, and urine leak).[198] Sonography is usually the first approach for evaluation of renal graft dysfunction but a renal scan can provide complementary information. A normal scan immediately posttransplant excludes mechanical complications. Serial scans during the first 1 to 3 weeks posttransplantation may detect early rejection 24 to 48 hours before biochemical abnormalities occur and can be used to monitor recovery from posttransplantation ATN. Classically, ATN presents with relatively preserved perfusion accompanied by delayed uptake and excretion although severe ATN can also present with diminished flow. Rejection presents as diminished flow with delayed uptake and excretion of the tracer.[198]

Chronic transplant nephropathy represents cumulative and incremental damage to nephrons from both immunologic and nonimmunologic causes. Imaging studies are obtained if the clinician suspects complications relating to renal blood flow, urine leak, urinoma, obstruction, abscess, hematoma, or lymphoma. Sonography is typically the first approach. A renal scan may provide complementary information regarding obstruction or a urine leak and ACE inhibition renography can detect renovascular hypertension.[151,198] A renal scan cannot distinguish between rejection and calcineurin-inhibitor nephrotoxicity.

Renal Cortical Scintigraphy (Pyelonephritis and Scar)

DMSA is the radiopharmaceutical of choice for imaging the renal cortex.[128,129,151,199] Static images are obtained 2 to 4 hours after injection and sedation is rarely needed. A normal scan demonstrates homogeneous concentration of the radiotracer throughout the cortex except for a lower concentration in the region of the collecting system. DMSA scans can measure relative function and identify functioning renal tissue in patients with congenital abnormalities. The studies are most commonly obtained in patients with suspected pyelonephritis to distinguish upper from lower urinary tract infections and to detect the presence of scar following an episode of acute pyelonephritis. Pyelonephritis and scarring are recognized by focal areas of decreased DMSA uptake in the renal parenchyma; however, any process that replaces, injures, or destroys normal cortical parenchyma will result in an abnormal scan.

Does a Child Presenting with a Febrile Urinary Tract Infection Have Pyelonephritis?

Pyelonephritis is a serious illness in the pediatric population; renal scarring from recurring infection remains an important cause for substantial long-term morbidity.[200] Clinical and experimental studies have demonstrated that scarring can be prevented or diminished by early diagnosis and aggressive therapy. In infants and young children, pyelonephritis is not always accompanied by high fever, an elevated sedimentation rate, and leukocytosis. Furthermore, a normal voiding cystourethrogram does not exclude acute pyelonephritis, and it is increasingly recognized that sonography and excretory urography cannot be used to exclude acute pyelonephritis in infants and children. Renal cortical (DMSA) scintigraphy is more sensitive for the detection of pyelonephritis than sonography (Fig. 10.39), and many investigators recommend cortical scintigraphy in the initial evaluation of children with suspected pyelonephritis. MRI and CT with contrast are also sensitive tests for the detection of pyelonephritis, but MRI is expensive, and there is the possibility of an allergic reaction to iodinated contrast given during the CT scan.

There is no consensus on the use of DMSA scans in the evaluation and follow-up of patients with urinary tract infection. The diagnostic algorithm depends on how the clinician

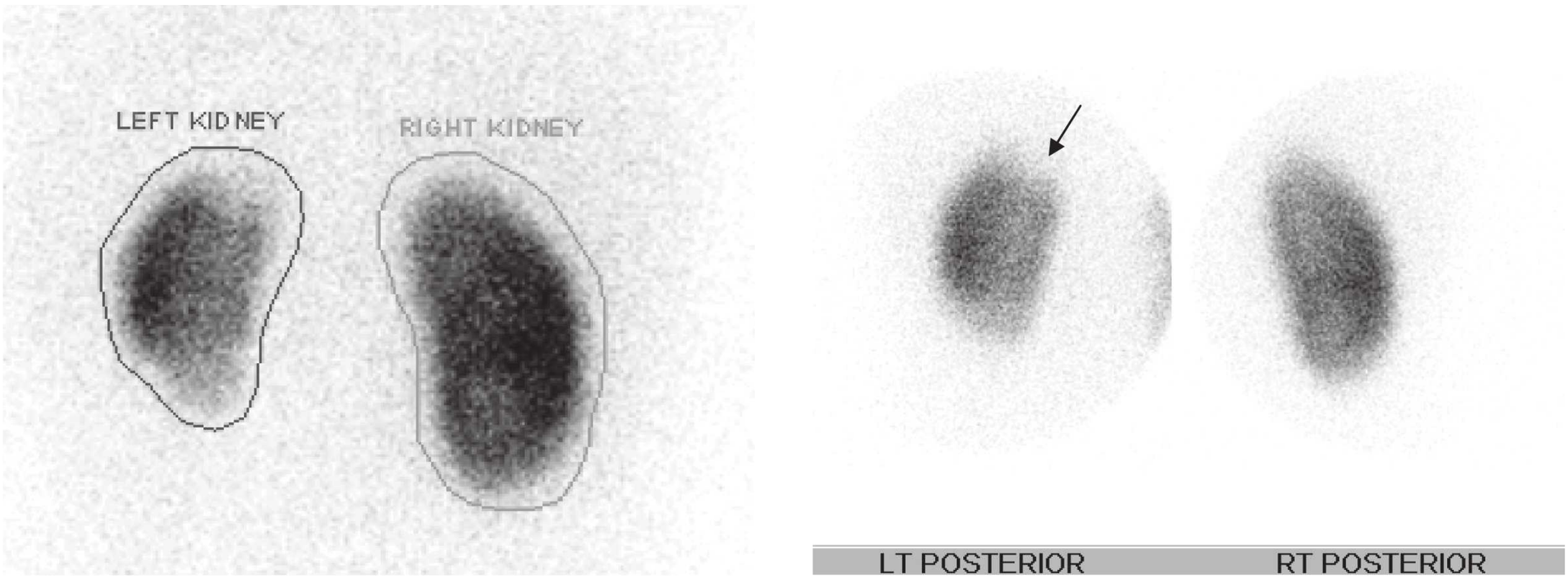

A B

FIGURE 10.39. A 6-year-old boy presented with fever, vomiting, a urinary tract infection, and an erythrocyte sedimentation rate of 98. **A:** A dimercaptosuccinic acid (DMSA) scan obtained with a parallel hole collimator shows the left kidney to be smaller than the right kidney and also suggests an area of decreased DMSA activity in the left upper pole. **B:** Additional images of each kidney were obtained using a pinhole collimator which provides better resolution than the parallel hole collimator. Pinhole images clearly show an area of decreased DMSA uptake in the superior pole of the left kidney (*arrow*) consistent with pyelonephritis; the normal right kidney is shown for comparison.

will use the information. Some institutions treat pediatric patients with suspected pyelonephritis empirically and only pursue diagnostic studies if the patient does not respond. In other institutions, patients with pyelonephritis receive more aggressive therapy and/or follow-up in the hope of reducing the risk of scarring and recurrent infection and, thereby, avoiding the subsequent development of hypertension or renal failure.[128,129,151,199]

Radionuclide Cystography

Vesicoureteral reflux, urinary tract infections, and renal scarring can lead to hypertension and chronic kidney disease; however, a large percentage of patients with pyelonephritis do not have reflux. Furthermore, reflux often resolves spontaneously. Management of patients with urinary tract infection and/or reflux tends to be individualized and varies from center to center. Reflux may be suspected based on an antenatal ultrasound showing ureteral or calyceal dilatation, a urinary tract infection in infants or young children, acute pyelonephritis, or documented reflux in a sibling. A conventional voiding cystourethrogram (VCUG) with fluoroscopy is usually the first test to detect and grade the degree of reflux. If follow-up studies are required, the patient can be followed by radionuclide cystography. The technique is accurate for detecting reflux, and the radiation dose to the gonads is much less than with a VCUG.[128,129,151]

Direct Radionuclide Cystography

The bladder is catheterized, and the study is performed by instilling saline containing approximately 1 mCi (37 MBq) of a ^{99m}Tc radiopharmaceutical into the bladder. These radiopharmaceuticals are not absorbed into the blood from the urinary bladder. Images are continuously acquired during filling of the bladder and subsequent voiding. Reflux can be quantitated by analysis of data recorded on the computer during the study.

Indirect Radionuclide Cystography

Bladder catheterization is not required. The patient typically receives an intravenous injection of ^{99m}Tc-MAG3 for evaluation of individual kidney function, urine drainage, and reflux; dynamic images are obtained during bladder filling, voiding, and after voiding. This technique avoids catheterization, but it is not as sensitive as direct radionuclide cystography for detecting reflux.

REFERENCES

1. O'Neill W. Sonographic evaluation of renal failure. Am J Kidney Dis. 2000;35: 1021–1038.
2. Marchal G, Verbeken E, Oyen R, et al. Ultrasound of the normal kidney: A sonographic, anatomic and histologic correlation. Ultrasound Med Biol. 1986; 12:999–1009. http://www.ncbi.nlm.nih.gov/pubmed/3547990
3. Behan M, Kazam E. The echographic characteristics of fatty tissues and tumors. Radiology. 1978;129:143–151. http://www.ncbi.nlm.nih.gov/pubmed/693867
4. Cook JH, Rosenfield AT, Taylor KJW. Ultrasonic demonstration of intrarenal anatomy. Am J Roentgenol. 1977;129:831–835. http://www.ncbi.nlm.nih.gov/pubmed/410246
5. Lafortune M, Constantin A, Breton G, et al. Sonography of the hypertrophied column of Bertin. AJR Am J Roentgenol. 1986;146:53. http://www.ncbi.nlm.nih.gov/pubmed/3510045
6. Davidson AJ, Hartman DS, Choyke PL, et al. Davidson's Radiology of the Kidney and Genitourinary Tract (3rd ed.). Philadelphia: WB Saunders; 1999.
7. Patriquin H, Lefaivre JF, Lafortune M, et al. Fetal lobation: An anatomoultrasonographic correlation. J Ultrasound Med. 1990;9:191. http://www.ncbi.nlm.nih.gov/pubmed/2184242
8. Troell S, Berg U, Johannson B, et al. Comparison between renal parenchymal sonographic volume, renal parenchymal urographic area, glomerular filtration rate and renal plasma flow in children. Scand J Urol Nephrol. 1988;22: 207–214.

9. Emamian SA, Nielsen MB, Pedersen JF. Intraobserver and interobserver variations in sonographic measurements of kidney size in adult volunteers. Acta Radiol. 1995;36:399–401.
http://www.ncbi.nlm.nih.gov/pubmed/7619620

10. Emamian SA, Nielsen MB, Pederson JF, et al. Kidney dimensions at sonography: correlation with age, sex, and habitus in 665 adult volunteers. AJR Am J Roentgenol. 1993;160:83–86.
http://www.ncbi.nlm.nih.gov/pubmed/8416654

11. Sargent MA, Long G, Karmali M, et al. Interobserver variation in the sonographic estimation of renal volume in children. Pediatr Radiol. 1997;27:663–666.
http://www.ncbi.nlm.nih.gov/pubmed/9252431

12. Miletic D, Fuckar Z, Sustic A, et al. Sonographic measurement of absolute and relative renal length in adults. J Clin Ultrasound. 1998;26:185–189.

13. Dinkel E, Ertel M, Dittrich M, et al. Kidney size in childhood: Sonographical growth charts for kidney length and volume. Pediatr Radiol. 1985;15:38–43.
http://www.ncbi.nlm.nih.gov/pubmed/4092904

14. Han BK, Babcock DS. Sonographic measurements and appearance of normal kidneys in children. AJR Am J Roentgenol. 1985;145:611–616.
http://www.ncbi.nlm.nih.gov/pubmed/3895872

15. Rosenbaum DM, Korngold E, Teele RL. Sonographic assessment of renal length in normal children. AJR Am J Roentgenol. 1984;142:467–469.
http://www.ncbi.nlm.nih.gov/pubmed/6607625

16. Cietak KA, Newton JR. Serial quantitative maternal nephrosonography in pregnancy. Br J Radiol. 1985;58:405–413.
http://www.ncbi.nlm.nih.gov/pubmed/3904902

17. Rottenberg GT, De Bruyn R, Gordon I. Sonographic standards for a single functioning kidney in children. AJR Am J Roentgenol. 1996;167:1255.

18. Gudinchet F, Meuli R, Regazzoni B. Compensatory renal growth in children and adults studied by Doppler sonography. J Clin Ultrasound. 1994;22:11–15.
http://www.ncbi.nlm.nih.gov/pubmed/8294571

19. Prassopoulos P, Gourtsoyiannis N, Cavouras D, et al. CT evaluation of compensatory renal growth in relation to postnephrectomy time. Acta Radiol. 1992;33:566.
http://www.ncbi.nlm.nih.gov/pubmed/1449882

20. Tapson JS, Owen JP, Robson PA, et al. Compensatory renal hypertrophy after donor nephrectomy. Clin Radiol. 1985;36:307.
http://www.ncbi.nlm.nih.gov/pubmed/3905198

21. Raj DS, Hoisala R, Somiah S, et al. Quantitation of change in the medullary compartment in renal allograft by ultrasound. J Clin Ultrasound. 1997;25:265–269.
http://www.ncbi.nlm.nih.gov/pubmed/9314109

22. Platt JF, Rubin JM, Bowerman RA, et al. The inability to detect kidney disease on the basis of echogenicity. AJR Am J Roentgenol. 1988;151:317–319.
http://www.ncbi.nlm.nih.gov/pubmed/3293376

23. Emamian SA, Nielsen MB, Pedersen JF, et al. Sonographic evaluation of renal appearance in 665 adult volunteers. Correlation with age and obesity. Acta Radiol. 1993;34:482–485.
http://www.ncbi.nlm.nih.gov/pubmed/8369185

24. Vade A, Lau P, Smick J, et al. Sonographic renal parameters as related to age. Pediatr Radiol. 1987;17:212–215.
http://www.ncbi.nlm.nih.gov/pubmed/3295730

25. Morin ME, Baker DA. The influence of hydration and bladder distension on the sonographic diagnosis of hydronephrosis. J Clin Ultrasound. 1979;7:192–194.
http://www.ncbi.nlm.nih.gov/pubmed/110840

26. Mosli HA, Rawas MM, Farsi HM. Mannitol-induced diuretic renal ultrasonography: A new technique. Urology. 1991;38:267–270.
http://www.ncbi.nlm.nih.gov/pubmed/1909474

27. Fried AM, Woodring MD, Thompson DJ. Hydronephrosis of pregnancy: A prospective sequential study of the course of dilatation. J Ultrasound Med. 1983;2:255–259.

28. Peake SL, Roxburgh HB, Langlois SLP. Ultrasonic assessment of hydronephrosis of pregnancy. Radiology. 1983;146:167–170.
http://www.ncbi.nlm.nih.gov/pubmed/6849041

29. Jeffrey RB, Federle MP. CT and ultrasonography of acute renal abnormalities. Radiol Clin North Am. 1983;21:515–525.

30. Paivansalo M, Huttunen K, Suramo I. Ultrasonographic findings in renal parenchymal diseases. Scand J Urol Nephrol. 1985;19:119–123.

31. Hricak H, Cruz C, Romanski R, et al. Renal parenchymal disease: Sonographic-histologic correlation. Radiology. 1982;144:141–147.
http://www.ncbi.nlm.nih.gov/pubmed/7089245

32. Rosenfield AT, Zerman RK, Cicchetti DV, et al. Experimental acute tubular necrosis: US appearance. Radiology. 1985;157:771–774.
http://www.ncbi.nlm.nih.gov/pubmed/3903859

33. Rivers BJ, Walter PA, Holm JC, et al. Gray-scale sonographic characterization of aminoglycoside-induced nephrotoxicosis in a canine model. Invest Radiol. 1996;31:639–651.
http://www.ncbi.nlm.nih.gov/pubmed/8889653

34. Nomura G, Kinoshita E, Yamagata Y, et al. Usefulness of renal ultrasonography for assessment of severity and course of acute tubular necrosis. J Clin Ultrasound. 1984;12:135–139.
http://www.ncbi.nlm.nih.gov/pubmed/6423686

35. Pardes JG, Auh YH, Kazam E. Sonographic findings in myoglobinuric renal failure and their clinical implications. J Ultrasound Med. 1983;2:391–394.
http://www.ncbi.nlm.nih.gov/pubmed/6632065

36. Walker JT, Keller MS, Katz SM. Computed tomographic and sonographic findings in acute ethylene glycol poisoning. J Ultrasound Med. 1983;2:429–431.
http://www.ncbi.nlm.nih.gov/pubmed/6632072

37. Kenney PJ, Brinsko RE, Patel DV, et al. Sonography of the kidneys in hemolytic uremic syndrome. Radiology. 1986;21:547–550.
http://www.ncbi.nlm.nih.gov/pubmed/3525450

38. Choyke PL, Grant EG, Hoffer FA, et al. Cortical echogenicity in the hemolytic uremic syndrome: clinical correlation. J Ultrasound Med. 1988;7:439–442.
http://www.ncbi.nlm.nih.gov/pubmed/3047422

39. Segel MC, Lecky JW, Slasky BS. Diabetes mellitus: the predominant cause of bilateral renal enlargement. Radiology. 1984;153:341–342.
http://www.ncbi.nlm.nih.gov/pubmed/6484164

40. Rosenfield AT, Siegel NJ. Renal parenchymal disease: Histopathologic-sonographic correlation. AJR Am J Roentgenol. 1981;137:793–798.
http://www.ncbi.nlm.nih.gov/pubmed/6974977

41. Di Fiori JL, Rodrique D, Kaptein EM, et al. Diagnostic sonography of HIV-associated nephropathy: New observations and clinical correlation. AJR Am J Roentgenol. 1998;171:713–716.
http://www.ncbi.nlm.nih.gov/pubmed/9725302

42. Schaffer RM, Schwartz GE, Becker JA, et al. Renal ultrasound in acquired immune deficiency syndrome. Radiology. 1984;153:511–513.
http://www.ncbi.nlm.nih.gov/pubmed/6385112

43. Schutz K, Siffring PA, Forrest TS, et al. Serial renal sonographic changes in preeclampsia. J Ultrasound Med. 1990;9:415–418.

44. Ten RM, Torres VE, Millner DS, et al. Acute interstitial nephritis: Immunologic and clinical aspects. Mayo Clin Proc. 1988;63:921–930.

45. Hiraoka M, Hori C, Tsuchida S, et al. Ultrasonographic findings of acute tubulointerstitial nephritis. Am J Nephrol. 1996;16:154–158.
http://www.ncbi.nlm.nih.gov/pubmed/8919233

46. Weber M, Braun B, Kohler H. Ultrasonic findings in analgesic nephropathy. Nephron. 1985;39:216–222.
http://www.ncbi.nlm.nih.gov/pubmed/3883209

47. Segasothy M, Abdul Samad S, Zulfigar A, et al. Computed tomography and ultrasonography: A comparative study in the diagnosis of analgesic nephropathy. Nephron. 1994;66:62–66.
http://www.ncbi.nlm.nih.gov/pubmed/8107955

48. Hoffman JC, Schnur MJ, Koenigsberg M. Demonstration of renal papillary necrosis by sonography. Radiology. 1982;145:785–787.
http://www.ncbi.nlm.nih.gov/pubmed/6755547

49. Braden GL, Kozinn DR, Hampf FE Jr., et al. Ultrasound diagnosis of early renal papillary necrosis. J Ultrasound Med. 1991;10:401–403.
http://www.ncbi.nlm.nih.gov/pubmed/1870185

50. Elseviers MM, De Schepper A, Corthouts R, et al. High diagnostic performance of CT scan for analgesic nephropathy in patients with incipient to severe renal failure. Kidney Int. 1995;48:1316–1323.

51. Toyoda K, Miyamoto Y, Ida M, et al. Hyperechoic medulla of the kidneys. Radiology. 1989;173:431–434.
http://www.ncbi.nlm.nih.gov/pubmed/2678257

52. Piccirillo M, Rigsby CM, Rosenfield AT. Sonography of renal inflammatory disease. Urol Radiol. 1987;9:66–78.
http://www.ncbi.nlm.nih.gov/pubmed/3303605

53. Hartman DS, Davis CJ Jr., Goldman SM, et al. Xanthogranulomatous pyelonephritis: Sonographic-pathologic correlation of 16 cases. J Ultrasound Med. 1984;3:481–488.
http://www.ncbi.nlm.nih.gov/pubmed/6392576

54. McGuire BB, Fitzpatrick JM. The diagnosis and management of complex renal cysts. Curr Opin Urol. 2010;20(5):349–354.

55. Bisceglia M, Senger GC, Stallone C, et al. Renal cystic diseases: A review. Adv Anat Pathol. 2006;13(1):26–56.

56. Ravine D, Gibson RN, Walker RG, et al. Evaluation of ultrasonographic diagnostic criteria for autosomal dominant polycystic kidney disease 1. Lancet. 1994;343:824–827.
http://www.ncbi.nlm.nih.gov/pubmed/7908078

57. Pei Y, Obaji J, Dupuis A, et al. Unif ed criteria for ultrasonographic diagnosis of ADPKD. J Am Soc Nephrol. 2009;20(1):205–212.
http://www.ncbi.nlm.nih.gov/pubmed/18945943

58. Bae KT, Commean PK, Lee JR. Volumetric measurement of renal cysts and parenchyma using MRI: phantoms and patients with polycystic kidney disease. J Comp Assist Tomography. 2000;24:614–619.
http://www.ncbi.nlm.nih.gov/pubmed/10966197

59. Levine E, Hartman DS, Meilstrup JW, et al. Current concepts and controversies in imaging of renal cystic diseases. Urol Clin North Am. 1997;24:523–543.
http://www.ncbi.nlm.nih.gov/pubmed/9275977

60. Hayden CK, Swischuk LE. Renal cystic disease. Semin Ultrasound CT MR. 1991;12:361–373.
http://www.ncbi.nlm.nih.gov/pubmed/1892695

61. Keith D, Torres VE, King BF, et al. Renal cell carcinoma in autosomal dominant polycystic kidney disease. J Am Soc Nephrol. 1994;4(9):1661–1669.

62. Kamholtz RG, Cronan JJ, Dorfman GS. Obstruction and the minimally dilated renal collecting system: US evaluation. Radiology. 1989;170:51–53.
http://www.ncbi.nlm.nih.gov/pubmed/2642347

63. Amis ES, Cronan JJ, Pf ster RC, et al. Ultrasonic inaccuracies in diagnosing renal obstruction. Urology. 1982;19:101–105.
http://www.ncbi.nlm.nih.gov/pubmed/7058574

64. Stevens S, Brown BD, McGahan JP. Nephrogenic diabetes insipidus: A cause of severe nonobstructive urinary tract dilatation. J Ultrasound Med. 1995;14: 543–545.
http://www.ncbi.nlm.nih.gov/pubmed/7563304

65. Riccabona M, Nelson TR, Pretorius DH, et al. In vivo three-dimensional sonographic measurement of organ volume: validation in the urinary bladder. J Ultrasound Med. 1996;15:627–632.
http://www.ncbi.nlm.nih.gov/pubmed/8866444

66. Kolman C, Girman CJ, Jacobsen SJ, et al. Distribution of post-void residual urine volume in randomly selected men. J Urology. 1999;161:122–127.

67. Middleton WD, Melson GL. Renal duplication artifact in US imaging. Radiology. 1989;173:427.
http://www.ncbi.nlm.nih.gov/pubmed/2678256

68. Bosniak MA, Rofsky NM. Problems in the detection and characterization of small renal masses. Radiology. 1996;198:638.
http://www.ncbi.nlm.nih.gov/pubmed/8628846

69. Leder RA, Dunnick NR. Transitional cell carcinoma of the pelvicalices and ureter. AJR Am J Roentgenol. 1990;155:713–722.
http://www.ncbi.nlm.nih.gov/pubmed/2119098

70. Grant DC, Dee GJ, Yoder IC, et al. Sonography in transitional cell carcinoma of the renal pelvis. Urol Radiol. 1986;8:1–5.

71. Igarashi T, Muakami S, Schichijo Y, et al. Clinical and radiological aspects of inf ltrating transitional cell carcinoma of the kidney. Urol Int. 1994;52: 181–184.

72. Raghavendra BN, Bosniak ML, Megibow AJ. Small angiomyolipoma of the kidney: sonographic-CT evaluation. AJR Am J Roentgenol. 1983;141: 575–578.
http://www.ncbi.nlm.nih.gov/pubmed/6603773

73. Siegel CL, Middletown WD, Teefey SA, et al. Angiomyolipoma and renal cell carcinoma: US differentiation. Radiology. 1996;198:789.
http://www.ncbi.nlm.nih.gov/pubmed/8628873

74. Weinberger E, Rosenbaum DM, Pendergrass TW. Renal involvement in children with lymphoma: Comparison of CT with sonography. AJR Am J Roentgenol. 1990;155:347–349.
http://www.ncbi.nlm.nih.gov/pubmed/2115266

75. Horii SC, Bosniak MA, Megibow AJ, et al. Correlation of CT and ultrasound in the evaluation of renal lymphoma. Urol Radiol. 1983;5:69–76.
http://www.ncbi.nlm.nih.gov/pubmed/6351400

76. Glicklich D, Sung MW, Frey M. Renal failure due to lymphomatous inf ltration of the kidneys: Report of three new cases and review of the literature. Cancer. 1986;58:748–753.
http://www.ncbi.nlm.nih.gov/pubmed/3524795

77. Villalon FC, Fernandez JE, Garcia TR. The hypoechoic halo: A f nding in renal lymphoma. J Clin Ultrasound. 1995;23:379.
http://www.ncbi.nlm.nih.gov/pubmed/7673455

78. Memel DS, Dodd GD 3rd, Shah AN, et al. Imaging of en bloc renal transplants: Normal and abnormal postoperative f ndings. AJR Am J Roentgenol. 1992;160:75–80.

79. Hanto DW, Simmons RL. Renal transplantation: Clinical considerations. Radiol Clin North Am. 1987;25:239–248.
http://www.ncbi.nlm.nih.gov/pubmed/3547472

80. O'Neill WC, Baumgarten DA. Ultrasonography in renal transplantation. Am J Kidney Dis. 2002;39:663–678.
http://www.ncbi.nlm.nih.gov/pubmed/11920331

81. Jurriaans E, Dubbins PA. Renal transplantation: the normal morphological and Doppler ultrasound examination. J Clin Ultrasound. 1992;20:495–506.
http://www.ncbi.nlm.nih.gov/pubmed/1328319

82. Lachance SL, Adamson D, Barry JM. Ultrasonically determined kidney transplant hypertrophy. J Urology. 1988;139:497–498.
http://www.ncbi.nlm.nih.gov/pubmed/3278128

83. Raiss GJ, Bree RL, Schwab RE, et al. Further observations in the ultrasound evaluation of renal allograft rejection. J Ultrasound Med. 1986;5:439–444.
http://www.ncbi.nlm.nih.gov/pubmed/3528522

84. McCarthy S, Rosenf eld AT. Ultrasonography in crossed renal ectopia. J Ultrasound Med. 1984;3:107.
http://www.ncbi.nlm.nih.gov/pubmed/6726857

85. Parvin SD, Rees Y, Veitch PS, et al. Objective measurement by ultrasound to distinguish cyclosporin A toxicity from rejection. Br J Surg. 1986;73: 1009–1011.

86. Absy M, Metreweli C, Matthews C, et al. Changes in transplanted kidney volume measured by ultrasound. Br J Radiol. 1987;60:525–529.
http://www.ncbi.nlm.nih.gov/pubmed/3304502

87. Nicholson ML, Williams PM, Bell A, et al. Prospective study of the value of ultrasound measurements in the diagnosis of acute rejection following renal transplantation. Br J Surg. 1990;77:656–658.
http://www.ncbi.nlm.nih.gov/pubmed/2200551

88. Slovis TL, Babcock DS, Hricak H, et al. Renal transplant rejection: Sonographic evaluation in children. Radiology. 1984;153:659–665.
http://www.ncbi.nlm.nih.gov/pubmed/6387788

89. Nicholson ML, Bell A, Burton PR, et al., Probability of rejection predicted from ultrasonographic measurement of renal transplant swelling. Br J Surg. 1993;80:1059–1062.

90. Swobodnik WL, Spohn BE, Wechsler JG, et al. Real-time ultrasound evaluation of renal transplant failure during the early postoperative period. Ultrasound Med Biol. 1986;12:97–105.
http://www.ncbi.nlm.nih.gov/pubmed/3526685

91. Amante AJ, Kahan BD. Technical complications of renal transplantation. Surg Clin North Am. 1994;74:1117–1131.
http://www.ncbi.nlm.nih.gov/pubmed/7940064

92. Pozniak MA, Dodd GD, Kelcz F. Ultrasonographic evaluation of renal transplantation. Radiol Clin North Am. 1992;30:1053–1066.
http://www.ncbi.nlm.nih.gov/pubmed/1518928

93. Hricak H, Mark AS, Alpers CE, et al. Sonographic evaluation of the rejecting ureter. Urol Radiol. 1986;8:25–31.
http://www.ncbi.nlm.nih.gov/pubmed/3523934

94. Katz JP, Hakki A, Katz SM, et al. Rejection of the ureter: a new component of renal allograft rejection. Transplant Proc. 1987;19:2200–2202.

95. Gottlieb RH, Voci SL, Cholewinksi SP, et al. Sonography: A useful tool to detect the mechanical causes of renal transplant dysfunction. J Clin Ultrasound. 1999;27:325–333.
http://www.ncbi.nlm.nih.gov/pubmed/10395128

96. Balchunas WR, Hill MC, Isikoff MB, et al. The clinical signif cance of dilatation of the collecting system in the transplanted kidney. J Clin Ultrasound. 1982;10:221–225.

97. Ghasemian SM, Guleria AS, Khawand NY, et al. Diagnosis and management of the urologic complications of renal transplantation. Clin Transplant. 1996;10:218–223.
http://www.ncbi.nlm.nih.gov/pubmed/8664523

98. Cunningham JJ, Bacani-Faulls M. Sonographic "White Line Sign" for detection of minimal mucosal thickening in renal transplants. Uroradiology. 1990;35:367–370.

99. Babcock DS. Sonography of wall thickening of the renal collecting system: A nonspecif c f nding. J Ultrasound Med. 1987;6:29–32.

100. Nicolet V, Carignan L, Dubuc G, et al. Thickening of the renal collecting system: A nonspecif c f nding at US. Radiology. 1988;168:411–413.
http://www.ncbi.nlm.nih.gov/pubmed/3293110

101. Khauli RB, Stoff JS, Lovewell T, et al. Post-transplant lymphoceles: A critical look into the risk factors, pathophysiology, and management. J Urology. 1993;150:22–26.

102. Pozniak MA, Kelcz F, Dodd GD. Renal transplant ultrasound: Imaging and Doppler. Semin Ultrasound CT MR. 1991;12:319–334.
http://www.ncbi.nlm.nih.gov/pubmed/1892693

103. Cullmann H-J, Prosinger M. Necrosis of the allograft ureter—evaluation of different methods in early diagnosis. Urol Int. 1990;45:164–169.
http://www.ncbi.nlm.nih.gov/pubmed/20691991

104. Bardelli M, Veglio F, Arosio E, et al. New intrarenal echo-Doppler velocimetric indices for the diagnosis of renal artery stenosis. Kidney Int. 2006;69(3): 580–587.
http://www.ncbi.nlm.nih.gov/pubmed/16407882

105. O'Neill WC, Bardelli M, Yevzlin AS. Imaging for renovascular disease. Semin Nephrol. 2011;31(3):272–282.
106. Vasbinder GB, Nelemans PJ, Kessels AG, et al. Diagnostic tests for renal artery stenosis in patients suspected of having renovascular hypertension: a meta-analysis. Ann Intern Med. 2001;135(6):401–411.
107. Radermacher J, Chavan A, Bleck J, et al. Use of Doppler ultrasonography to predict the outcome of therapy for renal-artery stenosis. N Engl J Med. 2001;344:410–417.
http://www.ncbi.nlm.nih.gov/pubmed/11172177
108. Krumme B, Hollenbeck M. Doppler sonography in renal artery stenosis—does the Resistive Index predict the success of intervention? Nephrol Dial Transplant. 2007;22(3):692–696.
http://www.ncbi.nlm.nih.gov/pubmed/22577447
109. Schwenger V, Keller T, Hofmann N, et al. Color Doppler indices of renal allografts depend on vascular stiffness of the transplant recipients. Am J Transplant. 2006;6(11):2721–2724.
http://www.ncbi.nlm.nih.gov/pubmed/17049059
110. Genkins SM, Sanfilippo FP, Carroll BA. Duplex Doppler sonography of renal transplants: Lack of sensitivity and specificity in establishing pathologic diagnosis. AJR Am J Roentgenol. 1989;152:535–539.
http://www.ncbi.nlm.nih.gov/pubmed/2644778
111. Baxter G, Rodger R. Doppler ultrasound in renal transplantation. Nephrol Dial Transplant. 1997;12:2449–2451.
http://www.ncbi.nlm.nih.gov/pubmed/9394347
112. Blaufox MD, Aurell M, Bubeck B, et al. Report of the Radionuclides in Nephrourology Committee on renal clearance. J Nucl Med. 1996;37(11):1883–1890.
http://www.ncbi.nlm.nih.gov/pubmed/8917197
113. Eshima D, Taylor A Jr. Technetium-99m (99mTc) mercaptoacetyltriglycine: update on the new 99mTc renal tubular function agent. Semin Nucl Med. 1992;22(2):61–73.
http://www.ncbi.nlm.nih.gov/pubmed/1534184
114. Marcus CS, Kuperus JH. Pediatric renal iodine-123 orthoiodohippurate dosimetry. J Nucl Med. 1985;26(10):1211–1214.
http://www.ncbi.nlm.nih.gov/pubmed/3900309
115. Stabin M, Taylor A Jr, Eshima D, et al. Radiation dosimetry for technetium-99m-MAG3, technetium-99m-DTPA, and iodine-131-OIH based on human bio-distribution studies. J Nucl Med. 1992;33(1):33–40.
http://www.ncbi.nlm.nih.gov/pubmed/1530968
116. Bubeck B, Brandau W, Weber E, et al. Pharmacokinetics of technetium-99m-MAG3 in humans. J Nucl Med. 1990;31(8):1285–1293.
117. Shikano N, Kanai Y, Kawai K, et al. Transport of 99mTc-MAG3 via rat renal organic anion transporter 1. J Nucl Med. 2004;45(1):80–85.
118. Taylor A Jr., Ziffer JA, Eshima D. Comparison of Tc-99m MAG3 and Tc-99m DTPA in renal transplant patients with impaired renal function. Clin Nucl Med. 1990;15(6):371–378.
http://www.ncbi.nlm.nih.gov/pubmed/2141307
119. Taylor A Jr, Clark S, Ball T Comparison of Tc-99m MAG3 and Tc-99m DTPA scintigraphy in neonates. Clin Nucl Med. 1994;19(7):575–580.
http://www.ncbi.nlm.nih.gov/pubmed/7924094
120. O'Reilly P, Aurell M, Britton K, et al. Consensus on diuresis renography for investigating the dilated upper urinary tract. Radionuclides in Nephrourology Group. Consensus Committee on Diuresis Renography. J Nucl Med. 1996;37(11):1872–1876.
http://www.ncbi.nlm.nih.gov/pubmed/8917195
121. Gordon I, Colarinha P, Fettich J, et al. Guidelines for indirect radionuclide cystography. Eur J Nucl Med. 2001;28(3):BP16–20.
122. Shulkin BL, Mandell GA, Cooper JA, et al. Procedure guideline for diuretic renography in children 3.0. J Nucl Med Technol. 2008;36(3):162–168.
http://www.ncbi.nlm.nih.gov/pubmed/18765635
123. Esteves FP, Taylor A, Manatunga A, et al. 99mTc-MAG3 renography: normal values for MAG3 clearance and curve parameters, excretory parameters, and residual urine volume. Am J Roentgenol. 2006;187(6):W610–617.
124. Russell CD, Taylor AT, Dubovsky EV. Measurement of renal function with technetium-99m-MAG3 in children and adults. J Nucl Med. 1996;37(4):588–593.
http://www.ncbi.nlm.nih.gov/pubmed/8691246
125. Van Nerom CG, Bormans GM, De Roo MJ, et al. First experience in healthy volunteers with technetium-99m L,L-ethylenedicysteine, a new renal imaging agent. Eur J Nucl Med. 1993;20(9):738–746.
http://www.ncbi.nlm.nih.gov/pubmed/8223766
126. Taylor A Jr, Thakore K, Folks R, et al. Background subtraction in technetium-99m-MAG3 renography. J Nucl Med. 1997;38(1):74–79.
127. Taylor A, Hansen L, Eshima D, et al. Comparison of technetium-99m-ll-EC isomers in rats and humans. J Nucl Med. 1997;38(5):821–826.
128. Piepsz A, Colarinha P, Gordon I, et al. Guidelines for 99mTc-DMSA scintigraphy in children. Eur J Nucl Med. 2001;28(3):BP37–41.
129. Rossleigh MA. Renal infection and vesico-ureteric reflux. Semin Nucl Med. 2007;37(4):261–268.
http://www.ncbi.nlm.nih.gov/pubmed/17544626
130. Prigent A, Cosgriff P, Gates GF, et al. Consensus report on quality control of quantitative measurements of renal function obtained from the renogram: International Consensus Committee from the Scientific Committee of Radionuclides in Nephrourology. Semin Nucl Med. 1999;29(2):146–159.
http://www.ncbi.nlm.nih.gov/pubmed/10321826
131. Piepsz A, Kuyvenhoven JD, Tondeur M, et al. Normalized residual activity: usual values and robustness of the method. J Nucl Med. 2002; 43(1):33–38.
132. Donoso G, Kuyvenhoven JD, Ham H, et al. 99mTc-MAG3 diuretic renography in children: a comparison between F0 and F + 20. Nucl Med Commun. 2003;24(11):1189–1193.
133. Bao J, Manatunga A, Binongo JN, et al. Key variables for interpreting 99mTc-mercaptoacetyltriglycine diuretic scans: Development and validation of a predictive model. Am J Roentgenol. 2011;197(2):325–333.
134. Taylor AT, Blaufox MD, De Palma D, et al. Guidance document for structured reporting of diuresis renography. Semin Nucl Med. 2011;42:41–48.
http://www.ncbi.nlm.nih.gov/pubmed/22117812
135. Taylor A, Nally J, Aurell M, et al. Consensus report on ACE inhibitor renography for detecting renovascular hypertension. Radionuclides in Nephrourology Group. Consensus Group on ACEI Renography. J Nucl Med. 1996;37(11):1876–1882.
http://www.ncbi.nlm.nih.gov/pubmed/8917196
136. Piepsz A, Tondeur M, Ham H. NORA: a simple and reliable parameter for estimating renal output with or without furosemide challenge. Nucl Med Commun. 2000;21(4):317–323.
137. Blaufox MD, Fine EJ, Heller S, et al. Prospective study of simultaneous orthoiodohippurate and diethylenetriaminepentaacetic acid captopril renography. The Einstein/Cornell Collaborative Hypertension Group. J Nucl Med. 1998;39(3):522–528.
http://www.ncbi.nlm.nih.gov/pubmed/9529303
138. Strauss BS, Blaufox MD. Estimation of residual urine and urine flow rates without urethral catheterization. J Nucl Med. 1970;11(2):81–84.
http://www.ncbi.nlm.nih.gov/pubmed/5410926
139. Sapirstein LA, Vidt DG, Mandell MJ, et al. Volumes of distribution and clearances of intravenously injected creatinine in the dog. Am J Physiol. 1955;181(2):330–336.
http://www.ncbi.nlm.nih.gov/pubmed/14376619
140. Bubeck B. Renal clearance determination with one blood sample: improved accuracy and universal applicability by a new calculation principle. Semin Nucl Med. 1993;23(1):73–86.
http://www.ncbi.nlm.nih.gov/pubmed/8469997
141. Schlegel JU, Hamway SA. Individual renal plasma flow determination in 2 minutes. J Urol. 1976;116(3):282–285.
http://www.ncbi.nlm.nih.gov/pubmed/785027
142. Gates GF. Split renal function testing using Tc-99m DTPA. A rapid technique for determining differential glomerular filtration. Clin Nucl Med. 1983;8(9):400–407.
http://www.ncbi.nlm.nih.gov/pubmed/6357589
143. Taylor A Jr, Corrigan PL, Galt J, et al. Measuring technetium-99m-MAG3 clearance with an improved camera-based method. J Nucl Med. 1995;36(9):1689–1695.
http://www.ncbi.nlm.nih.gov/pubmed/7658232
144. Bocher M, Shrem Y, Tappiser A, et al. Tc-99m mercaptoacetyltriglycine clearance: comparison of camera-assisted methods. Clin Nucl Med. 2001;26(9):745–750.
145. Taylor A Jr, Manatunga A, Morton K, et al. Multicenter trial validation of a camera-based method to measure Tc-99m mercaptoacetyltriglycine, or Tc-99m MAG3, clearance. Radiology. 1997;204(1):47–54.
146. Halkar R, Taylor A, Manatunga A, et al. Monitoring renal function: a prospective study comparing camera-based technetium-99m mercaptoacetyltriglycine clearance and creatinine clearance. Urology. 2007;69(3):426–430.
147. Tonnesen KH, Munck O, Hald T et al. Influence on the radiorenogram of variation in skin to kidney distance and the clinical importance hereof. In: Zum MM, Winkel K, Funck-Bretano JL, eds. Proceedings of the International Symposium on Radionuclides in Nephrourology. Stuttgart: Thieme; 1974.
148. Taylor A, Lewis C, Giacometti A, et al. Improved formulas for the estimation of renal depth in adults. J Nucl Med. 1993;34(10):1766–1769.
http://www.ncbi.nlm.nih.gov/pubmed/8410296
149. Gordon I, Piepsz A, Sixt R, et al. Guidelines for standard and diuretic renography in children. Eur J Nucl Med. 2001;28(3):BP21–30.

150. Liu Y, Ghesani NV, Skurnick JH, et al. The F + 0 protocol for diuretic renography results in fewer interrupted studies due to voiding than the F - 15 protocol. J Nucl Med. 2005;46(8):1317–1320.
http://www.ncbi.nlm.nih.gov/pubmed/21699777
151. Boubaker A, Prior JO, Meuwly JY, et al. Radionuclide investigations of the urinary tract in the era of multimodality imaging. J Nucl Med. 2006;47(11):1819–1836.
http://www.ncbi.nlm.nih.gov/pubmed/17079816
152. Kuyvenhoven J, Piepsz A, Ham H. When could the administration of furosemide be avoided? Clin Nucl Med. 2003;28(9):732–737.
153. Adeyoju AA, Burke D, Atkinson C, et al. The choice of timing for diuresis renography: the F + 0 method. BJU Int. 2001;88(1):1–5.
154. Brater DC. Diuretic therapy. N Engl J Med. 1998;339(6):387–395.
http://www.ncbi.nlm.nih.gov/pubmed/9691107
155. Hunsche A, Press H, Taylor A. Increasing the dose of furosemide in patients with azotemia and suspected obstruction. Clin Nucl Med. 2004;29(3):149–153.
http://www.ncbi.nlm.nih.gov/pubmed/15162982
156. Connolly LP, Zurakowski D, Peters CA, et al. Variability of diuresis renography interpretation due to method of post-diuretic renal pelvic clearance half-time determination. J Urol. 2000;164(2):467–471.
http://www.ncbi.nlm.nih.gov/pubmed/10893624
157. Conway JJ, Maizels M. The "well tempered" diuretic renogram: a standard method to examine the asymptomatic neonate with hydronephrosis or hydroureteronephrosis. A report from combined meetings of The Society for Fetal Urology and members of The Pediatric Nuclear Medicine Council—The Society of Nuclear Medicine. J Nucl Med. 1992;33(11):2047–2051.
http://www.ncbi.nlm.nih.gov/pubmed/1432172
158. Wong DC, Rossleigh MA, Farnsworth RH. Diuretic renography with the addition of quantitative gravity-assisted drainage in infants and children. J Nucl Med. 2000;41(6):1030–1036.
http://www.ncbi.nlm.nih.gov/pubmed/10855630
159. Frokier J, E.-J.A., Dissing T Antenatally detected hydronephrosis: the nuclear medicine techniques. In: Prigent A, Piepsz, eds. Functional Imaging in Neph□rourology. London and New York: Taylor and Francis; 2006.
160. Lorberboym M, Kapustin Z, Elias Z, et al. The role of renal scintigraphy and unenhanced helical computerized tomography in patients with ureterolithiasis. Eur J Nucl Med. 2000;27(4):441–446.
http://www.ncbi.nlm.nih.gov/pubmed/10805118
161. Bird VG, Gomez-Marin O, Leveillee RJ, et al. A comparison of unenhanced helical computerized tomography f ndings and renal obstruction determined by furosemide 99m technetium mercaptoacetyltriglycine diuretic scintirenography for patients with acute renal colic. J Urol. 2002;167(4):1597–1603.
162. Sfakianakis GN, Cohen DH, Braunstein RH, et al. MAG3–F0 scintigraphy in decision making for emergency intervention in renal colic after helical CT positive for a urolith. J Nucl Med. 2000;41(11):1813–1822.
http://www.ncbi.nlm.nih.gov/pubmed/11079488
163. Dawson DL. Noninvasive assessment of renal artery stenosis. Semin Vasc Surg. 1996;9(3):172–181.
164. Holley KE, Hunt JC, Brown AL Jr, et al. Renal artery stenosis. A clinical-pathologic study in normotensive and hypertensive patients. Am J Med. 1964;37:14–22.
http://www.ncbi.nlm.nih.gov/pubmed/14181143
165. Saf an RD, Madder RD. Ref ning the approach to renal artery revascularization. JACC Cardiovasc Interv. 2009;2(3):161–174.
http://www.ncbi.nlm.nih.gov/pubmed/19463421
166. van Jaarsveld BC, Krijnen P, Pieterman H, et al. The effect of balloon angioplasty on hypertension in atherosclerotic renal-artery stenosis. Dutch Renal Artery Stenosis Intervention Cooperative Study Group. N Engl J Med. 2000;342(14):1007–1014.
http://www.ncbi.nlm.nih.gov/pubmed/10749962
167. Plouin PF, Chatellier G, Darne B, et al. Blood pressure outcome of angioplasty in atherosclerotic renal artery stenosis: a randomized trial. Essai Multicentrique Medicaments vs Angioplastie (EMMA) Study Group. Hypertension. 1998;31(3):823–829.
http://www.ncbi.nlm.nih.gov/pubmed/9495267
168. Webster J, Marshall AF, Abdalla M, et al. Randomised comparison of percutaneous angioplasty vs continued medical therapy for hypertensive patients with atheromatous renal artery stenosis. Scottish and Newcastle Renal Artery Stenosis Collaborative Group. J Hum Hypertens. 1998;12(5):329–335.
http://www.ncbi.nlm.nih.gov/pubmed/9655655
169. Bax L, Woittiez AJ, Kouwenberg HJ, et al. Stent placement in patients with atherosclerotic renal artery stenosis and impaired renal function: a randomized trial. Ann Intern Med. 2009;150(12):840–848, W150–W151.
http://www.ncbi.nlm.nih.gov/pubmed/19414832
170. Wheatley K, Ives N, Gray R, et al. Revascularization versus medical therapy for renal-artery stenosis. N Engl J Med. 2009;361(20):1953–1962.
http://www.ncbi.nlm.nih.gov/pubmed/19907042
171. Baumgartner I, Lerman LO. Renovascular hypertension: screening and modern management. Eur Heart J. 2011;32(13):1590–1598.
172. Perez-Rodriguez J, Lai S, Ehst BD, et al. Nephrogenic systemic f brosis: incidence, associations, and effect of risk factor assessment—report of 33 cases. Radiology. 2009;250(2):371–377.
173. Rocha-Singh K, Jaff MR, Lynne Kelley E. Renal artery stenting with non-invasive duplex ultrasound follow-up: 3–year results from the RENAISSANCE renal stent trial. Catheter Cardiovasc Interv. 2008;72(6):853–862.
http://www.ncbi.nlm.nih.gov/pubmed/19006254
174. Gainer JV, Morrow JD, Loveland A, et al. Effect of bradykinin-receptor blockade on the response to angiotensin-converting-enzyme inhibitor in normotensive and hypertensive subjects. N Engl J Med. 1998;339(18):1285–1292.
175. Karanikas G, Becherer A, Wiesner K, et al. ACE inhibition is superior to angiotensin receptor blockade for renography in renal artery stenosis. Eur J Nucl Med Mol Imaging. 2002;29(3):312–318.
http://www.ncbi.nlm.nih.gov/pubmed/12002704
176. Kon V, Fogo A, Ichikawa I. Bradykinin causes selective efferent arteriolar dilation during angiotensin I converting enzyme inhibition. Kidney Int. 1993;44(3):545–550.
http://www.ncbi.nlm.nih.gov/pubmed/8231026
177. Taylor A, Blaufox MD, Dubovsky EV, et al. Society of Nuclear Medicine procedure guideline for diagnosis of renovascular hypertension 3.0. Procedure guidelines, Policy and Practice; 2003. Retrieved from www.snm.org.
178. Prigent A. The role of ACE inhibitor renography in the diagnosis of renovascular hypertension. In: Henkin RE, Boles MA, Dillehay GL et al., eds. Nuclear Medicine, 2nd ed. Philadelphia, PA: Elsiever; 2006.
179. Visscher CA, de Zeeuw D, de Jong PE, et al. Angiotensin-converting enzyme inhibition-induced changes in hippurate renography and renal function in renovascular hypertension. J Nucl Med. 1996;37(3):482–488.
http://www.ncbi.nlm.nih.gov/pubmed/8772652
180. Nally JV Jr. Provocative captopril testing in the diagnosis of renovascular hypertension. Urol Clin North Am. 1994;21(2):227–234.
http://www.ncbi.nlm.nih.gov/pubmed/8178390
181. Fommei E, Ghione S, Hilson AJ, et al. Captopril radionuclide test in renovascular hypertension: a European multicentre study. European Multicentre Study Group. Eur J Nucl Med. 1993;20(7):617–623.
http://www.ncbi.nlm.nih.gov/pubmed/8370384
182. Fommei E, Ghione S, Hilson AJW, et al. Captopril radionuclide test in renovascular hypertension: European Multicentre Study. In: O'Reilly PH, Taylor A, Nally JV, eds. Radionuclides in Nephrourology. Blue Bell, PA: Field & Wood, Medical Periodicals, Inc; 1994.
183. Erbsloh-Moller B, Dumas A, Roth D, et al. Furosemide-^{131}I-hippuran renography after angiotensin-converting enzyme inhibition for the diagnosis of renovascular hypertension. Am J Med. 1991;90(1):23–29.
http://www.ncbi.nlm.nih.gov/pubmed/1986589
184. Dondi M, Fanti S, De Fabrittiis A, et al. Prognostic value of captopril renal scintigraphy in renovascular hypertension. J Nucl Med. 1992;33(11):2040– 2044.
185. Kahn D, Ben-Haim S, Bushnell DL, et al. Captopril-enhanced 99Tcm-MAG3 renal scintigraphy in subjects with suspected renovascular hypertension. Nucl Med Commun. 1994;15(7):515–528.
186. Mittal BR, Kumar P, Arora P, et al. Role of captopril renography in the diagnosis of renovascular hypertension. Am J Kidney Dis. 1996;28(2):209–213.
187. Taylor A. Functional testing: ACEI renography. Semin Nephrol. 2000;20(5):437–444.
http://www.ncbi.nlm.nih.gov/pubmed/11022896
188. Helin KH, Tikkanen I, von Knorring JE, et al. Screening for renovascular hypertension in a population with relatively low prevalence. J Hypertens. 1998;16(10):1523–1529.
http://www.ncbi.nlm.nih.gov/pubmed/9814625
189. Huot SJ, Hansson JH, Dey H, et al. Utility of captopril renal scans for detecting renal artery stenosis. Arch Intern Med. 2002;162(17):1981–1984.
190. Roccatello D, Picciotto G, Rabbia C, et al. Prospective study on captopril renography in hypertensive patients. Am J Nephrol. 1992;12(6):406–411.
http://www.ncbi.nlm.nih.gov/pubmed/1292339
191. Fernandez P, Morel D, Jeandot R, et al. Value of captopril renal scintigraphy in hypertensive patients with renal failure. J Nucl Med. 1999;40(3):412–417.
http://www.ncbi.nlm.nih.gov/pubmed/10086704
192. Setaro JF, Saddler MC, Chen CC, et al. Simplif ed captopril renography in diagnosis and treatment of renal artery stenosis. Hypertension. 1991;18(3):289–298.
193. Eriksson P, Mohammed AA, De Geer J, et al. Non-invasive investigations of potential renal artery stenosis in renal insuff ciency. Nephrol Dial Transplant. 2010;25(11):3607–3614.

194. Taylor A. ACE inhibition renography in the evaluation of suspected renovascular hypertension. In: Prigent A, Piepsz A, eds. Functional Imaging in Nephro□ Urology. United Kingdom: Taylor and Francis; 2006.
195. Thorsson O, Bjuvang A, Granerus G. Advantages of standardized criteria for the interpretation of angiotensin-converting enzyme inhibition renography. Nucl Med Commun. 2009;30(6):449–454.
196. Fanti S, Dondi M, Guidalotti PL, et al. Bilateral symmetrical induced changes in captopril scintigraphy. J Nucl Med. 1998;39:86P.
197. Stavropoulos SW, Sevigny SA, Ende JF, et al. Hypotensive response to captopril: a potential pitfall of scintigraphic assessment for renal artery stenosis. J Nucl Med. 1999;40(3):406–411.
198. Dubovsky EV, Russell CD, Bischof-Delaloye A, et al. Report of the Radionuclides in Nephrourology Committee for evaluation of transplanted kidney (review of techniques). Semin Nucl Med. 1999;29(2):175–188.
http://www.ncbi.nlm.nih.gov/pubmed/10321828
199. Biassoni L, Chippington S. Imaging in urinary tract infections: current strategies and new trends. Semin Nucl Med. 2008;38(1):56–66.
200. Montini G, Tullus K, Hewitt I. Febrile urinary tract infections in children. N Engl J Med. 2011;365(3):239–250.
http://www.ncbi.nlm.nih.gov/pubmed/21774712